Managing Induced Seismicity Risks From Enhanced Geothermal Systems

A Good Practice Guideline

Zhou, Wen; Lanza, Federica; Grigoratos, Iason; Schultz, Ryan; Cousse, Julia; Trutnevyte, Evelina; Muntendam-Bos, Annemarie; Wiemer, Stefan

DOI
10.1029/2024RG000849

Publication date
2024

Document Version
Final published version

Published in
Reviews of Geophysics

Citation (APA)
Zhou, W., Lanza, F., Grigoratos, I., Schultz, R., Cousse, J., Trutnevyte, E., Muntendam-Bos, A., & Wiemer, S. (2024). Managing Induced Seismicity Risks From Enhanced Geothermal Systems: A Good Practice Guideline. *Reviews of Geophysics*, *62*(4), Article e2024RG000849. https://doi.org/10.1029/2024RG000849

AGU ADVANCING EARTH AND SPACE SCIENCES

Reviews of Geophysics

REVIEW ARTICLE
10.1029/2024RG000849

Managing Induced Seismicity Risks From Enhanced Geothermal Systems: A Good Practice Guideline

Wen Zhou[1], Federica Lanza[2], Iason Grigoratos[2], Ryan Schultz[2], Julia Cousse[3], Evelina Trutnevyte[3], Annemarie Muntendam-Bos[1], and Stefan Wiemer[2]

[1]Delft University of Technology, Delft, The Netherlands, [2]Swiss Seismological Service, ETH Zürich, Zürich, Switzerland, [3]University of Geneva, Geneva, Switzerland

Key Points:

- Induced seismicity can be caused by geothermal operations. These earthquakes can be operation-ending, or spur development moratoriums
- We review the breadth of literature and then synthesize "good practice" recommendations, in a modular format for simplicity
- Our guidelines provide a template for safe and responsible enhanced geothermal systems operations, while highlighting future research directions

Correspondence to:
R. Schultz,
Ryan.Schultz@sed.ethz.ch

Citation:
Zhou, W., Lanza, F., Grigoratos, I., Schultz, R., Cousse, J., Trutnevyte, E., et al. (2024). Managing induced seismicity risks from enhanced geothermal systems: A good practice guideline. *Reviews of Geophysics*, *62*, e2024RG000849. https://doi.org/10.1029/2024RG000849

Received 5 JUN 2024
Accepted 4 SEP 2024

Author Contributions:
Conceptualization: Wen Zhou, Federica Lanza, Iason Grigoratos, Ryan Schultz, Julia Cousse, Evelina Trutnevyte
Data curation: Wen Zhou, Federica Lanza, Iason Grigoratos, Ryan Schultz
Formal analysis: Wen Zhou, Federica Lanza, Iason Grigoratos, Ryan Schultz
Funding acquisition: Annemarie Muntendam-Bos, Stefan Wiemer
Investigation: Wen Zhou, Federica Lanza, Iason Grigoratos, Ryan Schultz
Methodology: Wen Zhou, Federica Lanza, Iason Grigoratos, Ryan Schultz
Project administration: Annemarie Muntendam-Bos, Stefan Wiemer

Abstract Geothermal energy is a green source of power that could play an important role in climate-conscious energy portfolios; enhanced geothermal systems (EGS) have the potential to scale up exploitation of thermal resources. During hydraulic fracturing, fluids injected under high-pressure cause the rock mass to fail, stimulating fractures that improve fluid connectivity. However, this increase of pore fluid pressure can also reactivate pre-existing fault systems, potentially inducing earthquakes of significant size. Induced earthquakes are a significant concern for EGS operations. In some cases, ground shaking nuisance, building damages, or injuries have spurred the early termination of projects (e.g., Basel, Pohang). On the other hand, EGS operations at Soultz-sous-Forêts (France), Helsinki (Finland), Blue Mountain (Nevada, USA), and Utah FORGE (USA) have adequately managed induced earthquake risks. The success of an EGS operation depends on economical reservoir enhancements, while maintaining acceptable seismic risk levels. This requires state-of-the-art seismic risk management. This article reviews domains of seismology, earthquake engineering, risk management, and communication. We then synthesize "good practice" recommendations for evaluating, mitigating, and communicating the risk of induced seismicity. We advocate for a modular approach. Recommendations are provided for key technical aspects including (a) a seismic risk management framework, (b) seismic risk pre-screening, (c) comprehensive seismic hazard and risk evaluation, (d) traffic light protocol designs, (e) seismic monitoring implementation, and (f) step-by-step communication plans. Our recommendations adhere to regulatory best practices, to ensure their general applicability. Our guidelines provide a template for effective earthquake risk management and future research directions.

Plain Language Summary Geothermal energy could play an important role in the future of climate-conscious energy. Enhanced geothermal systems (EGS) have the potential to unlock thermal energy trapped in impermeable rocks; hydraulic fracturing injects fluids under pressures high enough to stimulate fractures, increasing permeability. However, this process also has the potential to cause earthquakes. Induced earthquakes have the potential to end operations or cause development moratoriums. On the other hand, there are EGS operations that were able to adequately manage these risks. Here, we review the literature of cases, to synthesize material into a state-of-the-art understanding of seismic risk management. We provide "good practice" guidelines that spans multiple domains. Because of this breadth of topics, we advocate for a modular framework that covers seismic risk pre-screening, seismic hazard and risk evaluation, design of traffic light protocols, seismic monitoring considerations, and detailed communication plans. Overall, this review provides a template for future EGS projects to consider, while highlighting research directions needed for improved management of earthquake risks.

1. Introduction

1.1. Enhanced Geothermal Systems (EGS)

Geothermal energy is considered a source of clean, renewable, and sustainable energy and could play an important role in the energy transition to combat climate change. However, conventionally exploited hydro-geothermal energy resources are limited and only accessible in geologically favorable locations. Beneath the surface, temperatures increase significantly, normally with a gradient around 25°C/km (Criss, 2020). Thus, even for areas that are not in geologically favorable conditions, at 3–5 km depth temperatures reach around 100°C, making it possible to harness heat by injecting cold water, and extracting hot water (steam) that can be used for electricity generation or direct heating. However, low rock porosity and permeability restrict fluid flow.

Resources: Wen Zhou, Federica Lanza, Iason Grigoratos, Ryan Schultz
Software: Wen Zhou, Federica Lanza, Iason Grigoratos, Ryan Schultz
Supervision: Federica Lanza, Annemarie Muntendam-Bos, Stefan Wiemer
Validation: Wen Zhou, Federica Lanza, Iason Grigoratos, Ryan Schultz
Visualization: Wen Zhou, Federica Lanza, Iason Grigoratos, Ryan Schultz, Julia Cousse, Evelina Trutnevyte
Writing – original draft: Wen Zhou, Federica Lanza, Iason Grigoratos, Ryan Schultz, Julia Cousse, Evelina Trutnevyte
Writing – review & editing: Wen Zhou, Federica Lanza, Iason Grigoratos, Ryan Schultz, Julia Cousse, Evelina Trutnevyte, Annemarie Muntendam-Bos, Stefan Wiemer

Therefore, methods such as hydraulic stimulation or chemical stimulation are required to enhance rock permeability and fluid conductivity, leading to the creation of an EGS.

Conventionally, the hydraulic stimulation for EGS often intentionally targets formations with estimated natural small-scale fractures. The increase of fluid pressure in the reservoir induces slip along those fractures. Due to the heterogeneity and roughness of fractures, slip often creates dilatation, thus effectively creating pathways in the fracture network. In other cases, with enough fluid pressure, new fractures might be created, and proppants might be used to keep the fractures open. In either case, the induced slips can behave seismically, producing earthquakes that might be recorded or felt (Moein et al., 2023). Induced seismicity is thus an inevitable factor in EGS (E. L. Majer & Peterson, 2007; Zang et al., 2014).

Additionally, geothermal production (circulation of hot and cold fluids) could also induce earthquakes due to for example, pressure leaking to active faults (Schmittbuhl et al., 2021) or stress variations caused by heterogeneous temperature decreases (Parisio et al., 2019; Vörös & Baisch, 2022). Occasionally, mud loss during the drilling phase has also coincided with low-magnitude seismicity, often serving as a warning sign for future fault reactivation (Ellsworth et al., 2019; Muntendam-Bos et al., 2022). Thus, the inevitable factor of induced seismicity requires thorough seismic risk management on each stage of an EGS project.

1.2. Induced Seismicity Risk Management

Ideally, we want an EGS operation to generate only small magnitude earthquakes without any felt impact or risk to the nearby residents or personnel on site. This microseismicity can help to estimate the dimension of the reservoir and the efficiency of the stimulation, which are important factors for evaluating commercial production. However, larger events could potentially occur, imposing risks (e.g., noise nuisance, property damages, financial losses or personal injuries) on the residents and trigger financial/social consequences (e.g., project termination, social unrest, and obstacles for future development). Readers can refer to Table 27 in Ineris and BRGM (2023) and to Foulger et al. (2018) for a list of seismic incidents during geothermal operations.

The EGS project in Basel (Deichmann & Giardini, 2009; Häring et al., 2008) and the deep geothermal project in Strasbourg (Schmittbuhl et al., 2021) were terminated due to induced earthquakes of M_L 3.4, and M_L 3.6, respectively. The EGS project in Pohang, South Korea, caused the largest EGS-related earthquake, registering a magnitude of M_W 5.5 (U.S. Geological Survey; Woo et al., 2019). The Pohang earthquake resulted in dozens of hospitalizations, a fatality, over 75 million USD in direct damages to 57,000 structures, around 300 million USD in economic impact, and the termination of the project (Ellsworth et al., 2019; Kim et al., 2018). These highlight both the potential risk of induced seismicity (Box 1) and the need for improved assessment and management, before and during deep geothermal and EGS projects.

On the other hand, we have observed EGS operations in Soultz-sous-Forêts (France; Dorbath et al., 2009), Newberry (USA; Cladouhos et al., 2016), Cooper Basin (Australia; Holl, 2015), Paralana (Australia; Albaric et al., 2014), Blue Mountain (USA; Koirala et al., 2024; Norbeck & Latimer, 2023), Helsinki (Finland; Kwiatek et al., 2019) and Utah FORGE (USA; Moore et al., 2019), where induced seismicity did not pose unacceptable risk. Although not all of these cases achieved the expected conductivity for production. Examining the seismic risk management plans from those projects could potentially benefit future EGS initiatives.

This article aims to provide uniform and applicable good practice guidelines for managing induced seismic risk in EGS projects. It can serve as a reference for the EGS stakeholders including operators, regulators, independent experts, vendors, and residents, and it is based on existing documents and guidelines on induced seismicity. In particular, we draw insights from the existing guidelines in Europe (Baisch et al., 2016; Bohnhoff et al., 2018; Braun et al., 2020; Dialuce et al., 2014; Dutch Mining Act, 2003; FKPE, 2013; Ineris & BRGM, 2023; Kraft et al., 2020; Trutnevyte & Wiemer, 2017; Wiemer et al., 2017) and in the United States (E. Majer et al., 2012, 2013; Templeton et al., 2021, 2023; Walters et al., 2015). We also incorporate findings from the Geothermica project DEEP, which focused on the Utah FORGE EGS project (Moore et al., 2019; Pankow et al., 2023; Wannamaker et al., 2020) and consider information from analogous types of induced seismicity like hydraulic fracturing in the oil/gas industry (Atkinson et al., 2016, 2020; CAPP, 2019; Schultz, Skoumal, et al., 2020).

From a legal-requirement point of view, there is in general a lack of legislation regarding the permitting process and risk management for EGS projects. We hope this article could inspire more national legislation on EGS

Box 1. "Induced" Versus "Triggered".

Following McGarr et al. (2002), the adjective "induced" normally describes seismicity resulting from an activity that causes a stress change that is comparable in magnitude to the ambient shear stress acting on a fault, whereas "triggered" is used if the stress change is only a small fraction of the ambient stress level. Note that, in this article, we collectively refer to "induced" and "triggered" earthquakes as "induced seismicity". This is because it is difficult to distinguish them in practice, especially in near real-time, due to the very complex geomechanics involved (Ellsworth et al., 2019; E. Majer et al., 2012). Other publications have referred to (truly) "induced" seismicity using the term "driven" seismicity, to avoid ambiguity (Bommer & Verdon, 2024).

regulation to prevent nuisance, protect residents" properties, and safety, while developing EGS to achieve decarbonization and energy security needs.

1.3. Outline of the Guideline

The article comprises the following topics: (a) risk management framework, (b) seismic risk pre-screening, (c) comprehensive Seismic risk analysis (SRA) (for concerning projects), (d) traffic light protocols, (e) seismic monitoring, and (f) communication and outreach guidelines.

Throughout the article, we aim to clearly distinguish between good practice goals, recommendations, justifications, and examples. Herein, we define goals as the intended targets or purposes of a section, recommendations as the essential standards required to meet that goal, justifications as the scientific rationale for meeting the goals, and examples as concrete cases that implement this goal-recommendation-justification process. Because of these definitions, the words "goals" and "recommendations" will carry a special meaning in this article.

Specifically, we define recommendations based on (our informed opinion of) scientific consensus, which we anchor only to the most rigorously established and well-demonstrated concepts. This is done so that only clear and justifiable links are drawn between best science and best practices. This helps ensure that our recommendations are as universal and timeless as possible. In sections where scientific consensus has not been established, we will be clear as to these deficiencies and the current scope of open-ended research directions. Examples will cover state-of-the-art demonstrations—in some cases outlining multiple competing methods, because of this scope difference, relevant examples will likely evolve following the publication of this article.

This article structure was intentionally chosen to ensure that our good practices adhere to state-of-the-art science and regulatory best practices (Coglianese, 2018). We aimed to create guidelines that blend elements of both prescriptive and performance-based approaches (Box 2); in order to ensure effective risk reduction, while still fostering innovation. Our guidelines list specific frameworks when scientific consensus on certain topics has been reached, while remaining more open-ended when such consensus is lacking; to encourage further scientific research.

2. Induced Seismicity Risk Management Framework

Managing the risks associated with induced seismic activity is essential throughout the entire life cycle of an EGS project, from exploration (e.g., site selection, license acquisition, data acquisition) and planning (e.g., detailed operation planning, site preparation, drilling of monitoring wells, if applicable) to operation (e.g., drilling of injection and production wells, stimulation and circulation) and post-operation (i.e., after well shut-in or well abandonment). We thus propose the development of an Induced Seismicity Risk Management Framework (ISRMF) for each EGS project.

The ISRMF is designed to involve multiple stakeholders:

1. Regulator(s): the licensing and/or governing authority, normally linked to the local or national government.

Box 2. Definition of Prescriptive and Performance-Based Guidelines.

Rules, guidelines, or regulations can either be defined using prescriptive or performance-based approaches. Prescriptive standards tend to rigidly outline explicit details on what processes or methods are to be followed. Performance-based standards tend to define safety/quality metrics to be met, leaving the specifics on how to meet these targets flexible and open-ended. Performance-based approaches are also sometimes called outcome-based regulation or non-prescriptive regulation.

We note that the philosophical difference between these two approaches does not necessarily imply that performance-based guidelines will be lax or unsafe in comparison to their more prescriptive counterparts. It simply means that given two equivalent ways to describe a rule, the performance-based approach prefers the more generic one.

The flexibility of performance-based approaches can be advantageous. This is because it will be better able to accommodate unknown examples, variation in location specifics, or future technological developments. This also allows room for development of new technologies to meet (or exceed) safety/quality standards, by providing targets for innovation; these innovations then impart improved safety/quality, performance, or cost savings onto future projects.

However, for performance-based guidelines to be effective, clear and measurable target metrics are required. Thus, adequate monitoring systems need to be emplaced for compliance assurance. In cases where clear and measurable performance targets are unavailable, more prescriptive approaches generally tend to be favorable.

For a simplified example, a prescriptive guideline might recommend exactly how many seismic stations are needed to monitor for induced seismicity. This implicitly comes with assumptions about the type/scale of operation, geological setting, sources of noise, type/quality of sensors, and signal processing techniques being used. On the other hand, a performance-based guideline could outline the required target threshold for detection instead. This leaves room for future approaches (e.g., distributed acoustic sensing or machine learning) to reach these targets, without imposing the prior assumptions of the more prescriptive approach. However, this comes at the cost of additional complexity in the verification of monitoring performance.

In many regulatory applications, guidelines will blend both prescriptive and performance-based aspects together. In an effort to gain the advantages of one type, while simultaneously covering for deficiencies of the other type.

2. Operator(s): a company/organization that executes the EGS project and is responsible for the safety of the operations.
3. Independent experts: an independent group of experts who are not involved in the operational aspects of the EGS project or affiliated with the operator.
4. Vendors: a group of professionals, contracted to design or execute a specific task.
5. Affected communities and the general public: the target of protection of this guideline, they might refer to this guideline as an information resource.

Other existing guidelines include the EGS protocol by E. Majer et al. (2012, 2013), who proposed a seven-step risk management approach from an operators' perspective, in the USA. Their step-by-step approach is easy for operators to follow when executing an EGS project. In the Netherlands, Baisch et al. (2016) developed a multi-level framework for seismic hazard assessment of deep geothermal projects including EGS. In Switzerland, Trutnevyte and Wiemer (2017) built a framework of seismic risk governance for deep geothermal projects including EGS, which has mitigation measures recommended according to output from a seismic risk pre-screening (including stimulation and circulation). In France, Ineris & BRGM (2023) provide an overview of induced seismicity incidents from geothermal operations and recommend good practices for assessing and

mitigating induced seismic hazard. Other guidelines have covered the topic of induced seismicity risks in the past (e.g., Bohnhoff et al., 2018; Braun et al., 2020; Chen et al., 2020; Dialuce et al., 2014; Dutch Mining Act, 2003; FKPE, 2013; GEORISK, 2018; IMEPLS, 2016; Templeton et al., 2021, 2023; Walters et al., 2015). Our ISRMF is informed by these prior guidelines. Specifically, it can be used to produce a document similar to the Induced Seismicity Mitigation Plan as in E. Majer et al. (2012) and Pankow et al. (2023), which is delivered by the operator in the permitting process.

2.1. ISRMF Modules

In the current article, we redesign the step-by-step advice approach of E. Majer et al. (2012, 2013), while allowing tailoring based on various risk levels as in Trutnevyte and Wiemer (2017). Thus, recommendations are given as basic risk management components (Modules), which can be integrated to build an ISRMF. Here, we define as seismic risk the potential adverse impacts that a seismic sequence can have on the exposed individuals and structures as a collective, instead of focusing on the average probability that a single person will incur losses or physical harm. Hereafter, we provide a description of the six modules forming the risk management framework for EGS-induced seismicity. These modules are not defined in chronological order; instead, they can be flexibly integrated into the ISRMF (Figure 1).

2.1.1. Module 1—Seismic Risk Pre-Screening

Once an EGS project has been proposed by an operator, a seismic risk pre-screening (referred to as pre-screening hereafter) must be completed, as proposed by various studies (e.g., Baisch et al., 2016; Kraft et al., 2020; E. Majer et al., 2012; Trutnevyte & Wiemer, 2017), to classify the seismic concern level of the project as either low or high. Besides evaluating the level of concern (LoC), the pre-screening should indicate where the knowledge gaps are, in order to improve the assessment accuracy. If knowledge gaps are too large to draw a meaningful pre-screening, the operator initiates the data collection and research module. Once knowledge gaps are fulfilled, they re-run the pre-screening. Detailed description of Module 1 is given in Section 3.

2.1.2. Module 2—Data Acquisition and Research (D&R)

In cases where available data are limited to drive a meaningful pre-screening or comprehensive risk assessment (e.g., seismic hazard and risk analysis (SHRA)), data acquisition and research (D&R) should be conducted. As an example, the following procedures could be helpful to constrain fault activity and hazards:

As part of the pre-screening:

- Fault distribution mapping using field data acquisition (e.g., 2D/3D seismic, geological mapping).

As part of the comprehensive risk assessment:

- Collection of detailed fault geometry (e.g., 3D seismic, vertical seismic profile (VSP) surveys) and stress field (e.g., minifrac test).
- Derivation of ground-motion characteristics (e.g., building 3D *P*- and *S*-wave velocity models) and site-specific soil/rock conditions (e.g., near-surface surveys).

Given the strong variability in knowledge gaps and quick development of data acquisition and research, it is difficult to draw a guideline on how the D&R should be done. We thus do not provide a detailed description in this module. However, general principles such as open access policy and multiple stakeholders' involvement should be followed. Thus, we introduce the concept of learning targets (Section 2.3.2) to guide the process.

2.1.3. Module 3—Communication and Outreach

The operator involves all relevant stakeholders in the project in order to understand the social context, stakeholders' perceptions, and build a communication team and strategy.

In this article, we suggest a nine-step approach (see Section 7 for details):

- Step 1: Identifying stakeholders and their networks relevant to the project
- Step 2: Understanding the social context of the region
- Step 3: Setting up a multidisciplinary outreach team

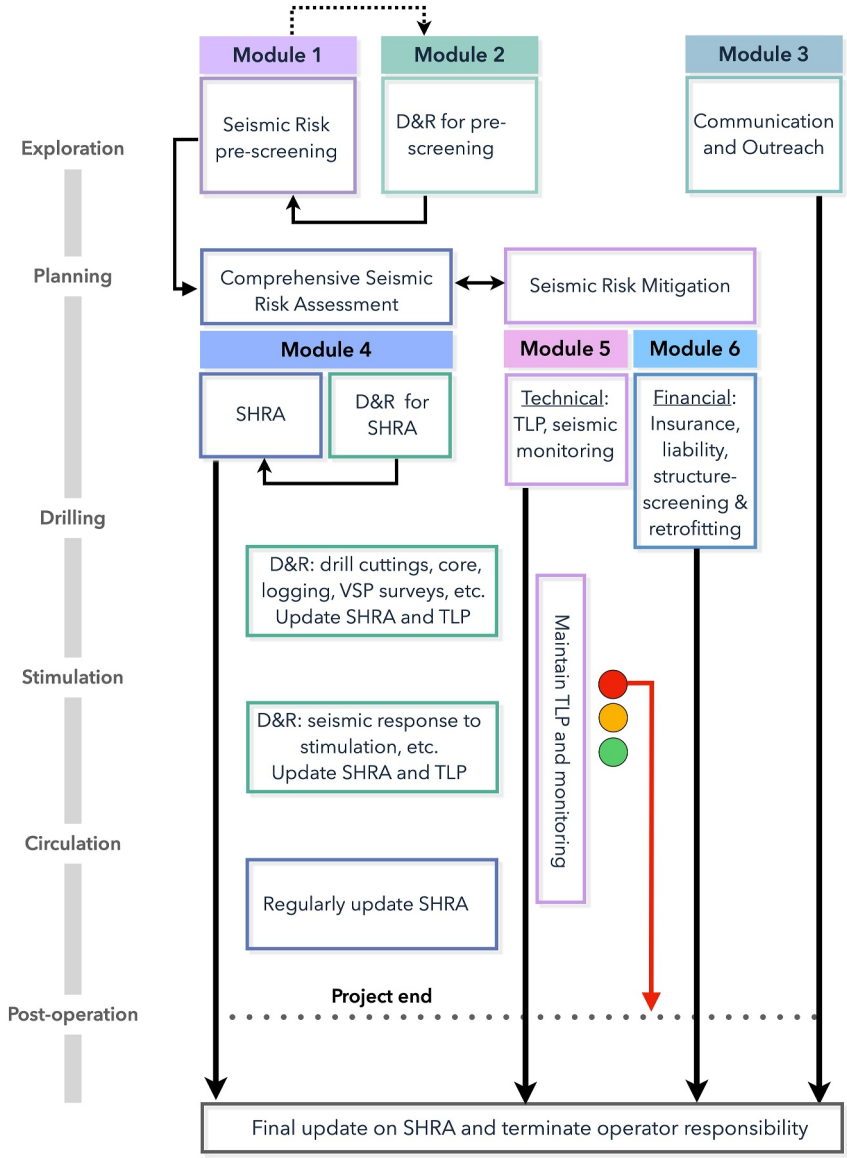

Figure 1. Schematic diagram of the Induced Seismicity Risk Management Framework. Interrelationships between component modules are shown alongside the timeline of drilling phases.

- Step 4: Acclimatizing the scale and scope of community participation
- Step 5: Setting up upstream discussions and partnerships between all stakeholders
- Step 6: Tailoring information to the social context and particular audience (i.e., target group)
- Step 7: Monitoring public perceptions in order to adapt the communication strategy
- Step 8: Developing a crisis plan
- Step 9: Giving regular updates about the project.

2.1.4. Module 4—Comprehensive Seismic Risk Analysis

For projects falling into the high-risk concern category, the operator will need to commission a comprehensive site-specific analysis to better assess the seismic risk related to hydraulic stimulation and fluid circulation activities at the EGS site. When compared to the pre-screening tool, this analysis is expected to require similar but more quantitative data to be collected, and a much more demanding analytical process that includes the construction of a seismic hazard and risk model, as well as complex calculations that will likely require the

establishment of a dedicated working group (independent experts or vendors; see Section 2.2). Details are given in Section 4.

2.1.5. Module 5—Technical Seismic Risk Mitigation Measures

Technical seismic risk mitigation measures should be in place before the start of the drilling of the operation and maintained through the project life cycle. The technical measures include: (a) building a seismic monitoring network (see Section 6), (b) establishing a TLP, and (c) outline operational mitigation strategies in the case of a yellow-light and red-light occurrence (see Section 5).

2.1.6. Module 6—Financial Seismic Risk Mitigation Measures

Financial risk mitigation measures should be conducted according to the risk analysis (Sections 4 and 5), and be in place before operation well drilling starts, and include (a) evaluating the seismic risk to the overall project financial risk estimation and management; (b) preparing for the worst-case scenarios:

- Clarify liability in the case of nuisance or damages from induced seismicity (Cypser & Davis, 1998).
- Developing a damage compensation scheme, seeking earthquake insurance for covering damages caused by induced seismicity, or contributing to an operator collateral fund (if available).
- Screening infrastructure to evaluate their resilience to shaking for high-risk projects. Optionally, building retrofitting could be used to reinforce fragile infrastructure.

Various financial mitigation measures, including but not limited to the example given above, are expected to be taken into account by the operator in their business plan. Given the variability of these measures for different countries and regions, we do not give a detailed description in the article. But the overall goal is to keep seismic risks in a financially tolerable range (e.g., Langenbruch et al., 2020). Including financial measures in the ISRMF is beneficial for protecting both the affected community and the operator from potential risks, and for maintaining project transparency.

2.2. Stakeholders' Roles in the ISRMF

2.2.1. Regulator

The regulator reviews the permit application, including the risk management plan, of the operator. The regulator must protect the interests of the public, while fostering innovation and competition within industry. Given that the seismic hazard on site might fluctuate as new data is collected, continuous supervision from the regulator is required. To aid the supervision process, we suggest that the regulatory and legislative authorities:

- Clearly define the suite of critical risk metrics (e.g., population nuisance, structural damages, local personal risk) and their corresponding thresholds, which will inform the pre-screening, the comprehensive SRA, and the design of the TLP.
- Work with the authoritative earthquake agency to densify the national/regional seismic network as soon as possible, to enhance the network for smaller events, establish an a priori baseline, and to provide independent measurements of possible induced events.

2.2.2. Operator

The operator is responsible for constraining the seismic risk within the regulator's acceptable thresholds across all phases of the project. We thus suggest that the operator:

- Deploy professional and experienced personnel to oversee the risk management of a project, which includes:
  - conducting or commissioning the continuous seismic risk assessment of the project (including the pre-screening), under the supervision of the regulator,
  - facilitating reasonable data requests from the regulator,
  - facilitating potential additional seismic monitoring needs,
  - following the agreed upon TLP,
  - facilitating potential operational changes to mitigate the seismic hazard.
- Implement a “learning from operation” strategy. Learning targets are defined for each project phase and should be reported to the regulator and the public by the end of each phase.

2.2.3. Independent Experts

The regulator may choose to appoint groups of experts to review the operator's risk management framework, the pre-screening and the comprehensive SRA, the seismic monitoring and the TLP. They can also produce alternative independent analyses for validation purposes. These expert groups should not be associated in any way with the operator.

2.2.4. Vendors

The operator (or the public) may choose to hire groups of professionals to fill needed expertise gaps. This may include designing/conducting the operator's risk management framework, the pre-screening, the comprehensive SRA, the seismic monitoring, and the implementation of their TLP.

2.2.5. Local Population

The local residents and businesses have the right to be informed of the potential risks posed by the project, including the process and the results of the pre-screening and of the comprehensive SRA, and mitigation measures. Reports related to the ISRMF should include a summary in plain language for the general public. Their concerns need to be addressed in accordance with the law.

2.3. ISRMF Workflow

Throughout the project life cycle, we provide a template for the ISRMF (Figure 1) using the six modules for EGS seismic risk management. Additionally, we introduce the concept of "learning targets" to guide the data acquisition in each phase of the ISRMF.

2.3.1. ISRMF Template

In this template, we divide the ISRMF workflow/modules into phases, based on the life cycle of an EGS project. Note that we assume Module 4 is required. In Section 3, we will discuss if the pre-screening (Module 1) indicates a low LoC, then Module 1 could replace Module 4 in each phase of the project.

2.3.1.1. Exploration Phase

During the exploration phase, Modules 1, 2, and 3 are initiated. Pre-screening (Module 1) and initial data acquisition (Module 2) will be used to inform if and how an EGS operation will move forwards. A series of exploratory wells might also be drilled and tested to facilitate the data acquisition process.

2.3.1.2. Planning Phase

During the planning phase (site preparation), a comprehensive seismic risk assessment (Module 4) may be required. Risk mitigation Modules 5 and 6 are designed, while communication (Module 3) is continued. If the operator decides to move forward, they should provide a detailed plan on how to implement the relevant modules.

2.3.1.3. Drilling Phase

During the drilling phase, the operator completes the wells needed for operations, while following their risk management plan (Modules 3, 4, and 5). We note that there is the potential for induced earthquakes starting at the drilling phase. Besides monitoring potential induced seismicity, the operator should also monitor drilling data such as mud losses, cuttings, well logs, and core recoveries, which might indicate the presence of faults (IMEPLS, 2016). After the drilling operation, the operator should continue D&R (Module 2) to analyze the data from drill cuttings/cores, well logs, VSP etc. and update the models of the SHRA.

2.3.1.4. Stimulation Phase

During the stimulation phase, the operator continues following their risk management plan (Modules 3, 4, 5, and 6), focusing on communication, real-time seismic monitoring and the TLP. After each stimulation, Modules 3, 4, 5, and 6 may need to be updated/verified based on the newly available data.

2.3.1.5. Circulation Phase

During the circulation phase (i.e., geothermal production), the seismic risks still exist but will likely be driven by different mechanisms compared to the stimulation phase. The operator continues following their risk management plan (Modules 3, 4, 5, and 6). After each circulation phase, Modules 3, 4, 5, and 6 may need to be updated/verified based on the newly available data.

2.3.1.6. Post-Operation Phase

At the end of the project, the wells are shut-in, plugged, and reclamation efforts commence. A project can end either from the natural completion of the wells' life cycle or prematurely due to a red-light event. The operator continues implementing Module 3, and the real-time seismic monitoring according to Module 5. Additionally, the operator should monitor for potential seismicity rate changes due to well shut-in, which might require updating Modules 4 and 6. The same happens if, after a sufficiently long period of monitoring, the seismicity rate and event magnitudes have decayed significantly. If the SHRA suggests that induced seismic risk has approached sufficiently low levels, the operator, regulator, and the independent expert group discuss terminating the responsibility of the operator. In this case, the operator hands over the monitoring system to the national earthquake agency for continued monitoring and maintenance, until the seismicity level approaches pre-project background levels.

2.3.2. ISRMF Learning Targets

Throughout this workflow, we suggest that the operator adopts the concept of "learning targets" (see Box 3) to guide D&R and assist in the efficiency and transparency of seismic risk management.

3. Seismic Risk Pre-screening (Modules 1 and 2)

In the proposed EGS seismic risk management framework, we suggest conducting a seismic risk pre-screening (referred as pre-screening hereafter) during the exploration phase of a project (Module 1; Seismic Risk Pre-Screening). This includes using existing data (Module 2; Data Acquisition and Research) to initially assess the LoC regarding the potential risks of induced earthquakes. The pre-screening should be conducted or commissioned by the operator and reviewed by the regulator (ideally after being reviewed/validated by independent experts). The process should be transparent, and the results should be made available to the public, if a comprehensive SHRA is not commissioned. The pre-screening is used to inform the suitability of subsequent analyses. For this purpose, we refer here to seismic risk as the potential adverse impacts that a seismic sequence can have on the exposed individuals and structures as a collective. More detailed risk analysis focusing on the average probability that a single person will incur losses or physical harm will be part of a more comprehensive SHRA (Module 4).

Goals of the seismic risk pre-screening

1. To utilize existing knowledge and project plans to provide an initial categorization of the project's LoC.
2. To identify knowledge gaps that will inform subsequent analyses and monitoring needs.

Note that the LoC is only a preliminary and qualitative estimation of seismic risk that uses incomplete information, thus it contains large uncertainty. A pre-screening for LoC should include important geological, operational and exposure factors and consider data quality. Public attitude toward the project should also be measured, given the strong benefit-risk relevance to the local population from EGS projects. When required, the comprehensive SHRA will supersede the pre-screening results.

The LoC categories serve as a reference for deploying further seismic risk mitigation measures (Modules 5 and 6). The LoC concept enables the operator to decide if the project is worth investing in, provides preliminary evidence for the regulator to evaluate the safety of the project, and communicates seismic risks transparently to the public (Table 1). Knowledge gaps and quality of existing data are contributing to the uncertainty of the pre-screening. Based on the identified gaps or data quality issues, the operator may conduct research and data acquisition (Module 2) to improve the quality of pre-screening.

If a "high" LoC is pre-screened, both a more comprehensive study on the seismic risk potential of the area (SHRA) and high-resolution seismic monitoring network are needed. The results of the detailed SHRA analysis supersede any pre-screening values and should inform the regulator's decisions on whether the project should be

Box 3. Learning From Operations.

The operator should define learning targets (in terms of gained knowledge) before each project phase that they need to reach. For example:

Before the exploration phase:
1. Are the population and infrastructure vulnerable to induced earthquakes?
2. Is the site geologically susceptible to induced earthquakes?
3. Will we get reliable geological data from geological and seismological agencies?
4. Will site amplification be an important element?

(…)

Before the drilling phase:
1. What data needs to be collected during drilling?
2. At what depth is it likely to encounter faults and fractures?
3. What is the mineral composition of the reservoir rock and how heterogeneous is the rock?
4. What is the in situ stress state from a mini-frac test? Do the principal stress directions agree with existing data?
5. Will there be mud losses and does that mean intersecting faults?

(…)

After each phase, the operator should review the results and determine how they should proceed with the project based on the new knowledge they have gained or not gained (Terrier et al., 2022). The learning targets and outcomes should be reported to the regulator and made open to the public to maintain transparency.

permitted, under which conditions and with which mitigation measures in place. A risk-based TLP to manage induced seismicity should be designed using site-specific models. According to the requirements of TLP, a high-resolution seismic monitoring network should be installed to reach both the necessary magnitude of completeness (Mc) and spatial resolution thresholds (Module 5; Section 6).

If a "low" LoC is pre-screened, the SHRA would still be informative but could be deemed optional by the regulator. Standard TLP thresholds required by the regulator might be used, and the regional backbone seismic monitoring network used if the backbone network meets the standard TLP requirements.

Recommendations for the seismic risk pre-screening

1. The LoC estimates should account for at least two main components of seismic risk: the seismic source characteristics (a combination of geological/tectonic and operational factors), and the characteristics of the exposed assets (including their fragility and potential consequences from nuisance or damages).

Table 1
Level of Concern Categories Resulting From the Pre-Screening and Corresponding Mitigation Measures

LoC category	Comprehensive SHRA	Traffic light protocol	Seismic monitoring
Low	Optional	Standard magnitude thresholds or informed by loss risk analysis	Coarse resolution meeting TLP requirement (e.g., regional backbone network)
High	Mandatory and consequential	Thresholds informed by site-specific risk analysis; an Adaptive TLP could be considered	High spatial and magnitude resolution meeting TLP requirement

Note. See Sections 5 and 6 for additional details of the impacts of level of concern (LoC) on traffic light protocols (TLPs) and seismic monitoring, respectively.

2. The pre-screening should be conducted or commissioned by the operator and should be accepted by the regulator (ideally after a review/validation from independent experts). The results and evaluation process of the pre-screening should be made public, if a comprehensive SHRA is not commissioned.
3. In the current absence of scientific consensus, various approaches could be used for pre-screening. The operator's decision on which pre-screening tool is to be adopted should be justified and agreed upon by the regulator (ideally with advice from independent experts).
4. The LoC should be updated if project plans change, or new knowledge is available. For example, from the comprehensive SHRA (Module 4; Section 4) or from the seismic monitoring (Module 5; Section 6).

It is important to stress that the existing pre-screening tools do not address the potential impact of long-term geothermal production on induced seismicity, due to the lack of comprehensive data from operational EGS projects. Data from conventional hydrothermal projects show that the thermal production has not resulted in large magnitude earthquakes, if the project is not located in an active fault region (see review by Buijze et al., 2019). However, in the case of EGS, available data is still too limited to draw definitive conclusions. Therefore, caution should be exercised, and mitigation measures must be sustained throughout the entire life cycle of an EGS project to monitor any anomalies during the heat production phase.

3.1. Key Factors for Pre-Screening

In general, the LoC is influenced by four main factors:

1. Geological and tectonic factors that influence the severity/frequency of earthquake hazards.
2. Operational factors that influence the occurrence and productivity of earthquakes.
3. Proximity, characteristics, and vulnerability of exposed assets (i.e., people and buildings).
4. Quality of data used to infer points 1–3.

Note that the attitude and perception of the local population could also significantly influence decision making. However, we suggest considering attitudes and perceptions separately as a legitimate concern (see Section 3.1.5).

3.1.1. Geological and Tectonic Factors

The geological/tectonic factors help evaluate the chance of having critically stressed faults around the project site. The basic principles involve keeping distance from active faults and seeking a less fractured (faulted) environment. This evaluation can be conducted through considering the following factors:

- Smallest distance to geologically known active or potentially active faults.
- Regional historical earthquake activity.
- Modeled tectonic seismic hazard levels around the site.
- Length of the proximal faults and those faults' triggering potential, that is, orientation with stress field.
- Potential for hydraulic pathways capable of transmitting pressure or stress changes to faults over a distance, whether horizontally or vertically.
- Lithology of formations near the operational target.

Note that near-surface conditions amplifying surface ground motion are considered in Section 3.1.3.

3.1.2. Operational Factors

The correlation between operations (stimulation and circulation) and seismicity remains a critical topic of induced seismicity. The direct response of seismicity to operations is still to be explored, while a few factors are known to be prone to induce or trigger fault slip events, including:

- Depth of the stimulation volume, which can serve as a proxy for the stress state and the proximity to basement faults.
- Net fluid injection volume, which has shown, in several cases, to have a linear relationship with the upper bound of the maximum observed magnitude (McGarr, 2014). However, it is important to recognize that these relationships can vary significantly from site-to-site.
- Fluid injection rate and pressure increase in the reservoir (Shapiro et al., 2010). The higher the flow rate and the pressure, the higher is generally the seismic hazard potential. Note that the stimulation strategy (e.g.,

single-/multi-stage, cyclical/monotonic injection rates, open-hole/perforated-casing) and the fluid composition might also influence the potential of induced seismicity.

- Temperature decrease during fluid-circulation (thermal production) causes stress changes in the subsurface due to thermal-elastic effect, which could trigger seismicity (N. T. Cao et al., 2022; Vörös & Baisch, 2022).
- Well orientation, which might influence the fluid-fracture/fault interconnection. To determine this, a detailed localized study is required.

3.1.3. Exposed Assets

The evaluation of seismic exposure should consider population density, building taxonomy, importance/fragility of assets, and local site conditions. Induced earthquakes can cause damage over an extended area (see Section 4 for details); thus, exposure data collection should cover a comparable region. The presence of highly critical infrastructure (e.g., nuclear power plants, dams, oil refineries, cultural heritage sites, long bridges), noise sensitive infrastructure (e.g., hospitals, sensitive laboratories), or buildings which are not designed for earthquake resistance, should be accounted for.

When considering the risks posed on structures and population, it is also important to consider the amplification of ground motion at each asset's location, due to near-surface soil/rock conditions (e.g., Van Ginkel et al., 2022) or topographic effects (e.g., Massa et al., 2014). In general, hard soil/rock has lower amplification than soft soil/rock (see Eurocode 8, CEN, 2004 for an example of site classifications).

3.1.4. Data Quality Factor

Data quality significantly influences the reliability of the pre-screened LoC. When data quality is limited, the pre-screening could be conservative, leading to higher apparent LoC. For example, by assigning a penalty on data quality to ensure that LoC is not underestimated because of poor data quality.

Here, we emphasize data quality considerations for a few examples of the geological/tectonic factors, which could be considered in the pre-screening:

- Seismic images (2D, 3D seismic reflection profiles, seismic velocity models); this data set is crucial for estimating hidden fault existence at a local scale. Sometimes this information may be supplemented with offsets from well logs. The best quality seismic data would be 3D seismic or multiple 2D seismic lines with dense coverage and deep penetration.
- Geological and tectonic maps (2D, 3D fault maps); these maps are often available from geological institutes and national topographic agencies. This data provides important information on regional scale faults. The resolution of these maps might be used as an indicator of data quality.
- Site characterization (e.g., soil profiles, surface geology maps, V_{S30} maps, or site amplification maps); since site characterization is also a crucial parameter for earthquake hazard, it is often available from national/regional geological institutes. The resolution of these maps might be used as an indicator of data quality. V_{S30}, the time-averaged *S*-wave velocity between the surface and 30 m depth, is a proxy metric for site amplification.
- Stress field (e.g., maximal horizontal stress direction and magnitude, faulting mechanism, regional borehole stress measurements, seismic anisotropy measurements); stress data is important for estimating fault activity, especially for seismically inactive regions. Indicators of stress field data quality could be the type of measurements and the proximity/relevance of the measurement site to the project site.
- Past earthquake activity (instrumental, historical, or paleoseismic); these data are often available through the national or regional earthquake agencies or from published studies. An important data quality factor is the completeness of the instrumental data through time, and the consensus behind historical or paleoseismic findings.

An important aspect of data quality is to identify knowledge gaps that need to be improved for site-specific risk assessment.

3.1.5. Public Attitudes and Concern

While public attitudes have sometimes been defined as a risk to an EGS project (Wiemer et al., 2017), it is crucial to think of public attitudes as a legitimate set of concerns to engage with, since the attitudes can both help and

Table 2
Summary of Pre-Screening Parameter Matrices for Four Existing Pre-Screening Tools

Pre-screening tools	Geology	Operations	Exposure	Public concern	Data quality	Low LoC	High LoC
Majer et al. (2012)	Brief	Brief	Detailed	–	–	Not defined	Not defined
Quick-Scan	Detailed	Detailed	–	–	–	<0.32	≥0.32
GRID	Detailed	Detailed	Detailed	Detailed	–	Cat. 0 and I	Cat. II and III
Ineris and BRGM (2023)	Detailed	Detailed	–	–	–	Level 0 and 1	Level 2 and 3

hinder the project. Contrary to the data quality score, determining a score for residents' attitudes is difficult. For example, the attitudes toward the project will likely evolve with time. A region could initially be enthusiastic about an EGS project, but this can change based on the dynamics and quality of communications among all stakeholders. In parallel to the pre-screening, initial assessment of attitudes and concerns is therefore important (Trutnevyte & Wiemer, 2017). To get an overall sense of attitudes toward the project in the initial stage of the project, steps 1 and 2 of Module 3, addressed in Section 7.1, may be followed. To obtain quantitative data on public attitudes, surveys to measure the attitudes and concerns of the general public could be used. To have deeper insights on how the local population perceives the project, face-to-face meetings, focus groups or interviews are preferred. These surveys and meetings should be repeated as the project progresses to monitor the evolution of the public opinion. However, the appropriate use of public attitudes together with pre-screening has not been well-researched; thus, we consider it an avenue for further study.

3.2. Existing Pre-Screening Tools

In the early stages of EGS projects, especially when available data are limited, diagnostic methods are often used for pre-screening seismic risks.

Notably, five pre-screening tools were developed for EGS or geothermal projects in general (Table 2):

1. E. Majer et al. (2012) proposed the first pre-screening process for EGS projects. This process focuses on analyzing ground shaking and exposure from the average expected induced seismicity and the “worst case” scenario (e.g., Wong et al., 2023). In E. Majer et al. (2012), the worst case and the risk boundaries are not defined and are expected to be judged by experts.
2. Quick-Scan is the first diagnostic tool developed by Baisch et al. (2016) for deep geothermal in the Netherlands. It has scores defined over geological/tectonic and operational parameters for induced seismicity potential. Thus, it only focuses on the seismic source and leaves the seismic risks to be estimated in a quantitative SHRA. This tool was particularly designed within a risk assessment framework for the geological conditions in the Netherlands (Baisch et al., 2016).
3. Geothermal Risk of Induced Seismicity Diagnosis (GRID), a diagnostic tool developed by Trutnevyte and Wiemer (2017) for geothermal activities specifically in Switzerland. Instead of focusing on a specific component of the seismic risks, GRID takes all components of SRA and adds social attitudes to define a LoC. A risk-matrix approach is then applied to these concerns to determine the concern categories.
4. Ineris and BRGM (2023) developed a decision tree tool to pre-screen the potential hazard level at geothermal projects. Similar to Quick-Scan, this tool focuses on induced seismicity potential from geological/tectonic and operational parameters. Specifically, it is designed to perform a first order hazard evaluation alongside the timeline of the project phases.

Other approaches, using statistical learning (van Eijs et al., 2006) or machine learning (Pawley et al., 2018) methods to assess the likelihood of encountering induced seismicity might also be used for the purpose of pre-screening the seismicity potential. Alternatively, geomechanical simulations to assess critical slip (Walsh & Zoback, 2016), when fault geometry and in situ stresses are known, have also been used for pre-screening purposes. These tools approach subsets of the pre-screening problem. With the development of EGSs, more data will become available, and as research into induced seismicity advances, more sophisticated tools will likely be developed.

3.3. How to Conduct the Pre-Screening

The implementation of pre-screening does not have an established scientific consensus. With time, new pre-screening tools will likely develop, and more sophisticated tools will be available. In the current stage, we recommend the risk pre-screening to be conducted with good confidence over the main factors: geological/tectonic and operation factors, exposure, and data quality, while taking public attitude and concern as an additional measure.

3.3.1. Referring to Previous Projects

Existing projects play a significant role in planning future projects, both societally and scientifically. Social reactions built from previous projects strongly influence the residents' attitudes. Knowledge of geology and of the relationship between operations and seismicity learned from previous projects are beneficial to guide the site-selection and operations design and also seismic risk assessments. Thus, it is important to refer to previous successful/unsuccessful projects during the pre-screening. When available, a project's pre-screening results should be compared against past projects' LoC and seismic response.

3.3.2. Iteratively Updating the Pre-Screening

Given the empirical nature of risk pre-screenings, they should be updated as soon as new knowledge has been gained. If the operational parameters have changed substantially during the project (e.g., deviated well crosses a fault, while a vertical well not crossing a known fault was the initial plan), or new geological/tectonic data (new faults are found during drilling) are available, the LoC should be re-evaluated.

As discussed in Section 3.1, geological/tectonic, operational, and exposure data are all crucial for performing reliable pre-screening. If data quality is poor enough to identify knowledge gaps (Section 3.1.4), it may be required to collect additional data. In case of data limitations, D&R (Module 2) could be implemented.

3.4. Data Acquisition and Research for Pre-Screening

When existing data cannot confidently appraise the LoC via pre-screening, Module 2 (D&R) should be implemented. The intention of this additional D&R would be to fill gaps in subsurface understanding needed to accurately appraise LoC. As the specifics of D&R will be site dependent, it would likely involve consulting the independent experts or vendors. Examples of additional D&R could include: (a) acquiring new field data (e.g., 2D/3D seismic, geological mapping) or re-processing and re-interpreting achieved geophysical data with state-of-the-art imaging methods to improve fault maps or site amplification maps; (b) Re-processing existing seismological data with template matching or machine learning methods to improve earthquake catalog; (c) conducting numerical simulation to study stress changes on existing faults, due to escalating fluid pressure or decreasing formation temperature.

4. Seismic Hazard and Risk Analysis (Module 4)

For projects whose LoC falls into the “high” risk category, the operator is instructed to conduct or commission a comprehensive site-specific analysis to better assess the seismic risk related to the stimulation activities at the EGS site (Module 4; Comprehensive Seismic Risk Assessment). The analysis should be reviewed by an independent expert group (on behalf of the regulator). In the end, the responsibility for the accuracy of the results should fall on the operator. The results of the SHRA supersede those acquired during the pre-screening (Module 1; Section 3).

Seismic hazard analysis (SHA) forecasts earthquake-caused ground shaking for a target location or region (Baker et al., 2021). SHA is typically divided into so-called deterministic (DSHA) and probabilistic (PSHA) approaches (Box 4). The primary difference is related to the treatment of the uncertainty behind the seismic source. Both approaches can consider the uncertainties behind the ground motion propagation (including site-effects) and eventually produce a probability of exceeding a certain ground shaking level. Notably, DSHA results in a seemingly narrower range of uncertainty, by masking the epistemic and aleatory uncertainties related to the seismic source. The two approaches can be used on their own, or they may be used together to provide complementary information of varying complexity for decision making.

Box 4. Deterministic Versus Probabilistic SHA.

Assuming identical ground motion modeling and rupture placement (near the injection point), DSHAs that assume the "maximum possible" magnitude as the earthquake scenario will always be more conservative than PSHAs, which also assign probabilities to smaller magnitudes. In that sense, if the seismic risk from such a DSHA is tolerable, then there is no need to conduct a more complex PSHA. However, DSHAs that adopt as "maximum credible" earthquake (maximum credible earthquake (MCE)) a magnitude smaller than the "absolute maximum" adopted by the PSHA may or may not be more conservative. In modern times, the probabilistic approach (PSHA) has prevailed, with very few exceptions (Bommer, 2022), and this is why we generally suggest it, especially when the data collection process enables it. PSHA has been used by the United States Geological Survey to produce 1-year hazard maps in areas with induced seismicity (e.g., Petersen et al., 2016), and by Convertito et al. (2012) and Bourne et al. (2015) to assess the time-dependent seismic hazard due to geothermal operations and fluid extraction, respectively. Several studies have gone one step further performing seismic risk assessment of varying complexity for the Groningen gas field (Crowley et al., 2019; van Elk et al., 2019), for an Enhanced Geothermal System in Basel (Mignan et al., 2015), for a HF sequence in the UK (Edwards et al., 2021) and for large-scale wastewater-disposal activities in Oklahoma (Grigoratos et al., 2021; Gupta & Baker, 2019).

Next, the seismic vulnerability analysis (SVA; Section 4.5) deals with the undesirable consequences of ground shaking, which include nuisance, personal injury, physical structural and non-structural damage to buildings and infrastructure, interruption of business and social activities, and the direct and indirect costs associated with such outcomes (Bommer, 2022). Seismic risk analysis combines SHA and SVA to quantify the probability of a certain level of loss being exceeded.

The SHRA may be performed prior to any reservoir stimulation taking place or after one or more stimulations have already occurred. As new local data are collected, the SHRA can undergo iterative updates on an ongoing basis. Obviously, the more local seismological and hydromechanical data are available, the more constrained the uncertainty behind the results will be.

When compared to the pre-screening (Module 1; Section 3), the SHRA is expected to require additional data to be collected, and a much more rigorous analytical process that includes the construction of a seismic risk model (Bommer, 2022; McGuire, 2004), as well as complex calculations that will likely require dedicated software packages (Pagani et al., 2014). Input data might include regional historical earthquake catalogs and strong-motion data, fault geometry, local stress field, hydraulic input of planned stimulations, portfolio of regional structures, population distribution, and regional site conditions.

Goals of the SHRA

1. To provide a comprehensive estimation of the expected seismic risk, using a more sophisticated approach compared to the pre-screening tools.
2. To demonstrate the range of uncertainty behind the modeled results, using tailored quantitative methods.
3. To inform cost-benefit analyses—allowing stakeholders to decide whether a project should start, continue, or acquire (additional) earthquake insurance.
4. To aid risk mitigation plans by informing the parametrization of the TLP.

Recommendations for the SHRA

1. The SHRA is the responsibility of the operator. It should be reviewed by an independent group of experts. The operator should accommodate any data requests and remain liable for its conclusions.
2. The SHRA should be based on established state-of-the-art models, with justification for their selection.
3. The SHRA needs to be updated when important new local data is acquired.
4. The analysis should cover multiple risk metrics, including population nuisance, structural damages, and personal injuries.

5. If the project is to be permitted, the SHRA results, methods, and data should be released in advance for public review.

The SHRA will most likely require a dedicated software engine to perform the calculations. We suggest using the OpenQuake engine (Pagani et al., 2014; Silva et al., 2014) for the hazard and risk calculations, which is a well-established and continuously supported open-source product of the Global Earthquake Model (GEM). Alternatives include OOFIMS (Franchin, 2014), SELENA (Molina et al., 2010), CARPA (ERN-AI, 2020), RiskScape (Paulik et al., 2023) or EQRM (Robinson et al., 2005). For a review of the available seismic risk engines see Hosseinpour et al. (2021). Finally, for hazard-only calculations one could use OpenSHA (Field et al., 2003), R-CRISIS (Ordaz et al., 2021), or REASSESS (Chioccarelli et al., 2019).

4.1. General Framework

Here, we outline the framework for performing a SHRA. A SHRA model for an EGS site should include the following components:

(a) a seismic source model, namely a set of one or multiple possible ruptures of specified sizes and hypocenters. In the case of PSHA, the rupture set is paired with corresponding probabilities of occurrence.
(b) a Ground Shaking Intensity Model (GSIM), estimating the spatial distribution of ground shaking levels given a certain earthquake magnitude, focal mechanism, and depth.
(c) a site-amplification model, capturing the effects of site conditions on ground motions.
(d) an exposure data set, containing the relevant assets that may be affected (e.g., structures, contents, people, roads).
(e) structure-specific fragility curves, capturing the structural or non-structural damages expected, given various levels of shaking.
(f) structure-specific consequence curves, capturing the direct or indirect economic, human or social losses, given various levels of damage.

The model components should be deemed applicable to the EGS location in question. A logic tree structure (Bommer & Scherbaum, 2008) that includes various models for each component is needed, unless a specific model can be validated against regional data. Logic trees are considered as the state-of-the-art tool to quantify and incorporate epistemic uncertainty which is the uncertainty related to the lack of knowledge (Abrahamson & Bommer, 2005; McGuire, 2004). Creating a logic tree involves selecting alternative models or model parameters for various components and then assigning weights to the different branches at each node to reflect (in a probabilistic way) the degree-of-belief of the analyst in each option (Bommer, 2012; Scherbaum & Kuehn, 2011). Crucially, the different models must be mutually exclusive and collectively exhaustive. Logic tree branching levels (Figure 2) are common for the Gutenberg-Richter (GR) parameters, the maximum magnitude, the GSIMs, and, in some cases, for the vulnerability curves. That said, the complexity of the structure of a logic tree can increase exponentially (Bommer, 2022). In the end, each branch of the logic tree is computed as a separate model-realization and taken into account based on its corresponding aggregate weight. More details about the computational mechanics are summarized in Box 5.

4.2. Seismic Source

Defining the characteristics of the seismic source is a very challenging and highly uncertain task of seismic risk modeling. This remains true for EGS projects, especially in terms of activity rates and magnitude range. Here, we attempt to introduce the key modeling parameters that need to be constrained, listing possible methods for their estimation, with future research expected to provide further implementation details.

In DHSA, the seismic source for an EGS stimulation is usually defined as:

1. one hypocenter that can form a rupture zone of a given aspect ratio and focal mechanism.
2. a fixed magnitude scenario.

In PHSA, the seismic source for an EGS stimulation can be defined as:

1. one or more hypocenters that can form rupture zones of a given aspect ratio following certain focal mechanisms.
2. a probability distribution for the magnitudes of each hypocenter, bounded by a maximum magnitude.

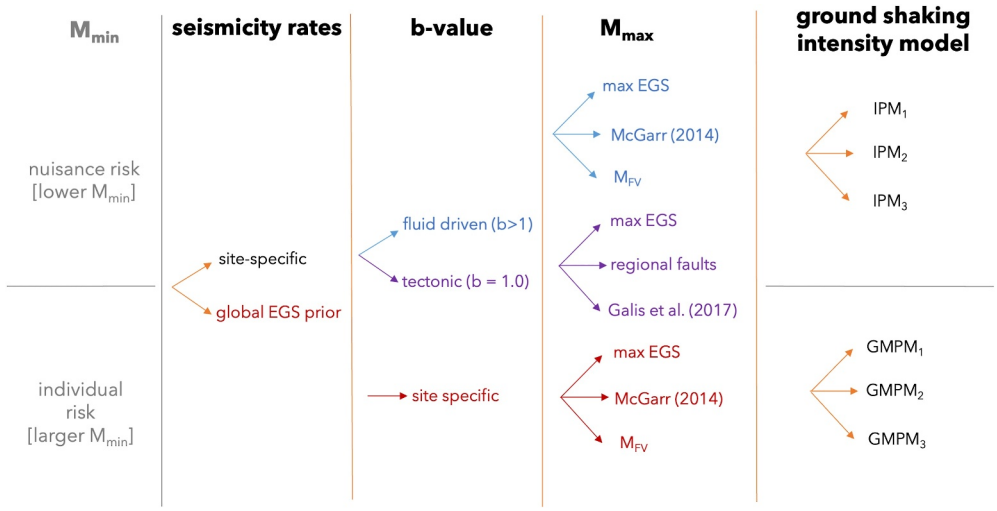

Figure 2. Illustrative example of a PSHA logic tree with four branching levels (weights not shown). The term "max EGS" represents the maximum recorded event at any Enhanced Geothermal Systems (EGS) site (currently M_W 5.5), while the term M_{FV} refers to the "lower bound" (finite volume) formulation in Shapiro et al. (2013). Intensity Prediction Model (IPM) stands for IPM and Ground Motion Prediction Model (GMPM) stands for GMPM. The term "global EGS prior" refers to an empirical model calibrated on past EGS data sets.

For EGS sites, the hypocenter of the seismic source is more or less known, since it is assumed/expected to be very close to the stimulation zone (less than 2 km away; Grigoratos et al., 2022; Zang et al., 2014)—analogous to observations of induced seismicity from hydrocarbon hydraulic fracturing (Schultz, Skoumal, et al., 2020). During circulation, the nucleation zone might be slightly further away. Furthermore, the focal mechanism can be potentially inferred from the local stress regime. The rest of the seismic source parameters, for example, the potential magnitudes and their frequency, are very difficult to meaningfully constrain before any local stimulation data are collected.

For EGS sites, the deterministic approach (DSHA) assumes a single (scenario) rupture with a predefined focal mechanism of the MCE, which is the largest magnitude reasonably expected during the human activities in

Box 5. Computational Framework of a SHRA.

For each simulated rupture many random fields of ground motion intensity measures (IMs) are generated (Kohrangi et al., 2016). The random fields are then used as input to the fragility model to estimate the damage severity that any given structure may suffer when subject to the predicted level of IM (Crowley & Bommer, 2006). Next, for each rupture and IM random field, the loss for the entire affected portfolio of structures is estimated by simply summing the losses predicted for each structure (given its damage state and value) in the footprint of the random field. This procedure is repeated for all random fields of each simulated rupture. Finally, the rate of exceeding any portfolio loss is empirically found by keeping track of the number of exceedances occurring over all the simulated realizations. This general approach to estimate earthquake risk to portfolios of structures at a regional level still holds for the case of induced seismicity, but given the peculiarities of the phenomenon, some modifications may be appropriate, especially in order to ensure that the traditional Poissonian recurrence models are valid (Grigoratos et al., 2021; Gupta & Baker, 2019). This approach also allows for implementation of spatial correlation between ground shaking at multiple sites from the same earthquake (Jayaram & Baker, 2009), due to common source and wave traveling paths and to similar distance to fault asperities. Incorporating spatial correlations improves the reliability of the risk estimates when dealing with spatially distributed structural portfolios (Park et al., 2007). This computational framework has been described further in Grigoratos et al. (2021).

Box 6. Methods for Computing the *b*-value.

The *b*-value should be computed following maximum likelihood methods such as Weichert (1980) or the ones outlined in Marzocchi and Sandri (2003). Least-squares fitting is usually not an appropriate regression method (Sandri & Marzocchi, 2007). Resampling to account for measurement/conversion uncertainties behind the cataloged magnitudes is strongly encouraged (Kwiatek et al., 2024; Taroni, 2022). The default magnitude binning interval should be 0.1 units (Marzocchi et al., 2020). A crucial step for the estimation of the *b*-value is the determination of the magnitude of completeness (Mc). The latter is the magnitude above which the overwhelming majority of earthquakes are reported in the available catalog. Small changes in the Mc can lead to impactful variations in the *b*-value, and thus to the hazard and risk. Examples of misrepresentations of Mc due to spatiotemporal variations in the performance of the seismic network can be found in Mignan (2012). The Mc could be estimated using more than one of the methods outlined in Zhou et al. (2018). If the *b*-value derived from traditional methods (Marzocchi & Sandri, 2003) differs by more than 0.2 units from the *b*-value derived following van der Elst (2021), then perhaps further sensitivity analysis is required.

question. This magnitude is selected based on historical seismicity, geological/tectonic considerations, and expert judgment (Bommer, 2002); MCE is usually smaller than the largest possible magnitude (M_{max}; Section 4.2.2), because it conceptually represents a finite return period.

4.2.1. Seismicity Rate Parameters

The PSHA takes into account numerous potential ruptures (of different sizes and potentially focal mechanisms) and their estimated probabilities of occurrence. This approach is expressed by a magnitude-frequency distribution, double-truncated by the minimum (Section 4.7) and maximum magnitude (Section 4.3). The most widely used magnitude-frequency distribution is the Gutenberg-Richter curve (Gutenberg & Richter, 1944), which has two parameters, the *a-value* (total rate of events above *M*0 in log10 scale) and the *b*-value (log-linear slope of the seismicity rate with magnitude). The *b*-value depends mainly on the local stress conditions and on the interconnectivity of the fracture network. Although hydraulic stimulation can alter both of these variables, the *b*-value is usually considered static, as far as the SHA calculations are concerned. During fluid injection operations, the *a-value* is often linked to the pressurization rate via a factor of proportionality (FoP), which is a proxy for how susceptible fault-stability is to pore-pressure changes (Grigoratos et al., 2022; Schultz et al., 2018; Shapiro et al., 2010). If a hydromechanical model is not available, the injection rate may be used as a proxy for the pressurization rate, as long as the latter is not decreasing (Shapiro, 2015).

Notably, the seismicity often continues even after the injection operations have ceased. The decaying seismicity rate after the injection rate has dropped significantly or is zero, can be modeled with a modified Omori law (Langenbruch & Shapiro, 2010; Schultz, Ellsworth, & Beroza, 2023). Even though the vast majority of events usually occur during the stimulation (Schultz, Ellsworth, & Beroza, 2022), the magnitudes of the trailing seismicity (after shut-in) can be relatively large or even the largest ones (Verdon & Bommer, 2020).

Even though the *a-value* fluctuates during a stimulation, for the purposes of the PSHA, it is taken as a static variable, expressed in cumulative terms. Its estimation is very difficult and requires local seismological and hydraulic data from past stimulations. The seismic response of the reservoir to future hydraulic input has to be calibrated using either statistical approaches (e.g., Shapiro, 2015) or physics-based hydromechanical numerical methods (e.g., Baisch et al., 2010; McClure & Horne, 2011). The former relies on crude assumptions for the underlying physics, while the latter requires several poorly constrained hydromechanical parameters and complex mathematical frameworks.

As far as the *b*-value is concerned, a local earthquake catalog is needed for calibration (Box 6). Even if that is feasible, *b*-values cannot be applied with confidence outside the magnitude range of their calibration. Furthermore, at moderate (above 4) or large magnitudes (above 6) the *b*-value will likely converge to the global (tectonic) average of 1.0 (Bell et al., 2013; Michael, 2014; Navas-Portella et al., 2019), given that the rupture is so extensive

Box 7. Largest Observed Magnitudes.

To date, the largest magnitude earthquakes linked to hydraulic fracturing stimulations for EGS projects are the M_W 5.5 Pohang, South Korea event (Ellsworth et al., 2019) and the M_W 3.7 Berlín, El Salvador event (Kwiatek et al., 2014). The largest magnitude decisively confirmed to be linked to hydraulic fracturing stimulations for oil and gas activities is smaller, M_W 4.6 in the Western Canada Sedimentary Basin (Atkinson et al., 2016; Mahani et al., 2017; Schultz et al., 2017). Larger hydraulic fracturing events (up to M_W 5.4) have been reported in the Sichuan Basin of China (Lei et al., 2017, 2019a; Zhao et al., 2023), although some of these cases are less conclusive because of data availability or other confounding long-term operations (Lei et al., 2019b; Sun et al., 2017). Seismicity during the production (circulation) phase of a geothermal project has reached magnitudes up to M_W 5.0 in the Geysers (Boyd et al., 2018; E. L. Majer & Peterson, 2007). Finally, a seismic swarm with magnitudes up to M5.4 in the North Brawley might have been triggered by aseismic slip originating from shallower geothermal wells (Im & Avouac, 2021).

that it has propagated outside the (limited) pore-pressure perturbed zone, along tectonically stressed faults. The *b*-value might also be affected by variations in the stress state within the injection/extraction zone (e.g., Cesca et al., 2014; Maxwell et al., 2009) or if a new fault is encountered (Zhang et al., 2022). For these reasons, we suggest either adopting magnitude-dependent *b*-values or including a branching level for the *b*-value in the logic tree, with equal weighting assigned to the locally calibrated *b*-value and the global average of 1.0 (Petersen et al., 2016).

If the SHRA is required prior to the first stimulation at the site, when no local data are available, both the MCE and the magnitude-frequency distribution are extremely uncertain variables, with very large influence on the final risk estimates. One way of tackling this problem is to assume that the site will respond in line with other global EGS stimulation for which the relevant parameters (MCE or FoP, *b*-value, and decay rate) are obtainable. All other EGS stimulations can be weighted based on how similar they are to the one in question. For example, the criteria could be depth, temperature gradient, lithology, average hourly fluid volume, injection protocol (monotonic, cyclical), or the ratio between the local Seismogenic Index (Shapiro et al., 2010) and the *b*-value.

4.2.2. Maximum Possible Magnitude

Any EGS-related SHA is bounded by the maximum possible magnitude (M_{max}) assigned to the stimulation under investigation. Note, that our definition of M_{max} is not (an estimate) of the largest observed earthquake, but rather the largest magnitude that this seismic source could accommodate. The M_{max} might be limited either due to tectonic constraints or due to the limited scope of the anthropogenic operations. Below we outline certain considerations that might inform the estimation of M_{max}. That said, this is a topic of ongoing research and debate. Thus, resorting, at least to a certain degree, to expert judgment might be an unavoidable outcome. In that case, a logic tree structure for the M_{max} might be an appropriate expression of the elevated uncertainty levels.

For stimulation-induced seismicity, assuming no runaway ruptures (i.e., self-sustaining outwards propagation via tectonic strain), M_{max} may be limited by the size of the rock volume perturbed by pore pressure (Shapiro et al., 2013) or the total injected fluid volume (Galis et al., 2017; McGarr, 2014). The method by Shapiro et al. (2013) requires data from at least one local stimulation, while Galis et al. (2017) require as input four geomechanical properties of the reservoir (bulk modulus of the reservoir rock, reservoir thickness, dynamic friction coefficient, background stress drop). The method of McGarr (2014) is the easiest to apply, but is also the least site-specific. All three methods use as input the total injected fluid volume (Box 8).

For tectonic seismicity and runaway induced ruptures, M_{max} is usually dictated by the size and interconnectivity of the local fault network and the expected stress drop (Box 7). The calculation employs empirical fault-scaling relations (e.g., Leonard, 2014) that infer the magnitude of an earthquake given the geometry and focal mechanism of a given rupture. Notably, these empirical relations have been derived from moderate to large magnitude earthquakes, with deeper hypocenters than the ones expected at EGS sites. Therefore, it is likely that the relations

Box 8. Available Equations to Calculate the M_{max} of Induced Earthquakes.

McGarr (2014) proposed a simple formula to compute an upper bound for the cumulative seismic moment that can be released during a fluid-induced earthquake sequence.

$$\Sigma M_0 = 2 * G * \Delta V \tag{1}$$

where G is the shear modulus, often assumed equal to 30 GPa, and ΔV is the net total injected fluid volume. The approach is based on volumetric changes inducing seismic slip in a linear fashion. It assumes that, on average, each fault patch is about half a seismic stress drop below the yield stress and so it only takes half as much stress change imposed by the volumetric change to induce seismic slip.

Assuming a *G-R* relation, one can employ the *b*-value to convert this cumulative seismic moment into a single maximum magnitude, which is given by:

$$M_0^{\max} = \frac{1-B}{B}\frac{2\mu\,(3\lambda+2G)}{3}\Delta V \tag{2}$$

where $B = 2b/3$. Assuming $\lambda = G$ and $\mu = 0.6$ this leads to:

$$M_0^{\max} = G * \Delta V \tag{3}$$

Then, the corresponding moment magnitude can be derived as:

$$M_W^{\max} = \frac{2}{3}\log_{10}\left(M_0^{\max}\right) - 6.033 \tag{4}$$

Galis et al. (2017) proposed an estimate for the maximum moment $M_0^{\max}$ that can be released during an arrested rupture based on the notion that such rupture is controlled by a competition between two sources of elastic energy: injection-induced fluid pressure and tectonic prestress. The contributions of these two sources are both positive. However, the energy contributed by injection-induced fluid pressure decays with increasing rupture size, whereas the energy contributed by tectonic prestress increases, thereby creating a trade-off between these two strain-energy sources. At the maximum arrest size, both contributions are comparable. The value of $M_0^{\max}$ is dependent on the total net injected volume ΔV with an exponent of 3/2 (instead of 1 for McGarr, 2014). The rest of the formulation includes various geomechanical parameters related to the target-reservoir that can be combined in a single parameter γ:

$$M_0^{\max} = \gamma * \Delta V^{3/2} \tag{5}$$

Galis et al. (2017) demonstrated that assuming $b = 1$, $\Sigma = 2/3\log_{10}\gamma - 6.07$, and at every time-iteration i, Σ is equal to Shapiro et al. (2010):

$$\Sigma_\gamma(i) = \log_{10}\left(\frac{N(i)}{10^{(-M_c)}\Delta V(i)}\right) \tag{6}$$

where N is the total number of events above Mc.

The so-called "lower-bound" formulation of Shapiro et al. (2013) assumed that a rupture can nucleate only within the stimulated rock-volume and cannot propagate outside of it. This applies a geometrical constraint on the 3D size of any rupture. As a proxy for the stimulated rock-volume one can fit an ellipsoid around the evolving seismicity cloud, to represent the expanding triggering front during pore-pressure diffusion. If the stimulation has not yet started, the evolving perturbed volume could be simulated using hydromechanical models. The formulation results in a maximum magnitude equal to:

$$M^{\max,L} = \log_{10}L^2 + \frac{2}{3}\left(\log_{10}\Delta\sigma - \log_{10}C\right) - 6.07 \tag{7}$$

where L denotes a characteristic scale of the stimulated volume (in meters), $\Delta\sigma$ is a static stress drop, and C is a geometrical constant close to 1. If $L_{\min} < L_{\text{int}} < L_{\max}$, Shapiro et al. (2013) found that:

$$L = \left[\frac{1}{3}\left(1/L_{\min}^3 + 1/L_{\text{int}}^3 + 1/L_{\max}^3\right)\right]^{-1/3} \quad (8)$$

often provides a good estimate of the characteristic scale. The values for $L_{\min}$, L_{int}, $L_{\max}$ are the principal axes of the fitted ellipsoid, while $\Delta\sigma$, Σ, and b are derived jointly using grid-search maximum likelihood regression, following the Poisson assumption.

overestimate the magnitude of small and/or shallow faults (Grigoratos et al., 2021). Alternatively, numerical simulations could be used to infer $M_{\max}$; for example, by combining physical understanding of dynamic fault slip and geological knowledge of the fault (e.g., Wentinck & Kortekaas, 2023). Notably, if the stimulation zone is within the shallow sedimentary cover, large-magnitude events (e.g., above magnitude 6) are arguably less likely (Bommer & Verdon, 2024). This is because these sedimentary layers tend to have lower stress drops (due to lower stiffness and frictional strength) and fewer and shorter faults (due to younger formation age). Furthermore, in general, shallow hypocenters (e.g., depth below 5 km) rarely produce large ruptures given that this would likely require rupture-propagation downwards into the crust, against increasing frictional strength and confining stress (Bommer & Verdon, 2024).

4.3. Ground Shaking Intensity

The primary predictor variables for the spatial distribution of ground motion are usually: magnitude, distance to the rupture, and site conditions (Boore et al., 1997). Additional variables may be included, such as style of faulting, depth to top of the rupture, depth to a velocity of 1 km/s, or others (Gerstenberger et al., 2020). Some Ground Motion Prediction Models (GMPMs) may incorporate additional constraints from physics-based simulations of ground shaking data. Usually, the output variables of a GMPM are spectral accelerations (SA) at different periods (e.g., 0.01–10 s), peak ground velocity (PGV), peak ground acceleration (PGA) or Arias intensity. A GMPM outputs a (log-normal) distributions of values, represented by the median and the logarithmic standard deviation. The distributions are usually truncated at three standard deviations (Strasser et al., 2008).

Applicable GMPM should have been calibrated with earthquake data compatible with the selected $M_{\min}$ (Section 4.6) and $M_{\max}$ values for the SHRA (Grigoratos et al., 2023; Box 9). They should also be compatible with the tectonic regime and focal depth of the site. Hybrid GMPM that combine recorded ground-motion data with 3D representations of Earth's structure in conjunction with dynamic kinematic representations of the earthquake source are also a viable alternative (e.g., Edwards et al., 2018). Site-specific GMPM should be derived when rich seismic data sets (both in terms of sample size and magnitude range) are available.

It is important to point out that ground motion estimates are very sensitive to the stress parameter assigned to the source (Baltay et al., 2013; Edwards & Fäh, 2013; Trugman & Shearer, 2018). This stress parameter is often informed by the measured stress drops at the site. Here, we should caveat that stress drop measurements can be highly uncertain due to factors such as data quality, source model assumptions, methodology, path/site effects, or instrumental response (Baltay et al., 2024). Overall, induced earthquakes do not appear to have significantly different stress drop than tectonic ones (Huang et al., 2017; Yu et al., 2020). That said, an inverse relationship between stress drop and proximity to the stimulation might exist at close (<2 km) distances (Goertz-Allmann et al., 2011; Kwiatek et al., 2014; Yu et al., 2020). Stress drops also depend on the focal mechanism (Allmann & Shearer, 2009; Hauksson, 2015; Oth, 2013), on the local lithology (Goebel et al., 2015), formation age (Bommer & Verdon, 2024), on the rate of tectonic deformation (Hauksson, 2015; Goebel et al., 2015), and likely increase with magnitude until magnitude values around 4 (Edwards & Fäh, 2013; Trugman et al., 2017). There is no scientific consensus on whether stress drop increases with depth; some studies favor this observation (Goebel et al., 2015; Oth, 2013; Trugman et al., 2017; Walter et al., 2017), while others do not (Abercrombie et al., 2021; Allmann & Shearer, 2009; Clerc et al., 2016; Hauksson, 2015; Jeong et al., 2021; Q. Wu et al., 2018). Notably, significantly lower stress drops tend to be observed in geothermal (Hauksson, 2015) and volcanic (Oth, 2013) areas, either due to high temperatures or due to the presence of fluids.

The variability in the near-surface geology is well known to have a strong influence on the level of amplification of seismic ground motion during an earthquake. The presence of low seismic velocity sediments overlying stiffer

Box 9. Examples of GMPMs and Treatment of Uncertainty.

GMPMs are inherently limited by the scarcity of data related to large shaking amplitudes, and/or near-source recordings. This is particularly challenging for stable continental regions, where low seismicity rates and typically sparse seismic networks exacerbate the lack of data (Gerstenberger et al., 2020). As far as induced events are concerned, due to their triggering process, they are likely to be of smaller magnitude and at shallower focal depth than typical tectonic earthquakes (Grigoratos et al., 2021). The focal depths of potentially induced events generally lie within the upper 6 km of the crust, making the seismic wave propagation more dependent on the heterogeneous properties of the uppermost crustal layers (Bommer et al., 2016).

To address these issues, several studies have developed region- or even sequence-specific GMPM for induced seismicity (Atkinson, 2015). Here, we exclude cases of mining-induced seismicity. Novakovic et al. (2018) and Zalachoris and Rathje (2019) developed GMPMs for Oklahoma (USA); Douglas et al. (2013) for low-magnitude earthquakes from geothermal areas in Europe; Sharma et al. (2013) for the Geysers Geothermal Area (USA), Edwards et al. (2018) for the Basel sequence (Switzerland), Sharma et al. (2022) for the St. Gallen sequence (Switzerland), and Cremen et al. (2020) for the Preston New Road HF sequence (UK). Finally, there are several GMPMs related to fluid-extraction based on the Groningen data (Bommer et al., 2016, 2017; Bommer, Edwards, et al., 2022; Bommer, Stafford, et al., 2022; Paolucci et al., 2020).

Notably, when Cremen et al. (2020) tested the model by Douglas et al. (2013) against the Preston New Road data, the fit was not satisfactory despite the broad similarities in magnitude range, focal depth, and tectonic setting. Furthermore, Grigoratos et al. (2021) demonstrated that even relations developed from similar data sets can exhibit very different attenuation functions. Therefore, it is very difficult to confidently select a GMPM unless it can be re-calibrated or at least tested against local data (Bommer & Stafford, 2020).

To deal with uncertainties, it is common practice to combine multiple GMPMs via logic trees. As explained in Gerstenberger et al. (2020), in practice, this approach begins with the selection of suitable GMPMs by first applying a criteria of quality assurance (Bommer et al., 2010; Cotton et al., 2006). Next, performance tests of the GMPMs with respect to a data set provide quantitative ranking of the models (e.g., Scherbaum et al., 2009). Sensitivity analyses and expert elicitation (e.g., Delavaud et al., 2012) can provide a final logic tree structure for GMPMs. That said, recent studies (e.g., Mak et al., 2017) have highlighted the inconsistency of a pure data-driven approach, in particular with a lack of independency of the data or incomplete (or biased) data sets that may favor one model over another.

Beyond the use of multiple GMPMs, the scaled backbone approach (Atkinson & Adams, 2013; Atkinson et al., 2014; Bommer, 2012; Douglas, 2018) provides an alternative for handling the wide range of uncertainties. In this approach, one GMPM is typically used to generalize the attenuation and magnitude- scaling behavior required for a specific tectonic region type for a range of magnitudes and distances. As explained in Boore et al. (2022), the selected backbone model is first adjusted to match the earthquake source and path characteristics of the target region, and then it is separately adjusted to account for the site- specific geotechnical profile. For a GMPM to be amenable to such host-to-target adjustments, the magnitude scaling of response spectral ordinates should be consistent with the theoretical scaling of Fourier amplitude spectra. In addition, the influence of individual source and path parameters should be clearly distinguished in the model to allow the adjustments to be applied individually, and reliable estimates of the source and path parameters from the host region of the GMPM should be available, as should a reference rock profile for the model. Using data analysis and judgment, upper and lower alternatives about the central GMPM are defined to capture the epistemic uncertainty of a representative suite of published GMPMs. A referenced backbone model allows tuning the size of the alternative branches while preserving statistical independence of the newly predictive models. This approach is gaining ground in recent years and its implementation details are outlined in Boore et al. (2022).

bedrock, especially near the surface, modifies earthquake ground motions by affecting amplitudes and frequency content. This phenomenon is referred to as seismic site response or site effects and is critical when assessing seismic hazard levels in a given area. It is usually dealt with by GMPMs in a crude way, using scaling based on the V_{S30} parameter. Site-specific site-amplification factors would be ideal (van Ginkel et al., 2022), if there is enough data to derive them.

Intensity Prediction Models (IPMs) have been developed to estimate Intensity Scales (e.g., modified Mercalli intensity (MMI)) for a given set of earthquake magnitudes and site distances. Unlike other IMs such as SAs or PGA, MMI depends solely on observations, such as felt intensities and structural damage (Wood & Neumann, 1931). Due to their simplified functional form, it is challenging to pair IPMs with specific site amplification models or focal

Box 10. Examples of IPMs.

Popular IPMs have been developed by Atkinson and Wald (2007), later revised by Atkinson et al. (2014), focusing on North American data above *M*3. Allen et al. (2012) developed a globally applicable IPM based on earthquakes with $M_w > 5$ for active crustal regions. Ahmadzadeh et al. (2020) developed an IPM for Iran, Le Goff et al. (2014) one for Portugal, Baumont et al. (2018) one for France and Dowrick and Rhoades (2005) one for New Zealand. None of the aforementioned IPMs is designed for very shallow small-magnitude earthquakes. A better fit would be the IPM by Teng et al. (2022), which is based on likely-induced earthquakes related to wastewater disposal in Texas, Oklahoma and Kansas, with magnitudes between *M*1.5 and 3.5 and hypocentral distances within 30 km. Alternatively, one could compute PGV or PGA estimates using an applicable GMPM, and then convert those to MMI using the conversion-relations of Schultz, Quitoriano, et al. (2021), originally derived for Central and Eastern US. That said, doubling the number of conversion-steps increases the uncertainty of the final output considerably.

mechanisms. Therefore, the data set used in their regression is a key factor for their applicability (Box 10). They also require fragility models that are explicitly developed for IPMs, to be paired with a certain exposure model.

4.4. Exposure

When conducting any type of SRA, it is important to understand which assets are exposed to the seismic hazard. These assets can be, for example, residential or industrial buildings, special buildings (e.g., schools, hospitals), roads, or critical infrastructure (e.g., bridges, pipelines, energy plants, dams, ports). Each asset has its own fragility against seismic loads and its own replacement cost. Individuals are also exposed entities, although their vulnerability is dependent on the structure they reside in at the time of the earthquake. These assets are aggregated at different spatial resolutions depending on data-availability. Notably, the spatial resolution itself can have an impact on the loss estimates (Dabbeek et al., 2021).

The buildings in the exposure model are classified according to their seismic performance using a building taxonomy that is based on national or international standards (e.g., the GEM Building Taxonomy, Brzev et al., 2013, as updated by Silva et al., 2018, 2022) that allows buildings to be classified according to a number of structural attributes. The main attributes that have been selected for the consistent definition of building classes are as follows:

- Main construction material (e.g., reinforced concrete, unreinforced masonry, reinforced/confined masonry, adobe, steel, timber).
- Lateral load resisting system (e.g., infilled frame, moment frame, wall, dual frame-wall system, flat slab/plate or waffle slab, post, and beam).
- Number of stories.
- Seismic design code level (pre-code, low, moderate, high).
- Lateral force coefficient used in the seismic design.

Each building is paired with a corresponding value for its structural elements (e.g., columns, slabs), non-structural elements (e.g., mechanical equipment, windows, cladding) and contents (e.g., furniture). The occupants of each building are also part of an exposure data set. Furthermore, special structures like bridges, dams, pipelines may also have their own, less standardized, taxonomy classes (FEMA, 2013; Pitilakis et al., 2014).

The SRA should take into account the entire relevant structural portfolio around the site. This can be ensured by including structures within at least a 100 km radius (Baker et al., 2021). Special considerations regarding dams, nuclear plants or other supercritical infrastructure may also be warranted. For both LoCs, the average number of people expected to experience felt seismicity within hundreds of kms (Schultz et al., 2021a) from the site during the stimulation and circulation phase of the EGS project should be evaluated. The impact radius of an earthquake

will depend on its magnitude, its focal depth, rupture propagation, fault geometry, and on the spatial distribution of the site conditions. For example, smaller or shallower expected maximum magnitudes might require smaller exposure distances. However, we caution that having to expand the exposure model if/when the assumed maximum magnitude is exceeded can be a time-consuming process at a critical decision-making moment.

Depending on the region, the exposure database could be compiled in an ad hoc fashion (e.g., from Census or government data). That said, a recent global compilation from GEM could also be utilized (Crowley et al., 2020; Yepes-Estrada et al., 2017, 2023), at least for the building data, if the lowest available spatial resolution meets the needs of the project. It contains information regarding structural and non-structural elements, contents and occupancy. We suggest adopting the lowest grid resolution possible, with indicative values ranging from 1 to 5 km (Papadopoulos et al., 2024).

4.5. Fragility and Vulnerability

According to the prevailing terminology, the terms fragility and vulnerability are similar but not identical, the former only captures physical damages, while the latter also captures the losses resulting from such damages. Any risk analysis assigns to each class of structure in its inventory a specific fragility (or vulnerability) curve that estimates the probabilistic distribution of damages (or losses) that this structure is expected to experience when subject to ground motions of different intensities. For the damages, modelers use standardized damage-states as labels, with typical cases being "light- damage", "significant damage", "heavy damage", and "collapse". The direct economic losses are measured in terms of loss ratio, which is defined as the ratio of cost of repair to cost of replacement. Other types of loss include population displacement, fatalities, or injuries. Indirect economic losses (such as business interruption or economic disruptions) are more difficult to model and are often neglected, even though they can be very important (Markhvida & Baker, 2023; Sousa et al., 2022). The IMs are usually related to the fundamental period of the structure (Silva et al., 2019), for example, 5% damped pseudospectral accelerations (SA) at 0.3s. That said, in recent years, more advanced IMs are gaining traction (Kohrangi et al., 2016).

Established sources of fragility and vulnerability models is GEM (Martins et al., 2021; Martins & Silva, 2020) and FEMA (FEMA, 2013), but there are numerous individual studies that have produced curves for specific structural typologies (e.g., Kallioras et al., 2019). Importantly, the adopted fragility curves should be compatible with the selected M_{min} and IM.

Notably, most fragility and vulnerability functions were developed for large (tectonic) events, at least larger than magnitude 5, and hence they might be biased toward higher loss estimates, compared to the short duration and high-frequency content of induced motions (Grigoratos et al., 2023). In general, these functions also ignore damage accumulation effects that might occur when buildings are subjected to a series of earthquakes (Papadopoulos et al., 2020). If more than one reliable fragility model is available for the exposed assets in question, a logic-tree approach can be applied there as well to capture the epistemic uncertainty. This implicitly assumes perfect damage-correlation over all assets, which might lead to skewed results.

4.6. Minimum Magnitude for Engineering Purposes

Notably, depending on the risk metric targeted by the analysis, there is a minimum magnitude (M_{min}), below which there is no engineering interest (Bommer & Crowley, 2017). In other words, the rupture is too short (in duration) or limited in frequency-content to cause any damage to the relevant structures, even at close distances. This M_{min} value represents the lower truncation of the magnitude-frequency distribution in the classical PSHA formulation. Furthermore, if the scenario earthquake adopted by the DSHA is lower than M_{min}, then no calculations are needed for the specific risk-metric in question.

Naturally, structural damages require a slightly larger M_{min} than non-structural damages, with the latter requiring a significantly larger M_{min} than nuisance calculations. When it comes to damages, the representative seismic design code level of the built environment plays a crucial role in determining a suitable M_{min} value. For example, the M_{min} value for structural damages in Groningen (no seismic code penetration) should be much lower than the one in Japan (very high seismic code and adoption levels).

Box 11. Minimum Magnitude Values.

M_{min} values linked to structural damages are to an extent typology-dependent; for example, an unreinforced-masonry building should be paired with a lower M_{min} than a reinforced-concrete wall building of similar height. Therefore, ideally one would use M_{min} values specific to both the taxonomy and the risk-metric, increasing considerably the complexity of the calculations for little real benefit. A more pragmatic approach assumes that a specific structural typology will dominate the risk metric results and chooses as M_{min} the value that corresponds to that typology.

Although exceptions may apply, typical indicative values for M_{min} are: 4 to 5 for structural damages (and fatalities), 3.5 to 4.5 for non-structural damages (Nievas et al., 2019) and 2 to 3 for nuisance estimates (Schultz, Quitoriano, et al., 2021). That said, in practice, for simplicity, a uniform M_{min} value is usually selected for both structural and non-structural damages, with a different one only for nuisance.

4.7. Risk Metrics

We propose the following risk-metrics as variables in decision making related to the permitting process, designing the TLP thresholds and in general regarding a project should be deemed too risky or not (Bommer et al., 2015; Grigoratos et al., 2023):

- aggregate nuisance level: mean total number of people feeling an earthquake.
- aggregate structural damages: mean total number of structures with at least "moderate" structural damages.
- aggregate non-structural damages: mean total number of structures with at least "severe" non-structural damages.
- local personal risk: mean probability of fatality for a person, who is continuously present without protection at a location.

These metrics encompass the entire duration of the human activity in question. Obviously, if a human activity is to be repeated multiple times (e.g., several stimulations over a number of weeks) then this should be taken into account. Both the list of risk metrics and their tolerance thresholds should be defined prior to the first SHRA by the regulator. Notably, local personal risk thresholds are mandated by law in certain countries (e.g., Netherlands).

To better contextualize these decision variables, one could express them as ratios of the equivalent ones for tectonic hazard. However, this assumes that the tectonic estimates are not only available, but that they have also been computed with sufficiently similar model components (e.g., GMPMs, fragility curves, etc.); this might be quite a challenging task.

Box 12. Definition of Damage-States and Nuisance Levels.

The damage-states adopted by the global risk map of GEM (Silva et al., 2020) or the ones from HAZUS (FEMA, 2013) could be used as reference points. E. Majer et al. (2013) also lists damage states for civil and buried structures. If the consequence function assumes different fatality ratios for daytime and nighttime, the mean of the two should be used. Indirect economic losses (such as business interruption or economic disruptions) are more difficult to model and are neglected here.

Regarding nuisance levels, the MMI scale defines various levels of felt shaking; the considerations outlined in E. Majer et al. (2013) can also inform this selection.

4.8. Deaggregation and Component Analysis

Deaggregation provides a breakdown of the modeled seismic risk estimates, allowing engineers and decision-makers to better understand the relative contributions of different earthquake sources (McGuire, 1995). It is

Table 3
Roles of Operator, Regulator, and Independent Expert Group on the Traffic Light Protocol

Participants	Roles
Regulator	Defines acceptable risk tolerance, uses risk principles to inform TLP design, ensures that the operator complies with regulations, enforces red-lights
Operator	Defines effective yellow-light mitigation strategies, complies with regulations, reports compliance to the regulator. Installs and maintains a monitoring network to ensure the efficacy of the TLP (and optionally the adaptive TLP). Optionally defines its own (lower) TLP thresholds
Independent expert group(s)	Provides authoritative seismic monitoring services and impartial scientific advice (e.g., calibrated M_L–M_W relationships)
Vendors	Provide seismic monitoring services and design/operate the TLP on behalf of the operator

the statistical decomposition of the probability of exceeding a certain hazard or risk metric, into the contributions from individual seismic sources or earthquake scenarios (Bazzurro & Allin Cornell, 1999; Goda & Hong, 2009; Hong & Goda, 2006). The results are usually plotted as probability mass functions for different values of magnitude, (hypocentral) distance, or are mapped along latitudinal and longitudinal surface coordinates. The spatial dimension of the deaggregation results might be relevant in case the EGS comprises multiple wells over a sizable geothermal play. If the EGS consists of just a few closely spaced wells, then only the decomposition in the magnitude domain is relevant. Notably, the latter is conceptually similar to how different scenario earthquakes are simulated to configure the red-light magnitudes in TLPs (Section 5.1.4).

One-at-a-time sensitivity analyses can also highlight whether the risk results are particularly sensitive to a specific logic-tree branching level, for example, to the GMPMs or the seismic source models. This would be an indication that additional effort should be put into reducing the uncertainty associated with this model component. Furthermore, component analysis could be utilized to highlight parts of the seismic risk model that are responsible for a significant portion of the losses. For example, if a specific building typology dominates the loss estimates, targeted retrofitting options or insurance coverage could be considered.

5. Traffic Light Protocols (Module 5)

The design of a Traffic Light Protocol (TLP, synonymously called a Traffic Light System) depends on a cross-examination and cooperation between the regulator, operator, and independent expert groups, as shown in Table 3. The operator then implements a plan to mitigate induced seismicity, which includes the seismic monitoring network and a reactive TLP (part of Module 5; Seismic Risk Mitigation).

In general, the TLP uses a three-stage response plan that governs the injection/extraction of fluids (Bommer et al., 2006):

- *Normal (green)*: operations continue as planned
- *Caution (yellow)*: operator implements seismicity-mitigation strategies
- *Stop (red)*: operation is (indefinitely) suspended

Note that the yellow-light can be further subdivided into sub-stages that implement increasingly effective mitigation strategies as the red-light is approached. Herein, (seismicity) mitigation strategies are defined as any operational changes made with the intention of reducing the growth in earthquake magnitude and frequency—in order to avoid encountering the red-light.

Goals of the TLP

1. The intention of the red-light is to provide the last-possible stopping-point, before exceeding an agreed upon tolerance to risk.
2. The intention of the yellow-light is to provide an adequate buffer, before the red-light, for an operator to enact their mitigation strategies—to ensure that the red-light is avoided.

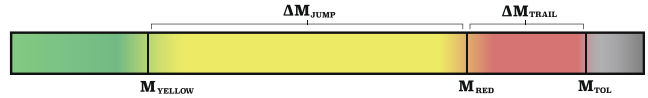

Figure 3. Schematic framework for a risk-based traffic light protocol, using magnitude thresholds.

Recommendations for the TLP

1. The construction of a TLP must be informed by seismic risk estimation methods.
2. Red-lights need to account for trailing seismicity: aftershock-like earthquakes that continue to occur after an operation has stopped, which can be larger in magnitude than the events during stimulation (Schultz, Ellsworth, & Beroza, 2022; Watkins et al., 2023). In this sense, the red-light should trigger the operational stop an adequate "distance" before the agreed upon risk tolerance.
3. Yellow-lights need to account for magnitude jumps: sudden increases in the largest event in a sequence—to minimize the chance of moving straight from green-to-red.

We note that any event size (magnitude or ground motion) based TLP has uncertainty and cannot prevent intolerable events, thus supplementary measurements should be considered during decision making (see Section 5.2).

These core recommendations are illustrated in Figure 3. Risk-based approaches are used to estimate M_{TOL}, a threshold magnitude that is expected to exceed a tolerance to risk (if it occurs). The red-light threshold (M_{RED}) is then stepped back from M_{TOL} by an amount we anticipate that magnitudes could change after an operation has stopped ($\Delta M_{\mathrm{TRAIL}}$). The yellow-light threshold (M_{YELLOW}) is then stepped back from M_{RED} by an amount we anticipate that magnitudes could jump during an operator's mitigation (ΔM_{JUMP}). We note that this figure is a simplification, in order to illustrate these concepts.

5.1. Risk-Based Traffic Light Protocols

In the following, we provide justifications and examples that illustrate how a risk-based TLP could be designed for EGS operations in a geothermal setting. We organize these points based on questions and answers to TLP design.

5.1.1. How to Select Risk Tolerances?

Seismic risks are multifaceted and can include nuisance, infrastructure damages, economic losses, and personal safety. Seismic risks can also vary by local or aggregate types: being either the impacts to an individual or the group, respectively. Using risk to decide when an operation needs to stop is justified, since these metrics are most closely tied to the consequences of induced seismicity and most easily understood by the impacted stakeholders.

Tolerances to each of these risks need to be clearly defined and communicated for a region/project—preferably in cooperation with all the affected stakeholders. Ideally, tolerances are defined via legislation or policy direction, which gives the regulator mandate or authority to govern industrial activities. Alternatively, tolerances can be inferred from prior TLPs or operation-ending earthquakes. The risk metrics, types, and tolerances that are relevant for a region/project might vary depending on:

- Familiarity, willingness, and consent of the local communities to cope with earthquake ground shaking risks.
- History of regulation, energy projects, and induced seismicity in a region.
- Policy orientation and social/cultural norms.
- Criticality of the energy project.

5.1.2. Why Are Magnitudes Used for Thresholds?

The majority of thresholds used in conventional TLPs are magnitude-based, given that magnitude can be calculated rapidly from a coarse network. Under special circumstances, magnitudes may even be determined from a single station (Lockman & Allen, 2005; Y. M. Wu et al., 2006). Often this arises due to practical needs and

Box 13. Hypothetical Example for a High LoC Project.

If a risk-based analysis determined that an $M_{TOL} = 3$ was determined to be associated with an operation-ending amount of nuisance or social unrest, then a red-light threshold of $M_{RED} = 2$ could be chosen. This is 1 magnitude lower than the risk-based target, considering that 90% of historical projects with hydraulic fracturing have trailing event magnitude differences smaller than magnitude +1 ($\Delta M_{TRAIL} = 1$) (Schultz, Ellsworth, & Beroza, 2022). Similarly, the yellow light could be $M_{YELLOW} = 0$, considering 90% of historical projects have magnitude jumps lower than 2 ($\Delta M_{JUMP} = 2$) (Verdon & Bommer, 2020); or 99% chance based on a Gutenberg-Richter distribution, with a *b*-value of 1 (Schultz, Ellsworth, & Beroza, 2022). So, there is a 90%–99% chance the project does not encounter a green-to-red jump.

considerations: regulatory/mitigatory decisions need to be made robustly, in rapid response to incoming (and uncertain) information. Induced seismicity often occurs in seismically quiescent regions that are (initially) poorly monitored. As well, operations (like EGS stimulations or hydraulic fracturing) are transient and may become numerous—targeting sites/plays and then moving on. Magnitude is also a more homogeneous metric compared with ground motions, which are only available at the measurement point. It is likely that these reasons also play a role in why local magnitude (M_L) is most often used to define TLP thresholds, rather than moment magnitude (M_W), which requires additional subsurface information (e.g., velocity model) and complex models. That said, a well-calibrated magnitude scale is essential for an effective TLP, because the link between magnitude and potential risks should be as accurate as possible (e.g., Luckett et al., 2019; Roy et al., 2021).

However, M_W could be implemented as the magnitude scale used for the TLP, if robust and reliable real-time estimation is available down to the monitoring thresholds. Practical issues aside, M_W would be preferable to M_L since it is based on the physical quantity of seismic moment from the earthquake, is used pervasively throughout hazard/risk estimation approaches (e.g., within GMPMs), and does not saturate at large magnitudes.

In cases where there are monitoring stations co-located either with the operation or exposed assets, ground shaking measurements can be used to directly supplement the TLP decision making process. Better yet, direct measures of risk impacts could also supplement the TLP decision making process. We note that seismic risk estimation approaches (Module 4; Section 4) can be used to translate magnitudes into seismic hazards or risks, and vice versa. There, uncertainties in geophysical parameters can be taken into account when designing a magnitude-based TLP threshold.

5.1.3. Simplified Examples of Designing Red-Light Magnitude Thresholds

When M_{TOL} has been determined for a given risk tolerance, models of magnitude jumps and trailing seismicity can be used to inform how far back (in magnitude) an operator needs to stop. These concepts were previously illustrated in Figure 3, where M_{RED} needs to be set back from M_{TOL} (by ΔM_{TRAIL}) and M_{YELLOW} needs to be set back from M_{RED} (by ΔM_{JUMP}). Two simplified examples are described in Boxes 5.1 and 5.2. Note that the estimation of M_{TOL} will not depend on the pre-screened LoC category—it will only depend on jurisdictional risk tolerances, the portfolio of (exposed) assets, and geological conditions in the vicinity of the operation.

These two simplified examples highlight how the basic concepts of trailing seismicity and magnitude jumps can be used to define TLP red- and yellow-light thresholds. In practice, we want to unify these concepts in a rigorous method that simultaneously considers risk-based tolerances, magnitude jumps, and trailing seismicity.

5.1.4. How Are Risk Tolerances Transformed Into Red-Light Magnitude Thresholds?

By constructing models to estimate seismic risks from any scenario earthquake magnitude, the risk tolerance can be converted into a red-light magnitude (Ader et al., 2020; Douglas & Aochi, 2014). Typical risk concerns are nuisance, damage, and a probability of personal risk concern. An example of a detailed workflow is developed by

Box 14. Hypothetical Example for a Low LoC Project.

If a risk-based analysis determined that an $M_{TOL} = 4$ event could be associated with intolerable housing damage, then a red-light threshold of $M_{RED} = 3.3$ could be chosen. This is 0.7 magnitude lower than our risk-based target, considering ~75% historical projects have trailing event magnitude differences smaller than +0.7 ($\Delta M_{TRAIL} = 0.7$) (Schultz, Ellsworth, & Beroza, 2022). The yellow light could then be $M_{YELLOW} = 2.3$, considering 60% historical projects have magnitude jumps lower than 1 ($\Delta M_{JUMP} = 1$) (Verdon & Bommer, 2020); or a 90% chance based on a Gutenberg-Richter distribution, with a *b*-value of 1 (Schultz, Ellsworth, & Beroza, 2022). So, there is a 60%–90% chance the project does not encounter a green-to-red jump.

Schultz et al. (2021a), and illustrated in Figure 3 and the Box 15 below. In prior work, these concepts have been applied to prospective EGS induced seismicity (Schultz, Muntendam-Bos, et al., 2022; Yaghoubi et al., 2024). The approaches used draw from the previously described seismic risk/hazard estimation concepts (Module 4; Section 4). We anticipate that there may be additional methods developed to assist in the construction of risk-based TLP thresholds. For example, by estimating magnitudes of intolerable events (M_{TOL}) for a given location or using the mathematical framework of deaggregation of seismic risk (Section 4.8).

Box 15. A Risk-Based Red-Light Workflow (Schultz et al., 2021a).

To determine a red-light magnitude, we can use a workflow that simultaneously incorporates concepts of trailing seismicity, risk estimation, and risk tolerances.

Assuming a red-light threshold, scenarios of earthquake magnitudes are randomly drawn from a trailing seismicity model. Trailing seismicity models are used in place of seismogenic rate models (which are difficult to constrain a priori), since we are only interested in the last-possible stopping-point before exceeding an amount of risk.

The remaining steps straightforwardly use concepts from PSHRA (Module 4; Section 4). Trailing events are translated into an expected amount of hazard, via a GMPM (Section 4.3). Given a proposed location for the operation (and simulated trailing magnitudes), we can estimate the degree of hazard via ground shaking intensity. Ground shaking is then translated into risk via a combination of exposure (Section 4.4) and vulnerability/fragility models (Section 4.5). Essentially, if we know where assets are and how they respond to ground shaking, we can estimate the impact. These impacts can be of various risk types (e.g., nuisance, damage, or fatality) and various risk scopes (e.g., aggregate amounts to a population or local chances for an individual). The process is probabilistically repeated to estimate median/mean amounts of potential risk impacts and provide a measure of uncertainty (e.g., Section 4.1) as a function of the red-light magnitude. For this location, as the red-light threshold increases, so does the level of "acceptable" risk implicitly taken. This process quantifies the amount of risk taken, as a function of red-light magnitude. Since the earthquake location, wave propagation, and exposure profile are physically constrained (for a given/potential site), the red-light magnitude becomes the critical variable.

Given known tolerances to risk (Section 4.7), it is possible to use this approach to determine the appropriate red-light for when an operation would need to stop—to ensure that these risk tolerances are not exceeded. This can be accomplished by observing the graphical intersection between the risk tolerances and estimated risk curves (Figure 4). In this sense, we can work backwards from risk tolerances (using risk modeling) to infer an appropriate red-light threshold for any possible site (Figure 5).

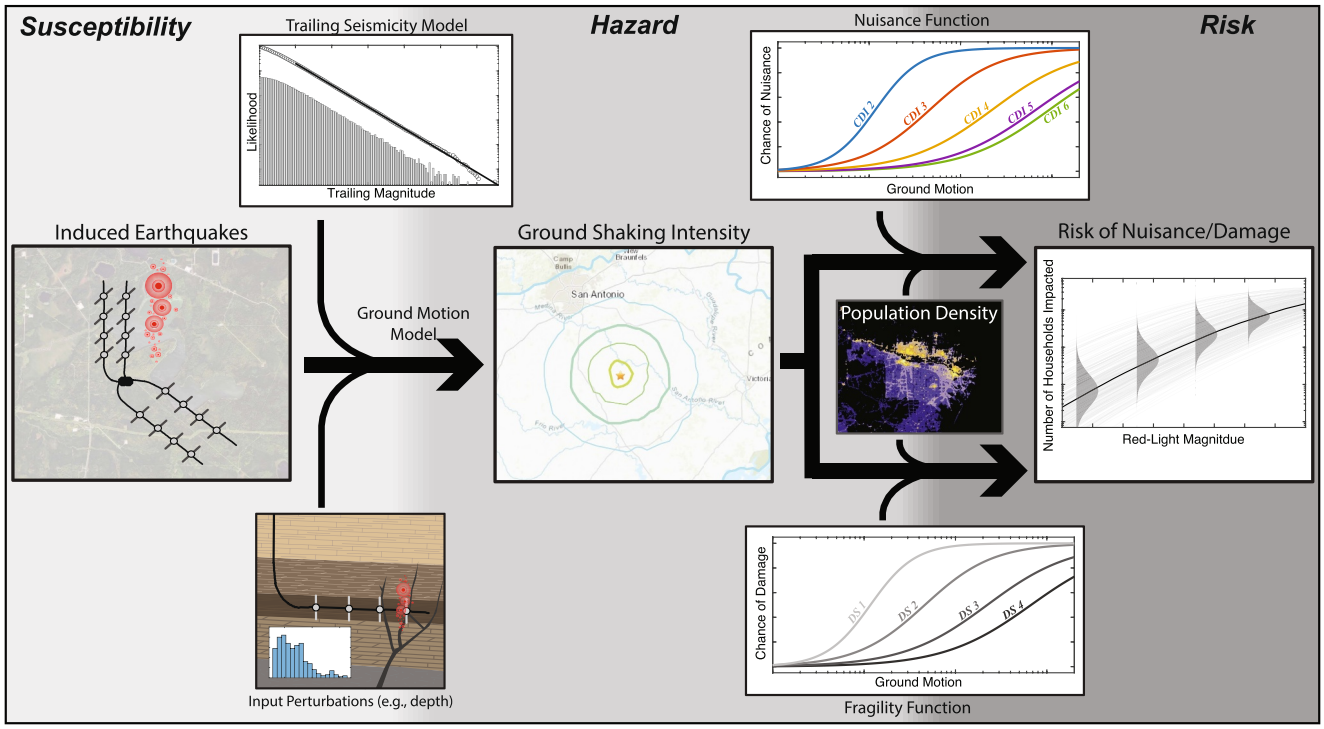

Figure 4. An example workflow of a risk-based traffic light protocol. Scenarios of earthquake magnitudes following a red-light event are randomly drawn from a trailing seismicity model. These scenario red-light events pass through the hazard/risk workflow to estimate the amount of expected risk. Figure is adapted from Schultz, Ellsworth, and Beroza (2023), Schultz, Baptie, et al. (2023).

5.1.5. Can Red-Light Thresholds Vary for the Same Risk Tolerance?

Currently, many countries have adopted TLP thresholds at a national or regional scale, with values ranging between M_L 0.5–4.0 (Braun et al., 2020; Ineris & BRGM, 2023; Schultz, Beroza, et al., 2020; Schultz, Ellsworth, & Beroza, 2023; Verdon & Bommer, 2020). Ideally, TLP thresholds should be informed by risk-based principles. Notably, the same risk tolerance can mean different red-light thresholds from region-to-region, since assets and their exposure to risk can vary spatially.

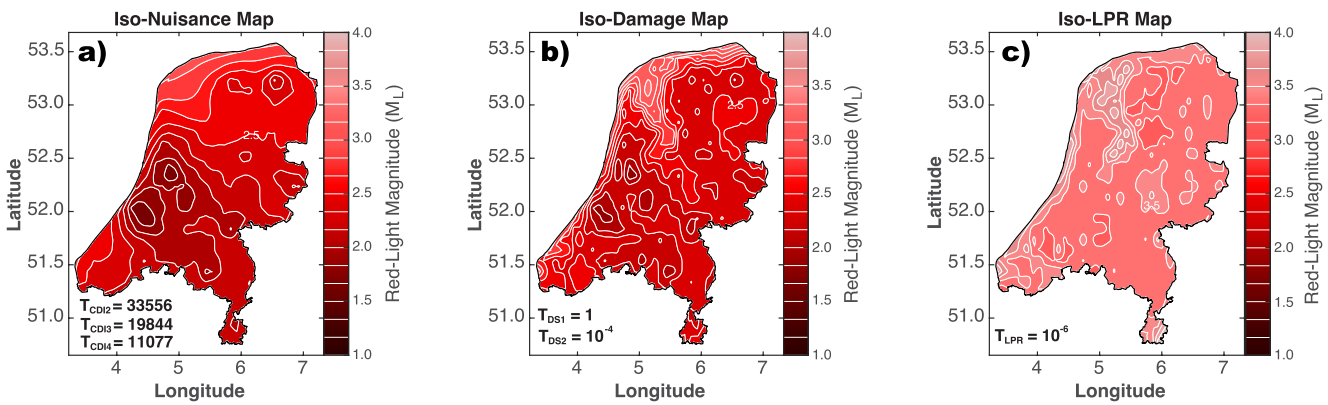

Figure 5. An example of traffic light protocol red-light thresholds determined using risk-based methods. Given known/inferred tolerances to risks of nuisance (a), damage (b), and fatality (c), an appropriate stopping point is determined for all enhanced geothermal systems locations in the Netherlands. Tolerances to risks (text labels) were either inferred from past operation-ending events (a, b) or based on national legislation (c). Multiple metrics of risk could be considered by using the lowest red-light estimate (at a given site location). This approach automatically considers the potential for trailing seismicity. Figure is adapted from Schultz, Muntendam-Bos, et al. (2022).

First, the red-light magnitude can vary, depending on:

- The tolerance of the local population to seismic risks
- Location and fragility of exposed assets (exposure factors, population density, critical infrastructures)
- Regional physics of wave propagation, ground motion, and site amplification
- Variations in the anticipated amount of trailing seismicity

Second, the magnitude of the largest trailing event also varies, depending on:

- Spatial variations in seismogenic model: *b*-values and the productivity of trailing seismicity (Schultz, Ellsworth, & Beroza, 2022; Verdon & Bommer, 2020).

5.1.6. What Are the Limitations of a TLP?

The framework of a TLP is based on the assumption that induced earthquake magnitudes will grow with time, providing some warning or reaction time for an operator to enact mitigation strategies. It also assumes that the enacted mitigation strategies will be effective in reducing the probability of larger magnitude events. Likely, these deficiencies are potential avenues for future research.

We emphasize that the TLP for the stimulation phase of the EGS project can differ from the TLP during the production (circulation) phase of the geothermal project. Currently available magnitude jump and trailing seismicity models (Schultz, Ellsworth, & Beroza, 2022; Verdon & Bommer, 2020), are developed for stimulation, which might also be used for the circulation phase with caution. Future developments on seismogenic models are needed to properly address the circulation phase.

5.1.7. Lower TLP Thresholds From the Operator's Perspective

An operator may opt to take a more conservative approach than the regulator's regionally defined guidelines. This could be informed by additional information the operator has regarding the subsurface conditions for induced seismicity susceptibility, the severity of earthquake impacts/consequences, or simply the operator's (lack of) appetite for risk. Note that the seismic monitoring network's design should be adjusted to meet the revised yellow-light threshold (Table 4).

5.1.8. Mitigation Strategies for TLPs

Mitigation strategies are the reactive measures employed by the operator to ensure that induced seismicity does not continue to grow to unacceptable levels. Currently, there is no consensus or rigorously established approaches on how to most effectively mitigate induced seismicity. Said another way, currently there is no "silver bullet" to prevent further earthquakes. Here, future research would be beneficial; specifically, to disentangle and quantify the efficacy of mitigation in a variety of geological, seismotectonic, and operational settings. Openly accessible data sets will be crucial to establish scientific consensus on mitigation.

Typical mitigation strategies include reduction of stimulation rate/pressure, implementing gradual changes to pumping rates, operational pauses, reorganizing the stage stimulation schedule, changing stimulation designs (e.g., soft "cyclic" stimulation (Hofmann et al., 2019)), flowing back between stages, reducing total injection volume, skipping problematic stages, or ultimately pad/well abandonment. Other non-operational mitigation measures can include public outreach, relocation of infrastructure/personnel, building retrofitting, or financial compensation schemes (Bommer, 2022; Module 6). Yellow-light mitigation strategies (and the communication channels to execute them) should be outlined and agreed upon before the operation begins. Ideally, test case scenarios would be practiced in a hypothetical setting before the operation begins. Examples of detailed mitigation strategies are available in prior documents (Ader et al., 2020; Braun et al., 2020; Gischig et al., 2019; E. Majer et al., 2013; Pankow et al., 2023; Yaghoubi et al., 2024). The design of mitigation plans/strategies can also straightforwardly adapt from the analogs in hydraulic fracturing for shale gas (CAPP, 2019; Schultz, Skoumal, et al., 2020).

Operators encountering a red-light should shut-in their operation as soon as reasonably practicable. They should follow jurisdictional shut-in safety guidelines to avoid causing any other operational risks/concerns (e.g., well integrity issues). Details of a "generic" red-light shut-in procedure should be previously agreed upon, at the discretion of the regulator. This may include mitigatory strategies such as a gradual shut-in procedure (Segall &

Table 4
Mc Threshold and Location Precision/Accuracy Targets and Their Corresponding Network Parameters for a General Case Featuring a Field-Scale Enhanced Geothermal Systems Project in Rural, and Urban Contexts

LoC	Detection threshold suggestions (Mc)[a]	Locations accuracy/precision suggestions[a]	Example of backbone instrumentation for detection, location, & magnitude determination[b]	Example of accuracy/ precision of locations[b]
Low	Mc < M_{YELLOW}	Resolve fault/fracture at ~M_{RED}	– 3C broad-band sensors at the surface	Horizontally: ±0.5 km
			– Typically, at least 5 stations	
	and	and	– Typically, at least 1 strong motion sensor in the center of the array	
	Mc < M_{felt}	Spatial resolution < half the inter-pad spacing[c]	– Optionally shallow borehole stations	
High	Mc < M_{YELLOW}-1.0	Resolve fault/fracture at ~M_{YELLOW}	– 3C broad-band sensors at the surface	Horizontally: ±0.06 km
			– Typically, at least 7 stations	
	and	and	– Typically, at least 1 strong motion sensor in the center of the array	
			– Shallow borehole stations	
	Mc < 1.0	Spatial resolution < half the inter-stage spacing[d]	– Geophone chains in deep wells	

[a]Refer to the text for examples of numerical simulation approaches for modeling Mc levels and location accuracy. [b]Note that the two example columns can change on a case-by-case basis, thus we advise to follow the Mc and locations accuracy targets rather than the given (example) prescription. [c]Only valid in case of multiple pads. [d]Only valid in case of multiple stages.

Lu, 2015) or well flow back. Specific details of the shut-in procedure could vary on a case-by-case basis, again at the discretion of the regulator.

Triggering a red-light likely means the end of an operation, so the urgency of yellow-light mitigation strategies should reflect this finality. A reduction of the TLP level after triggering a red-light should be properly investigated (and only considered in exceptional cases), with input from the independent expert group, acceptance from the regulatory authorities, and with consent from the impacted community/stakeholders.

5.2. Supplementary TLP Considerations

The threshold of a conventional TLP is magnitude based. A risk-based red-light threshold must choose some probabilistic value of risk tolerance (e.g., a median amount of nuisance impacts or mean fatality chances) and is based on empirically/statistically derived models—guaranteeing that it will never be completely effective. Furthermore, magnitude is not a complete indicator of earthquake physics and risk consequences. Thus, other supplementary indicators should be used when available. These supplementary considerations are aimed at better understanding how the underlying geophysics, geology, or monitoring uncertainties could impact the earthquake sequence(s); this information should inform how the operator reacts during the yellow-light.

The following are important to consider:

1. Spatial distribution/orientation of seismicity. Well-resolved clouds of seismicity (after accounting for location uncertainty) generally indicate the least problematic scenario of stimulated fracture networks. Plane-like features can be more concerning, depending on their orientation within the stress field. For example, planes subparallel to the maximum stress direction are likely hydraulically stimulated fractures in tensile failure. On the other hand, planar features oriented along critically stressed directions indicate fluid is reactivating a larger fault in shear slip. Operations encountering fault reactivation in shear slip should proceed with heightened caution, especially if multiple stages intersect different points of the same fault. Suggestions here are analogous to those for hydraulic fracturing for shale gas (CAPP, 2019; Schultz, Skoumal, et al., 2020).
2. Events with a large distance from the injection point should raise attention, as that likely indicates pressure conduits linked to distant faults. Faults that are distant from the operation will be more difficult to control, due to relatively larger lag time between operational changes and induced earthquakes.
3. Rates of seismicity are often used as a supplementary metric within existing TLPs. This is often included to account for cases where a large event was statistically expected to occur, but still has yet to be observed. For example, by triggering a yellow-light either if an M_{YELLOW} event is encountered or if ten M_{YELLOW}-1.0 events are recorded within a given timeframe.

4. Proxies for the seismic response of the reservoir like the seismogenic index (Shapiro et al., 2010), the seismic injection efficiency (Kwiatek et al., 2019), and the seismic moment release (Bentz et al., 2020). These metrics have implications for the growth of earthquake magnitudes during injection.
5. The Gutenberg-Richter *b*-value. Often hydraulic fracturing operations observe larger *b*-values (∼2.0) during fracture stimulation. Fault reactivation is usually associated with smaller tectonic values (∼1.0). This transition in *b*-value has been observed in hydraulic fracturing cases where fracture stimulation inadvertently reactivates faults (Maxwell et al., 2009). Generally speaking, the smaller the *b*-value the greater the seismic risk.
6. The amount of trailing seismicity observed. The initial TLP design will have made assumptions about the productivity of trailing events. How this deviates from the initial assumption will have important implications for the current operation (Schultz, Baptie, et al., 2023). Generally speaking, more trailing events means that operations would need to mitigate (or end) further back from the tolerance threshold M_{TOL} (i.e., the red-light would need to be lowered).
7. Additional risk or hazard related information: such as felt reports, damage/loss reports, or ground shaking metrics.

5.3. Updating the TLP

The uncertainty of the TLP thresholds predominantly lies within accurately estimating the seismogenic model (Section 4.2), GMPM (Section 4.3), exposure (Section 4.4), and vulnerability/fragility model (Section 4.5), which are also key components of the risk analysis workflow (Module 4; Section 4). As development within a project or play progresses, new data will become available, which could be used to update the SHRA and TLP (Figure 6).

Box 16. Research Considerations for Improved TLP Updating.

The probability of magnitude jumps used in the TLP are statistically obtained from large data sets. It is possible to achieve site-specific estimation, if seismicity data is available, through an ensemble (logic tree) of various models available in the literature, such as Shapiro et al. (2013), McGarr (2014), Galis et al. (2017), van der Elst et al. (2016), and W. Cao et al. (2020). Some of these models incorporate the injection strategy, others use the extent of the seismicity cloud as a proxy for the largest possible rupture, and others use purely statistical methods based on the magnitude-frequency distribution. Research into the efficacy of models will be required (Schultz, 2024).

Additionally, at the early stage of the stimulation operation, operations could consider incorporating information from a seismogenic fault injection test (SFIT) as proposed by Schultz, Ellsworth, and Beroza (2022) to constrain the site-specific $\Delta M_{\mathrm{TRAIL}}$ following well shut-in. This parameter is one of the most sensitive to perturbing red-light thresholds (Schultz et al., 2021a) and site-specific measurements have been suggested as a TLP correction metric (Schultz, Baptie, et al., 2023). Note that constraining trailing seismicity through a SFIT is currently being developed and its limitations are not yet fully understood, for example, it involves a small volume, which might not be representative for the entire reservoir. Alternatively, if multiple stimulations are involved, the seismicity during and after the early-stage stimulations could be used to constrain the $\Delta M_{\mathrm{TRAIL}}$.

For a low LoC project, we suggest that a TLP is designed. For a high LoC project, we suggest periodic updates to the TLP alongside gains in knowledge and the progress of the project, following the recommendations in Section 2 (Module 2). Optionally, high LoC projects can consider updating their TLP in real-time, which is accomplished through the Adaptive TLP.

5.4. Adaptive Traffic Light Protocols (ATLP)

The TLP has its simplicity for implementation and regulation, thus should always be conducted for EGS projects. But some of the shortcomings of traditional TLPs are that they are reactive, they do not forecast future seismic activity or risk, and there is limited application for real-time monitoring optimization. Thus, continued research and development into both traditional TLP and Adaptive Traffic Light Protocols (ATLP) are advised. ATLPs are an alternative decision-support tool that aims to provide operators with continuously updated estimates of seismic

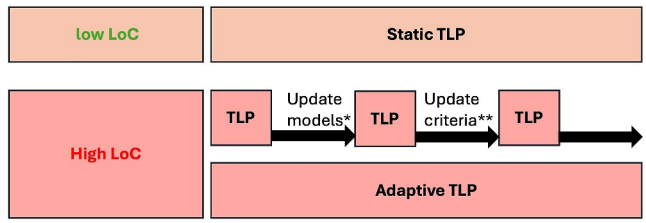

Figure 6. Schemes on updating a traffic light protocol (TLP) or Adaptive Traffic Light Protocols. *The TLP should be updated each time significant improvements are made to underlying models or criteria (e.g., ground motion prediction, trailing seismicity, risk tolerance). **Appropriate yellow-light reactions to supplementary considerations should be updated as information is shared amongst the operators on how the play responds to injection.

hazard and risk forecasts during reservoir operations (Figure 7; Box 17). This approach is currently at a low technology readiness level, as it has not been tested in a real project so far.

Below, we suggest the following protocols if ATLPs are deployed:

- An ATLP Expert Panel, selected by the operator and the regulator, composed of independent subject matter experts and communication experts, should be created whose purpose is to provide thresholds for the ATLP, run the ATLP, and communicate response levels of the ATLP to the public and other project stakeholders. ATLP updates should be given through the online web interfaces dedicated to seismic monitoring, as outlined in Section 6.3 on data sharing.
- Clear threshold level criteria defining when an increase in response level is necessary must be defined in advance. Threshold criteria include (but are not limited to): probability of exceeding certain earthquake magnitudes, the probability of a felt/damaging/fatal event, or a ground shaking intensity (Bommer et al., 2017; Gischig et al., 2020).
- A clear description of the mitigation actions and emergency response plans at each of the TLP levels should be agreed upon before the start of operations.

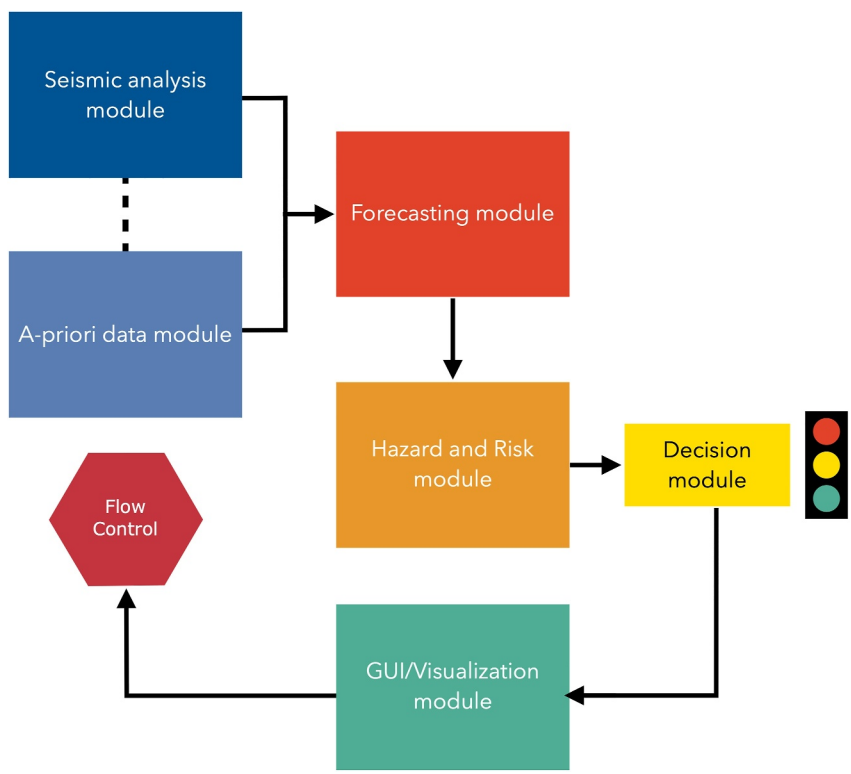

Figure 7. Simplified scheme of the adaptive traffic light protocols workflow.

Box 17. Adaptive Traffic Light Protocols (ATLP).

ATLP are built to capture the reservoir evolution based on a range of key parameters (e.g., permeability, pressure, temperature, seismicity, injection rates, etc.). They are fully probabilistic, data-driven (in the sense that microseismic data are integrated in real-time to update geo-mechanical and statistical seismicity forecasting models) and risk-based by integrating hazard, exposure, and vulnerability (Grigoratos et al., 2021; Langenbruch et al., 2020; Mignan et al., 2017; Mizrahi et al., 2024; Wiemer et al., 2014). The ATLP should therefore, at any point in time, integrate all available information on the reservoir evolutions into the best possible forecast.

- Sensitivity pre-testing of the ATLP for the minimum amount of data needed.
- Adequate near-real-time data input (including fast data transfer) from the seismic monitoring system must be in place. Hydraulic and seismic data acquisition systems must be synchronized to one reference time base to allow for the forecasting models to run.

6. Seismic Monitoring (Module 5)

In this Section (part of Module 5; Seismic Risk Mitigation), we aim to harmonize the monitoring guidelines that are currently available at national levels. These new standards are designed to encompass the different phases of an EGS project life cycle (ranging from initial planning and drilling to stimulation and post-operation stages) as well as the different LoC categories as assessed by the available methods previously discussed in Section 3 (Module 1).

Goals of seismic monitoring

1. To provide supporting earthquake information, at a resolution sufficient to inform safety-relevant, decision-making processes (e.g., TLP).
2. To reduce the uncertainties in seismic risk estimates, through measurements that update a priori assumptions.
3. To demonstrate an operational transparency that fosters trust with the impacted community and stakeholders.
4. To provide guiding subsurface information for future operations.
5. To characterize the properties of the reservoir for production optimization.

Recommendations for seismic monitoring

1. Seismic monitoring networks must be designed to detect sufficiently small earthquakes, well before decisions need to be enacted (e.g., the yellow-light).
2. Seismic monitoring networks must be designed to spatially resolve earthquakes (e.g., identifying pre-existing faults and event migration patterns) to adequately aid mitigation decision making.
3. To update risk estimates, seismic monitoring networks must be designed to reduce uncertainties (e.g., event magnitudes, locations, ground shaking metrics, fault geometry, potential for hazard/risk, and the general understanding of the subsurface).
4. Seismic monitoring networks need to be tailored toward both short-term and long-term risk scenarios.
5. All seismic monitoring data should be shared using open and FAIR (Findability, Accessibility, Interoperability, and Reuse) data practices. Sharing could occur after a brief (and optional) embargo period.
6. Seismic monitoring is the responsibility of the operators, with the requirement that information is shared with all the other groups. This is to ensure that the operator is meeting their monitoring targets.

We note here that the provided recommendations do not include guidelines regarding the acquisition of active source seismic data (e.g., reflection seismic, VSP, or multi-channel surface wave survey), which should be considered when pre-screening and site-specific SHRA analysis is required (as described in Sections 3 and 4; Modules 1 and 4). We also note that for a low LoC project, if a red-light event (or an unexpectedly high level of seismicity) occurs, it would require a re-assessment of the pre-screening analysis and previously appraised LoC.

For each of the LoC categories, a different level of monitoring sensitivity is required as either case could still potentially trigger a red-light. Stricter monitoring sensitivity/targets for high LoC reflects the need for increased scrutiny over more worrisome projects (and vice versa). Two critical measures of monitoring sensitivity are the magnitude of completeness (Mc, see Box 18) and spatial resolution. To avoid non-uniform spatial completeness,

Mc targets must be reached before advanced techniques such as template matching and/or repeater detectors are applied.

Box 18. Magnitude of Completeness (Mc).

In an earthquake catalog, the magnitude of completeness (Mc) is defined as the minimum magnitude above which the overwhelming majority of earthquakes in a space-time volume are detected. This minimum magnitude depends on the number and spatial density of seismic stations (Mignan et al., 2011). Mc can be estimated with a variety of statistical methods (Schorlemmer & Woessner, 2008; Wiemer & Wyss, 2000; Woessner & Wiemer, 2005; Zhou et al., 2018); some of these methods assume a Gutenberg-Richter law (Gutenberg & Richter, 1944) for the magnitudes above the completeness threshold.

Below, we list our justifications for and quantifications of Mc thresholds that a seismic monitoring network should reach to accommodate risk assessment studies and risk mitigation measures (e.g., TLP, see Section 5). Seismic monitoring must reach detection thresholds based on:

(a) *Felt ground shaking*: Felt ground shaking is one of the first undesirable impacts encountered by stakeholders from an induced earthquake. Thus, adequately resolving felt events should be one of the monitoring objectives. Here, we define the size of the minimum felt event (M_{felt}) as the smallest magnitude expected to cause nuisance to stakeholders. M_{felt} depends on the site conditions, focal depth, population density, and time of occurrence. Most felt events are usually larger than $M2.5$, under rare circumstances they might be as low as $M1.0$ (e.g., close to population with significant site amplification during the night). However, in areas with no exposed population this value could be arbitrarily large. The network Mc should be equal or smaller than M_{felt}. For example, shaking intensity data could be used to inform when felt events are being approached, through calibration of IPMs or GMPMs.

(b) *Yellow-lights:* Yellow-lights define the period when mitigation strategies should be enacted. Thus, adequately resolving yellow-light events should also be a monitoring objective. The Mc should be small enough to allow enough data to be collected and used for yellow-light mitigation strategies. For example, the data may be used to inform earthquake recurrence models, namely the parameters of magnitude-frequency distributions (e.g., *b*-value, seismicity rate, seismogenic index), magnitude jumps, and maximum magnitude after shut-in (trailing magnitude). This could be achieved by setting the Mc lower than the yellow-light, depending on the LoC category.

The event spatial resolutions are supplementary considerations for the SHA or magnitude-based TLP. Below we list our justifications for spatial resolution thresholds that a seismic monitoring network should reach for mapping pre-existing faults and accommodate other supplementary TLP measures (Section 5.2):

(a) *Fault delineation:* The orientation of a fault within the ambient stress field is a key factor for determining the susceptibility for slip reactivation. Furthermore, distinguishing between shear fault reactivation and fracture stimulation is an important supplementary measure in effectively reacting to problematic induced seismicity (Section 5.2). Thus, adequately resolving relative hypocentral trends of induced earthquakes should be a monitoring objective. Because of this, the seismic monitoring network must be capable of resolving fault sizes/orientations on scales encountered during the TLP. Furthermore, this data can be used to inform regional seismotectonics, in situ stress information, or subsurface hydraulic connectivity.

(b) *Causation assessment:* Identifying if an earthquake is natural or induced (and attributing it to the correct operation) is a key step in effective mitigation. Spatial information is important for distinguishing between natural and/or competing anthropogenic operations (Davis & Frohlich, 1993; Foulger et al., 2023; Verdon et al., 2019). Thus, adequately resolving absolute hypocentral locations must also be a monitoring objective. As the density of these competing natural/anthropogenic sources increases, so must the monitoring resolution —to ensure that sources can be distinguished unambiguously. The spatial resolution of the monitoring network will need to be smaller than the lateral spacing of sources to accomplish this task.

Note also that the event focal mechanism is also an important parameter for stress estimation, reservoir characterization, and seismic hazard. Here, we assume the network capacity on resolving event location is correlated with resolving focal mechanism, and do not take it as an independent measure.

We also note that for reservoir characterization, seismic monitoring is pivotal for reconstructing a detailed map of faults, fractures and fluid pathways being developed during stimulation/production phases. To illuminate such structures, a seismic network should be able to characterize very small events (microseismicity). We provide the caveat that over-focusing on the spatial domain sometimes results in discarding events with higher location uncertainty, affecting catalog completeness in the magnitude domain. Within reasonable constraints, the latter should remain a priority for the catalogs to remain useful for the development of earthquake recurrence models (*a*/*b*-value, magnitude jumps).

6.1. Seismic Network Design

Concerning the technical specifications for a microseismic monitoring network, a universally recognized standard practice has not yet been established. Various thresholds such as the number of stations, azimuthal gap, location accuracy, magnitudes, dynamic range, sampling rates, etc., differ significantly and are tailored based on specific project requirements, highlighting a considerable reliance on a project-to-project basis (e.g., Ineris & BRGM, 2023). Here, we propose a standardization of practices based on the Mc and event spatial resolution as a function of the LoC categories (Table 4).

Note that if the LoC changes with time, the monitoring targets will change and thus the network sensitivity should also change accordingly.

6.1.1. Low LoC Category

For this category, the seismic monitoring network should ensure accurate/precise locations and source parameters of induced earthquakes, as well as the operation of a conventional magnitude-based TLP (see Section 5). This data is also collected to validate/refute the hypothesis that the operation is indeed low LoC. For example, if a red-light is encountered for a low LoC project/region, this should trigger a reassessment of pre-screening efficacy. Thus, monitoring standards must be adequate enough to perform a causation/risk assessment in the case that unexpectedly high levels of seismicity/risk is encountered.

Below we list the targets for the network-Mc and spatial resolution thresholds (Table 4):

- Mc threshold:

  The seismic network should be able to detect and characterize seismicity at a Mc lower than the yellow-light and M_{felt} within the expected source region. However, if induced seismicity occurs beyond the expected source region, the latter should be reassessed and enlarged to include greater distances. The target Mc threshold value can be obtained through numerical simulation scenarios where different numbers of sensors and array geometries are tested (e.g., Kraft et al., 2020; Section 6.1.1).

- Spatial resolution threshold:

  The choice of a target location accuracy/precision should be set so that stimulation fractures can be clearly distinguished from shear fault reactivation for events of magnitudes approaching the M_{RED} threshold. Moreover, the location accuracy should allow for distinguishing between competing anthropogenic operations (inter-pad spacing). To achieve this, numerical simulation scenarios to calculate the location accuracy/precision of earthquakes down to the completeness level should be performed (see Section 6.1.1). As location uncertainties are highly dependent on the velocity model used in their calculation, we suggest, for this category, to use locally-derived 1-D or 3-D velocity models.

We suggest planning the network taking into account the existing national monitoring network as, depending on the local density of the stations, the number of new stations to be deployed could be reduced (Kraft et al., 2020). Included stations from the national network should be accessible in real-time and incorporated in the calculation of magnitudes and locations. We also suggest to co-locate accelerometers at the station closest to the expected injection point, and close to the exposed community. Apart from dedicated high-quality instruments, budget

instruments for example, RaspberryShake seismometers/accelerometers, might be also used to further improve the network performance.

An example scenario for designing a seismic network for a project in the low LoC category is provided in Box 19.

Box 19. Example Scenario for a Low LoC Category.

If we had a case where the red-light was set at M4.0 and the yellow-light at M2.0, then the seismic network should be able to spatially resolve faults capable of hosting M4 events and detect events down to M2.0. Earthquakes of M4.0 have an average fault length of ∼500 m (Zoback & Gorelick, 2012). Thus, the seismic network should be able to achieve a relative location accuracy of ±0.5 km horizontally.

Generally, for a low-risk area (e.g., rural), and a field-scale EGS project in a strike-slip stress regime, the seismic network is composed of at least five regional/local stations with a geometrical configuration to allow an azimuthal gap smaller than 120°. This should ensure a minimum redundancy in case of station failure. For the same general case, Kraft et al. (2020) recommended that the epicentral distance of the stations to the expected injection point should be about two times the planned operation depth, but less than ∼10 km. This is to guarantee good sensitivity (e.g., detection capability) while allowing to constrain earthquakes depth.

6.1.2. High LoC Category

For this category, the seismic monitoring network should ensure near real-time accurate/precise locations of induced earthquakes, as well as the operation of a risked-based TLP (see Section 5) or, if possible, an ATLP. This data is also collected to improve the understanding of induced seismicity: to improve source/forecast models (Gaucher et al., 2015; Mizrahi et al., 2024), to accurately model hazard/risk and react to recorded events. Thus, monitoring standards must be adequate enough to reduce relevant uncertainties in magnitude estimation, earthquake locations, ground motion metrics, and the geometry of fault structures. As well, this information should be informative enough to adequately improve the understanding of the subsurface (e.g., seismotectonics, in situ stress state, hydraulic connectivity).

Below we list the targets for network-Mc and spatial resolution thresholds (Table 4):

- Mc threshold:

  The network design should include a comprehensive numerical modeling study to infer the minimum magnitude of completeness level needed to fulfill the microseismic monitoring as well as reservoir characterization targets. The derived Mc should be at least 1.0 magnitude units less than the yellow-light set in the TLP within the source region and less than M1.0 to allow for meaningful statistical analysis of the frequency magnitude distribution. The choice of decreasing the Mc thresholds by at least one magnitude lower than the yellow-light enables the consideration of magnitude jumps and still provides adequate room to execute operational changes. The modeling should also include testing different array geometries and different combinations of instrumentation (e.g., surface dense array patches, co-located geophones and fiber optic technologies, i.e., DAS). Comparison of the noise levels at the sites of the different seismic instruments and network design should also be performed.

- Spatial resolution thresholds:

  The monitoring network location accuracy/precision target should be sufficient to distinguish between stimulated fractures and shear fault re-activation for events of magnitudes near M_{YELLOW}, so that an appropriate reaction plan can be implemented by the operators. Additionally, the spatial resolution should be able to link each earthquake cluster to its causal stage. To achieve this, numerical simulations that verify the spatial resolution down to the completeness level should be performed (see Section 6.1.1). To improve the absolute location accuracy/precision and source depth determination, we suggest performing checkshots and perforations to calibrate the velocity model and to orient the borehole sensors (Akram & Eaton, 2013). Ideally, the

velocity model should be calibrated prior to the stimulation. If available, velocity information from active seismic surveys, VSP and crosshole tomography should be integrated into the velocity model used for event location.

The baseline network should include surface stations (a mix of high-gain sensors and low-gain accelerometers) in a number as indicated by the Mc numerical modeling. A possible add-on to the baseline monitoring at the surface is the installation of dense surface arrays which have been demonstrated to reduce the noise level, and thus reducing the magnitude of completeness significantly (Fiori et al., 2023). In addition, during stimulations, geophone chains in one deep borehole have been demonstrated to lower the Mc levels. Boreholes are crucial for establishing a detailed high-precision catalog of the induced seismicity produced during the stimulation phase. This is because by going closer to the source and away from the near surface, the effect of noise is reduced, and smaller events are more easily detected. If high temperature graded sensors are available, their deployment should be attempted, however we caution that Mc numerical modeling should not solely depend on the performance of these sensors until the technology is proven to be reliable. This is also due to the fact that such equipment is typically deployed in certain (critical) phases of the project only. Additional instrument types (e.g., shallow borehole stations, surface DAS and borehole DAS cables) may be also necessary depending on the noise levels and results from the numerical modeling of Mc.

An example scenario for designing a seismic network for a project in the high LoC category is provided in Box 20.

Box 20. Example Scenario for a High LoC Category.

If we had a case where the red-light was set at $M4.0$ and the yellow-light at $M2.0$, then the seismic network should be able to spatially resolve faults capable of hosting $M2$ events and detect events down to $M1.0$. Earthquakes of $M2.0$ have an average fault length of ∼60 m (Zoback & Gorelick, 2012). The combined seismic network (surface + boreholes) should be able to achieve an absolute location accuracy of ±60 m horizontally near the injection well.

Generally, for a high-risk area (e.g., urban) and a field-scale EGS project in a strike-slip stress regime, the seismic network should include at least 5 surface stations to ensure redundancy in case of failure and an azimuthal gap smaller than 90°. At least one geophone chain in a deep monitoring well is recommended (Maxwell et al., 2010), although multiple are significantly better. Additionally, dense surface arrays can also provide complementary monitoring improvements (Cochran et al., 2020; De Landro et al., 2020; Fiori et al., 2023). Importantly, the network should ensure a minimum redundancy in case of station failure.

6.1.3. Numerical Modeling Tools for Network Design and Optimization

The Mc determination is a function of the attenuation and the noise conditions at the recording sites (Kraft et al., 2020). Below we list few well-known numerical or statistical approaches to calculate either noise levels, variations of Mc, station accuracy, location accuracy, or a combination of these four:

- Optimization method for regional scale microseismic monitoring networks (Kraft et al., 2013). This method is based on the simulated annealing approach proposed by Hardt and Scherbaum (1994), which aims to minimize the volume of the error ellipsoid of the linearized earthquake location problem (D-criterion). The method samples the solution space for the optimal network configuration by testing many different sizes and geometries of D-optimal networks; it can handle 3-D velocity models, and directly incorporate the calculation of seismic body-wave amplitudes at arbitrary stations.
- Seismic Network Evaluation through Simulation method (D'Alessandro et al., 2011). This method uses numerical simulations to evaluate the performance of hypocenter location of a seismic network. Inputs needed are the station locations and their noise levels, a velocity model, and empirical relationships to estimate the variance in residual travel times.
- Probability-based magnitude of completeness (Schorlemmer & Woessner, 2008). This empirical method estimates both station-specific and regional time-dependent Mc values as a function of network properties (e.g., phase data, attenuation relations) instead of earthquake samples (e.g., event-size distribution).

- Bayesian magnitude of completeness (Mignan et al., 2011). It provides network-specific spatial relationships between Mc and the proximity to the *n*th nearest seismic stations. The statistical regression behind the method was later improved, in line with hierarchical Bayesian modeling (Feng et al., 2022).

Additional comments regarding noise levels:

- To select best surface sites, bedrock installations should be preferred over sediment/alluvial layers. A quantitative site selection procedure is described in Plenkers et al. (2015).
- Noise analysis before the final installation of a seismic station should be conducted (preferably over a 7-day period). The noise level should also be continuously addressed during the operational phase of the project.
- If the required noise level conditions are not met, it is suggested to use shallow boreholes (80–150 m depth or as a function of the site conditions).
- To enhance signal-to-noise ratio (SNR), and as an alternative to shallow boreholes, surface dense arrays can be employed as it enables stacking over closely located stations which have coherent waveforms. When designing dense arrays, it is important to consider noise-frequency content, target Mc, and source depths.
- Indicatively, for baseline surface monitoring, to resolve felt nearby events, Kraft et al. (2020) recommended that seismic stations should be located on sites such that the noise level in the 5–40 Hz frequency band should not exceed an amplitude of 100 nm/s, and the ground velocity of 600 nm/s can be recorded with SNR of at least 6 in this frequency range (see also Box 21).

Box 21. Noise Levels.

The SNR is sometimes set in order to accurately time the phase arrival onsets (Ruigrok et al., 2023; Zeiler & Velasco, 2009). We note that the numerical modeling softwares for modeling location precision/network performance usually use the maximum amplitude of the body wave onset rather than the arrival time which is the first break of the wavetrain onset (Kraft et al., 2020). If the signal is not impulsive, which is often the case, the onset will have much smaller SNR than the one estimated from the model.

Additional suggestions for all risk levels, deployed at the field scale for a single pad:

- Three-component seismic instruments should be preferred to allow for a clear distinction of seismic wave types (*P*- and *S*-waves) and orientation (particle motion); this should provide better earthquake locations, especially for small events that are recorded/visible only at a single station.
- In case of sensitivity saturation of the recording instruments, we suggest co-locating an accelerometer at the station closest to the expected source region. The accelerometer should be able to measure strong ground motions up to at least 1 g.
- Seismic stations must be synchronized to a common time reference with a precision of 1 ms. Hydraulic data and other geophysical measurements should be also synchronized to the same time reference with the same precision. Recommendation is for using a digital data acquisition system of 24-bit and a global position system (GPS)-based field timing system.
- Performing tests recording for new instruments besides an existing calibrated instrument, to ensure manufacturing parameters are reliable, gains and dynamic ranges are set properly, and instrument three components are correctly responding to its design.
- During instrument deployment, ensure that the instrument orientation has been accurately determined.
- Real-time transfer of continuous waveform data should be implemented. This implies setting up a telemetry system.
- The surface monitoring system should be in place and operational before the start of the project drilling phase to test data workflows and procedures (see Section 5.3) and establish background levels of seismicity. We suggest at least 6 months of seismic measurements for all risk categories. However, this value can vary between operations, projects, and jurisdictions (e.g., 3–12 months).

Table 5
Seismic Network Management by Level of Concern (LoC) Category

	LoC category: Low	LoC category: High
Continuous recordings	Yes	Yes
Real-time processing	Within 1 hr	Within 10 min
Seismic monitoring responsible personnel	Yes, remote	Yes, on-call
TLP personnel	Yes, remote	Yes, on-call
ATLP personnel	Not needed	Suggested, on-call
Operational manager overseeing all activities	Yes, on-call	Yes, on-call[a]
Reporting to regulators and public	Yes	Yes

[a]For critical phases of the operation (e.g., stimulation) it could be advisable to have responsible staff on-site.

6.2. Seismic Network Management

Baseline seismic monitoring and reservoir characterization networks follow different monitoring protocols as they are tailored to long-term and short-term risk, respectively. The following guidelines focus on the reservoir monitoring protocols and recommendations for deep geothermal projects in the different LoC categories.

Before the start of operations (drilling, stimulation, circulation), it is important to plan discussions and coordination meetings with all the parties involved in order to detail the monitoring activities and data acquisition parameters (see Section 6.3). Instruments should be tested and assembled beforehand. We suggest implementing TLP for all LoC projects. Section 5 includes recommendations to design thresholds for yellow and red-lights, which should be the responsibility of the regulators. Proper sensitivity (Mc) targets for each LoC category are outlined in Section 6.1. We remark here that for high-risk categories it is suggested to have an operational manager on site who is responsible for integrating the seismic and hydraulic groups, so that all groups are always fully informed of timing and changes in operations. In general, network operations are the primary responsibility of the operators with external surveillance and collaboration with the operators of the national networks (for baseline monitoring).

Below we report in detail the seismic network management for both low and high LoC categories (see also Table 5).

6.2.1. Low LoC Category

During the drilling and operational phase of the project, personnel tasked with providing real-time seismic monitoring (e.g., generating earthquake catalogs) can operate remotely. A TLP is recommended, and it can also be run remotely. Seismic waveform data should be analyzed in near-real time (within 1 hr) to detect, associate, locate, and determine magnitudes of seismic events. If any additional station is added to the baseline seismic network by the operator in order to reach the sensitivity level (Mc) required for this category, the operator should ensure continuous recording. This task should be performed by the operator. Reporting to regulators and the public during and after the stimulation should follow the data policies outlined in Section 6.3 and the communication guidelines described in Section 7 (Module 3).

6.2.2. High LoC Category

During the drilling and operational phase of the project, personnel tasked with providing real-time seismic monitoring (e.g., generating earthquake catalogs) need to be on-call. The responsible personnel running the TLP should be also on-call. An ATLP is not mandatory, but if implemented, details regarding the ATLP should be established with the operations team. The expectations for the ATLP should be established and there should be a process to decide the probabilistic thresholds (e.g., exceeding probability of a felt/damaging event or as a function of nuisance). The ATLP groups should also test the sensitivity of the system for the minimum amount of data needed, given the variety of data sets. Importantly, a plan for exchanging data and communicating between the different groups needs to be established and tested in advance of the stimulation activity. Further guidelines specific to ATLP protocols are described in Section 5.4.

Seismic waveform data should be analyzed in near-real time (within 10 min) to detect, associate, locate, and determine magnitudes of seismic events. This task should be performed by the operator. As previously mentioned, for this category, it is important to appoint an operational manager to oversee all the monitoring (seismic and hydraulic) groups, so that all groups are always fully informed of timing and changes in operations. Reporting to regulators and the public at all phases of the project should follow the data policies outlined in Section 6.3 and the communication guidelines described in Section 7 (Module 3).

6.3. Data Management Recommendations

In deep geothermal projects, many different activities and parameters have to be monitored and many different expert teams have to be coordinated. In preparation for seismic monitoring for all project categories, some key elements should be decided in the planning phase before arriving at the field and all groups, both the seismic and hydraulic team, participating in monitoring should participate in this aspect of the planning. It is essential that all data and documents refer to common standards and reference systems. Below we report best practices regarding data acquisition, data sharing and dissemination.

6.3.1. Data Acquisition

Specific data acquisition items to be decided on by all teams involved in monitoring activities include:

- The reference time and any potential timing issues between all the different sensor systems. The universal time (UTC) should be adopted, and the accuracy of the measurements should be indicated.
- The coordinate reference system. Relative measurements (e.g., depths) should be clearly described with reference to the chosen coordinate system.
- Reports should use SI units for all quantitative parameters. Otherwise, transformation must be indicated.
- Details of data integration, file/waveform formats and archiving procedures should be agreed beforehand. We suggest the SEED format for seismic data. If this is not possible (e.g., for DAS and geophone chains), a procedure and a correspondent conversion tool to transform the data format should be outlined and provided.
- Sampling rate should be adequate to avoid aliasing and record the spectral content of events. Although here we do not explicitly suggest an exact value for the minimum sampling rate to be used, for local/regional seismic networks 100 Hz sampling rate should be already sufficient, whereas higher sampling rates on the order of kHz are commonly used for borehole sensors and DAS cables that capture smaller events at closer scales.
- The metadata (and any changes from the initial settings) of all sensors and digitizers must be documented in detail.

6.3.2. Data Communication

An alarm system (via SMS and/or email) should be in place. This system should provide real-time information on automatic event origins (and subsequent manual refinements) to the regulators, as well as independent monitoring agencies. As part of the trust-building strategy toward the public and authorities, independent monitoring agencies should be authoritative for TLP-relevant magnitudes. The regulator should be authoritative for TLP-relevant decisions when events reach the yellow or red levels.

6.3.3. Data Sharing

We recommend publishing earthquake catalogs and hypocenter maps in near real-time on a dedicated web interface for all interested parties (operator, regulator and the public). This website can be hosted by the national seismic agency. Besides event origin time, location, magnitude, or event type (e.g., natural earthquakes, induced earthquakes, quarry blasts, landslides), there should be a clear label on whether the event is automatically or manually processed. This can help improve acceptance, support, and trust by the public/local communities. Indeed, including earthquakes not felt by the public will help the public to understand that not every earthquake is a problem, and a transparent exchange of information is in place (see also Section 7.3). Moreover, it facilitates the project oversight and allows scientists to further analyze the data and thus improve the overall state-of-knowledge of induced earthquakes within the research community.

Following the FAIR principles, hydraulic data, raw seismic waveforms, associated metadata (e.g., instrument locations, instrument response functions), and event catalogs should be archived throughout the lifetime of the

project. For the seismic data, the databases should be available in standard seismological data formats such as miniSEED, QuakeML, and data request and transfer schemas, such as SEEDLink and FDSN StationXML should be set up. Similarly, time-stamped hydraulic data including flow rates, stimulation pressure, proppant placed, stage locations should be also accessible openly. It is highly recommended that the data should be made available to third parties immediately or, if necessary, after an embargo period, to allow for verification, quality control and the application of advanced analysis methods (e.g., double-difference relocation methods, template matching, moment tensor determination). The length of the embargo period can be agreed upon jointly by the regulator and the operator. We note that however, access to seismic or hydraulic information relevant for the TLP should be made available to analysts immediately, even if an embargo is in place.

Additionally, related information such as the seismic velocity model used for the computation of the event locations, the magnitude calculation method and formulas, scaling relationship between locally established magnitude and moment magnitude, changes to processing routines, equipment failures and changes to network performances, should be shared. Open science data sharing practices have already been successfully implemented in regulatory frameworks that manage induced seismicity in Alberta, Canada (Schultz, Yusifbayov, & Shipman, 2020).

7. Communication and Stakeholder Involvement (Module 3)

The aim of this Section is to provide good practice guidelines for communication and social engagement for EGS geothermal projects (Module 3; Communication and Outreach). We define communication here as a multi-way process where all stakeholders receive and provide information. It is crucial to understand that risk communication is a discussion between different stakeholders and not a one-way information provision from the project operator or from experts to the public. The guidelines focus on communication with the local population (i.e., living close to the project site), but also gives an overview of dynamics between the different stakeholders involved in the implementation of a project. The guidelines are informed by a review of academic papers as well as reports from industry in 13 different countries. While these guidelines may be used for any EGS project, the specific measures taken always need to be tailored to the social context. Herein, social context refers to how the social, political, historical, economic, regulatory, and media environment impacts the choices and experience of stakeholders. Because of this, there exists no "one-size-fits all strategy" when it comes to (risk) communication (Trutnevyte & Ejderyan, 2018).

Goals of communication and stakeholder involvement

1. To facilitate open, transparent, and two-way exchange of knowledge between all stakeholders.
2. To provide an impartial and balanced education on the geothermal project, especially around concepts needed to make informed decisions regarding potential risks and benefits.
3. To foster trust and build a sense of community amongst the stakeholders.

While induced seismicity is at the center of challenges faced around the development of EGS projects and has been at the forefront of public debates (Giardini, 2009; Stauffacher et al., 2015), past research and projects have shown that perceived risks of a project (e.g., seismic events) depend on different aspects such as the perceived fairness of the project (McComas et al., 2016), the quality of the relationship with the project developer (Weber & Brian, 2014) as well as the overall quality of the communication strategy (Ejderyan et al., 2019). Therefore, communication guidelines must cover a larger breadth of issues than seismic risk mitigation only.

Stakeholder involvement is a necessary part of risk management and governance, especially when there is uncertainty about a risk which is the case for deep geothermal energy systems (IRGC, 2020). The public is the most important target group. For this target group, risks are assessed on the basis of personal experience (e.g., exchanges with peers), hearsay or media reports (Weber & Brian, 2014). The public includes both the affected public and the general public (IRGC, 2020). The former are individuals who will directly experience the positive and/or negative impacts from the EGS project, while the latter are individuals who are not directly affected and are part of the general public opinion on the issue (IRGC, 2020). While most efforts will be directed toward the affected public, attending to the general public is highly relevant as its opinion may affect the view of the affected public.

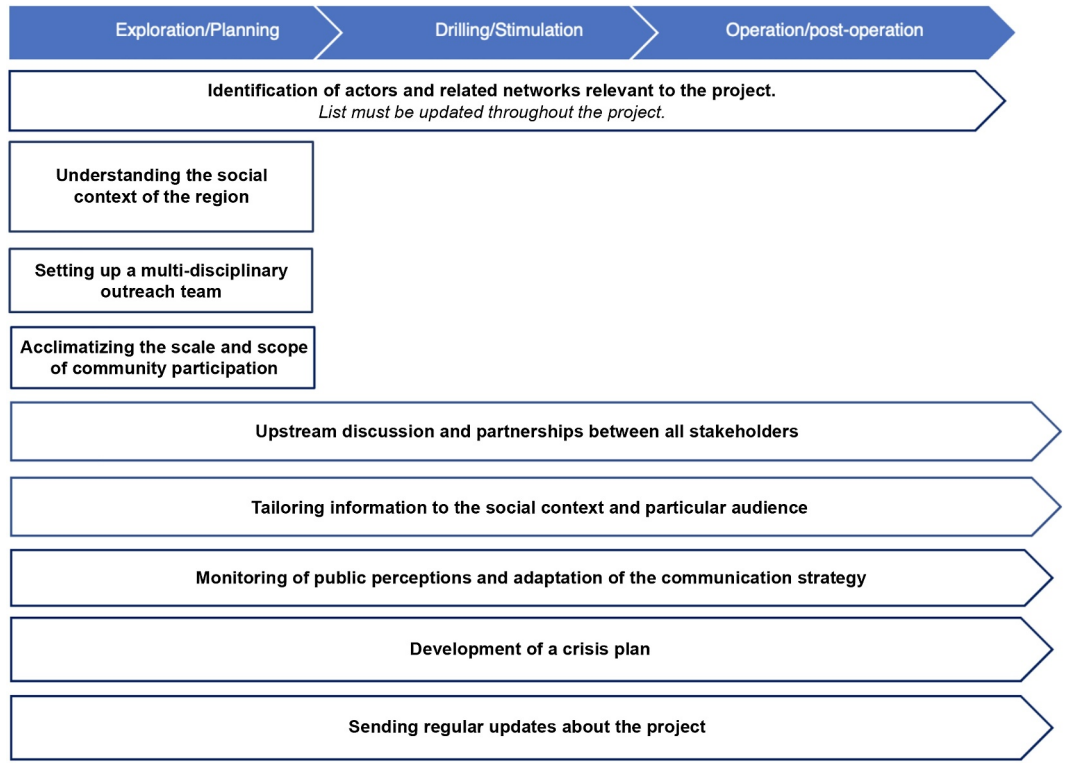

Figure 8. Summary of the general communication guidelines throughout the operational life cycle.

Recommendations for communication and stakeholder involvement

1. Communication plans must start in the earliest phases of an operation, including an identification of stakeholder networks and an understanding the social context of the region.
2. Communication plans need to understand the social context of the region.
3. Outreach teams must consist of multidisciplinary experts that are providing credible and trustworthy information.
4. Stakeholders should be able to participate in the governance process, including decisions impacting them.
5. Information should be disseminated in regular intervals and tailored for the audience—with monitoring of public perceptions updating the communication strategies.
6. Crisis plans must be prepared/practiced in advance, to ensure that key messages are communicated quickly and received well.

7.1. General Guidelines for Communication

The proposed communication guidelines consist of nine steps throughout the lifetime of the project (Figure 8).

Step 1—Identification of actors and related networks relevant to the project

Communication efforts should start in the early phases of the project (Cousse et al., 2021). EGS project developers should identify all relevant stakeholders through the connections they have with their project before defining their communication and engagement strategies (Vargas-Payera et al., 2020). These stakeholders may not be directly impacted by the project but yet have a strong weight in its success in terms of acceptance (e.g., non-governmental organizations (NGOs), general public). Among the key stakeholders, local politicians have a strong relevance as the affected population may have high trust in them. Local politicians are often able to build a bridge between the population and the other stakeholders and can give insights on how to communicate to the population. Politicians at the state and national levels have an important role to support the project developers too as EGS can help reach environmental objectives defined at the state or national level. It may however be deceptive to think that it is enough to have politicians on one's side. The legitimacy of a project always requires the approval of the

population. Without this approval, politicians may prove to be unreliable partners (Weber & Brian, 2014). The media should further be considered as an important intermediary to the public population. Other important stakeholders are the permitting authorities, the investors, and other special stakeholders, including the chambers of industry and commerce, other geothermal project developers, homeowners' and landowners' associations, NGOs and other associations with local or regional roots (e.g., citizens' climate lobbying groups) (Weber & Brian, 2014).

It is crucial to identify "local champions," which could support the project as they can indeed considerably influence the public perception (Chavot et al., 2019). For example, in the case of the St. Gallen project, the local city councilor in charge of relaying messages had a positive impact on the communication as he showed personal affiliation and dedication to the project (Diehl et al., 2017; Ejderyan et al., 2019). It is further important to identify a list of local associations which represent the diverse views and interests of the community (Weber & Brian, 2014). To build a relevant network of stakeholders, a snowball sampling technique can be used. In this technique, participants (i.e., stakeholders already identified) are asked to assist in identifying other potential subjects.

Step 2—Understanding the social context of the region

Where do conflicts (if any) originate from? What can be learned from them? What are the attitudes of local stakeholders? What kind of inconveniences will there be for the population during construction and operation? How far away are the residential areas? Are there any critical facilities nearby? The history of a town or region is very important as well as the experience of the population with similar infrastructure projects. EGS project developers can gain insights on the pulse of the local population by looking at press archives, news, social media or by conducting surveys. Such insights will reveal acceptance issues that could crop up at later stages in the process (Chavot et al., 2020). For example, if a region wishes to assert its autonomy with respect to the country where geothermal energy production is regulated at a national level, opposing geothermal energy may be a way to declare its autonomy while not necessarily implying opposition to the technology per se (Chavot et al., 2020). Understanding the social context is also highly relevant to know where potential misbeliefs about the project exist among the population (Spampatti et al., 2022). In situations with high uncertainties, such as it is the case with EGS projects, misinformation is more likely to emerge. Distinguishing the nature and origins of misinformation can be very useful to initiating a debunking strategy and to address the public's misconceptions appropriately (Dallo et al., 2022).

Step 3—Setting up a multidisciplinary outreach team

The choice of the outreach team is critical as the latter will be the "face of the project" and, consequently, will have a direct impact on how the community perceives the project and its operators (E. Majer et al., 2013). Providing information about the project is important but good communicators or moderators are needed for this and should be identified early on (Ruef et al., 2020). The outreach team should consist of communication specialists who consult with management, the industry, scientists, government officials, company stakeholders, and citizens groups (Chavot et al., 2018; E. Majer et al., 2013). The outreach team should clearly define the processes for both internal and external communications for the project. A community liaison group should be set up that represents different positions and needs from the population (e.g., Parish, local councilors, local residents and business representatives, or other interested agencies). This group not only creates requirements but is also a liaison as it has direct links with the population and can favor trust. In addition, a community liaison manager may be assigned to oversee the interactions with local residents to ensure that any problems or concerns are addressed quickly and personally (Law et al., 2019). To fit the project into the social environment, the outreach team should have considerable knowledge of politics, the population, and of the media landscape, in addition to social and technical skills (Weber & Brian, 2014).

Step 4—Acclimatizing the scale and scope of community participation

Considering population's preferences for specific participation formats allows the anchoring of a project to the social context and for appropriate ways of engaging the population (Chavot et al., 2018). Possible participation formats are highlighted in Table 6, according to their degree of participation (Trutnevyte & Wiemer, 2017; Weber & Brian, 2014). If participation is offered, there should be room for adaptation, leading to acceptance

Table 6
Opportunities for Participation Based on Weber and Brian (2014) and Trutnevyte and Wiemer (2017)

Degree of participation	Type	Description
Low	Consultation procedures (two-way)	Opportunity is offered to the population to have a stake in the decision-making process through a moderated dialog. It is particularly important here to clearly communicate in advance how much leeway is available to take into account preferences from the population
	Cooperation	Project is planned jointly by consensus and moderated by a neutral party. This option is mostly used when conflicts exist or are expected
High	Financial participation	Financial participation is offered to the municipality and its citizens during the phase where the project is less risky

compromises in the project design (Chavot et al., 2019; Dallo et al., 2022). A problematic approach is to promise cooperation and participation when the population in the end has no say or is not involved (Hirschberg et al., 2014; Holenstein, 2016). When the scale of participation is selected, formal commitments to the local and wider population should be made. Formal commitments can relate to information exchange, transparency, mitigation measures, addressing concerns, promoting cooperation, and additional benefits (Law et al., 2019). Together with these formal commitments, the mandates and responsibilities of all stakeholders should be made transparent (E. Majer et al., 2013). The population needs to be told (a) what kind of information they can expect, (b) what is not possible to communicate, (c) why, when and where they can have access to the information, (d) and who is going to distribute the information (Dallo et al., 2022).

Step 5—Set up upstream discussions and partnerships between all stakeholders

For building trust with the community and subsequently having constructive exchanges, communication strategies should not only aim to inform relevant stakeholders (i.e., downstream discussion), but should enable them to become involved in the governance process (Dallo et al., 2022; Trutnevyte & Wiemer, 2017). Trust requires personal contact, genuine interest in the opinion of others as well as reliable and transparent action (Weber & Brian, 2014). Projects that proceed without upstream discussion involving local populations may encounter strong opposition from elected officials and inhabitants (Chavot et al., 2019). Stakeholders of a project, who have good knowledge of their population as well as of the overall social context (e.g., employment, economy, education) will be better equipped to demonstrate how the project can support the community (E. Majer et al., 2013) and to understand negative public perceptions and to remedy those (e.g., pre-screening the LoC). Connecting the project to the local environment, social identity, and local politics will favor trust and relation building (Chavot et al., 2019), which are essential for the success of the project. In addition, multi-way stakeholders engagement may allow to reveal challenges linked to the project that experts may have not thought of.

These upstream discussions should start in the planning phase and close attention should be paid to raising interest in the project in order for all interested stakeholders and members of the community to have a chance to participate. In cases where the population was involved too late, communication efforts tended to be not successful (Weber & Brian, 2014). At the same time, efforts should be made to present and discuss mitigation measures to deal with the risks evoked to the population (Trutnevyte & Wiemer, 2017). It is a matter of negotiating how great the risk is and what safety measures are to be taken. Importantly, communicators need to be aware that perception of risks is different between laypeople and experts. Forums for dialog need to be created where the different stakeholders can express their perspectives, concerns and fears about the information received. For these discussions, face-to-face meetings should be used as a core tactic whenever it is possible.

Step 6—Tailoring information to the social context and particular audience (i.e., target group)

Rather than trying to convince, information should be geared to the needs and concerns of the particular audience (Dallo et al., 2022; Weber & Brian, 2014) and should be consistent between the different actors providing information (E. Majer et al., 2013). Information that does not address the risk perceived by the population will not be effective. Specifically, the information must address the concerns, misconceptions, needs of the population and be tailored to socio-demographic aspects, practical knowledge, beliefs, and motivations (Dallo et al., 2022; Karytsas & Polyzou, 2021). The dialog process must correspond exactly to the region and the project being analyzed (Holenstein, 2016).

It is better for project developers to provide information about particularly relevant topics at an early stage and on their own initiative, induced seismicity, noise, steam hazards, radon etc. (Weber & Brian, 2014). Openly talking about the risks will give less room to interpret them, and thus less room for rumors and misconceptions (Weber & Brian, 2014). It is further important to present the benefits and risks of deep geothermal projects in terms of their overall contribution to energy production (i.e., compared to other energy sources). This will mitigate the risk that the population perceives that the information is provided to them in a biased way.

Step 7—Monitoring public perceptions and adapting the communication strategy

The outreach team needs to consider the changing aspects of a social context when planning communication and engagement processes (Chavot et al., 2020; Trutnevyte & Wiemer, 2017). The changes in perceptions and concerns need to be monitored. This monitoring can be done through public meetings, interviews or surveys. For example, as soon as residents become aware of a project being planned in their neighborhood, they will expect clear answers on the expected benefits and risks (Chavot et al., 2020). To be ready for the latter, demonstrating that the project is well conceived, placing any associated risk in the proper social context and developing key messages that resonate with the community is crucial (Benighaus & Bleicher, 2019; E. Majer et al., 2013; Robertson-Tail et al., 2018).

Step 8—Developing a crisis plan

To limit the loss of confidence that comes with a crisis, the crisis plan must specify how to react to which type of crisis and the roles assumed by different stakeholders (Weber & Brian, 2014). The plan should also highlight the key messages that are to be communicated to the population in case of crisis because fast reaction will be key. For this, it is recommended to make a list of possible negative events, such as various magnitudes of induced earthquakes alongside associated damage and then prepare how to communicate transparently about each of them (Weber & Brian, 2014).

Step 9—Giving regular updates about the project

Announcements about the project (positive and negative) should be made regularly. Everyone (local population, politicians, associations, media), should be informed about the project more or less at the same time. Strategically proceeding with the announcement allows the EGS project developers to make full use of communication opportunities, occupying the population space early on, instead of leaving the sovereignty of interpretation to others (Weber & Brian, 2014).

7.2. Guidelines Specific to Communication Around Seismicity

Experience from several projects has shown that the population will be more tolerant to induced seismicity if they have been forewarned. This tolerance will be further increased if the benefits of the operation are clearly conveyed (McComas et al., 2016). Continued outreach, education, and communication are thus crucial elements to help the community understand the meaning of induced seismicity and microseismicity (Pankow et al., 2023). Communication regarding induced seismicity should be conducted with a variety of stakeholders (e.g., population, media, regulators, elected officials) during the various phases of the project and should occur pre-stimulation, during stimulation and post-stimulation. As with general communication about geothermal projects, timing of communication is critical (Dallo et al., 2022). For this, it could be useful to create a publicly available database with up-to-date information recording events. The database should quantify risk, record incidents, build up a record of risks and be made publicly accessible. It may record current activities but also anticipate future operations (e.g., risks of drilling in urban environments should be mapped proactively) (Master Plan Geothermal Energy in the Netherlands, 2018).

Furthermore, it is important to be mindful that technologies are perceived to be riskier, the more their consequences are "unknown" (effects unobservable or delayed) and the more they provoke a sense of "dread" (negative consequences potentially catastrophic and uncontrollable) (Bassarak et al., 2017; Slovic, 1987). Based on this, increasing familiarity with the underground and drilling activities appears important. In this regard, Law et al. (2019) suggests arranging events for the population where people are able to visit the underground through videos or virtual reality, providing interactive/live information or classes about geothermal energy in the curriculum.

Research has further shown that it may be most effective to use a combination of both numerical and verbal descriptions of probability when talking about earthquake risk (Dallo et al., 2022; Knoblauch et al., 2019). Verbal descriptions should not be used alone as they are often interpreted in different ways (Dallo et al., 2022). Given that it can take experts some time to analyze whether an earthquake has occurred naturally or was induced, it is crucial for operators to immediately communicate that they investigate the nature of the event while they do not know if the event is related to geothermal activities (Dallo et al., 2022).

A crisis plan specific to seismic risk requires to develop and implement a protocol that specifies the steps stakeholders must take in the event of earthquakes. The TLP should be used to define the acceptable levels of disturbance and the latter should be presented to all relevant stakeholders, including the population (Trutnevyte & Wiemer, 2017). A "calling tree" should also be built for the project management to be notified in case of seismicity. A "calling tree" is a hierarchical communication plan that indicates who should be informed when an event/emergency happens. The institution responsible for seismic monitoring in the region or country should inform the relevant stakeholders immediately in case of seismic events. The details of this "calling tree" should also be made available to the population (Pankow et al., 2023).

Abbreviations Glossary

a-value	Gutenberg-Richter *a-value*
ATLP	Adaptive Traffic Light Protocol (synonymously Adaptive Traffic Light System)
b-value	Gutenberg-Richter *b*-value
DAS	Distributed Acoustic Sensing
DSHA	Deterministic Seismic Hazard Analysis
EGS	Enhanced Geothermal System
FAIR	Findability, Accessibility, Interoperability, and Reusability
FoP	Factor of Proportionality
FORGE	Frontier Observatory for Research in Geothermal Energy
G-R	Gutenberg-Richter
GMPM	Ground Motion Prediction Model
GSIM	Ground Shaking Intensity Model
GRID	Geothermal Risk of Induced seismicity Diagnosis (Trutnevyte & Wiemer, 2017)
IM	Intensity Measure
IPM	Intensity Prediction Model
ISRMF	Induced Seismicity Risk Management Framework
LoC	Level of Concern
Mc	Magnitude of Completeness
M_{felt}	Magnitude expected to cause nuisance to stakeholders
M_L	Local Magnitude
M_W	Moment Magnitude
MMI	Modified Mercalli Intensity
M_{min}	Minimum magnitude for engineering purposes
M_{max}	Maximum possible magnitude
MCE	Maximum Credible Earthquake

PSRA	Probabilistic Seismic Risk Analysis
PSHRA	Probabilistic Seismic Hazard and Risk Analysis
PSHA	Probabilistic Seismic Hazard Analysis
SHA	Seismic Hazard Analysis
SHRA	Seismic Hazard and Risk Analysis
SNR	Signal to Noise Ratio
SRA	Seismic Risk Analysis
SVA	Seismic Vulnerability Analysis
TLP	Traffic Light Protocol (synonymously a Traffic Light System)
VSP	Vertical Seismic Profile
Σ	Seismogenic Index

Data Availability Statement

Data were not used nor created for this research. Some figures were reproduced from past studies (Schultz et al., 2021a, 2021b; Schultz, Muntendam-Bos, et al., 2022).

Acknowledgments
This project is subsidized through the Cofund GEOTHERMICA, which is supported by the European Union's HORIZON 2020 programme for research, technology development and demonstration under grant agreement no. 731117. We thank Verónica Antunes, Falko Bethmann, Laura Ermert, Toni Kraft, Claudia Finger, Rémi Fiori, Ernie Majer, Kris Pankow, Floris Post, and Philippe Roth for their comments during drafting. We are grateful to Michèle Marti, Irina Dallo, Chritopher Katis, and Olivier Zingg for their insights for Section 7 (Module 3). We would like to thank Julian Bommer and an anonymous reviewer for their comments that helped to improve this manuscript. Open access funding provided by Eidgenossische Technische Hochschule Zurich.

References

Abercrombie, R. E., Trugman, D. T., Shearer, P. M., Chen, X., Zhang, J., Pennington, C. N., et al. (2021). Does earthquake stress drop increase with depth in the crust? *Journal of Geophysical Research: Solid Earth*, *126*(10), e2021JB022314. https://doi.org/10.1029/2021JB022314

Abrahamson, N. A., & Bommer, J. J. (2005). Probability and uncertainty in seismic hazard analysis. *Earthquake Spectra*, *21*(2), 603–607. https://doi.org/10.1193/1.1899158

Ader, T., Chendorain, M., Free, M., Saarno, T., Heikkinen, P., Malin, P. E., et al. (2020). Design and implementation of a traffic light system for deep geothermal well stimulation in Finland. *Journal of Seismology*, *24*(5), 991–1014. https://doi.org/10.1007/s10950-019-09853-y

Ahmadzadeh, S., Doloei, G. J., & Zafarani, H. (2020). New intensity prediction equation for Iran. *Journal of Seismology*, *24*(1), 23–35. https://doi.org/10.1007/s10950-019-09882-7

Akram, J., & Eaton, D. (2013). Impact of velocity model calibration on microseismic locations. In *SEG technical program expanded abstracts* (pp. 1982–1986). https://doi.org/10.1190/segam2013-0795.1

Albaric, J., Oye, V., Langet, N., Hasting, M., Lecomte, I., Iranpour, K., et al. (2014). Monitoring of induced seismicity during the first geothermal reservoir stimulation at Paralana, Australia. *Geothermics*, *52*, 120–131. https://doi.org/10.1016/j.geothermics.2013.10.013

Allen, T. I., Wald, D. J., & Worden, C. B. (2012). Intensity attenuation for active crustal regions. *Journal of Seismology*, *16*(3), 409–433. https://doi.org/10.1007/s10950-012-9278-7

Allmann, B. P., & Shearer, P. M. (2009). Global variations of stress drop for moderate to large earthquakes. *Journal of Geophysical Research*, *114*(B1), 286. https://doi.org/10.1029/2008JB005821

Atkinson, G. M. (2015). Ground-motion prediction equation for small-to-moderate events at short hypocentral distances, with application to induced-seismicity hazards. *Bulletin of the Seismological Society of America*, *105*(2A), 981–992. https://doi.org/10.1785/0120140142

Atkinson, G. M., & Adams, J. (2013). Ground motion prediction equations for application to the 2015 Canadian national seismic hazard maps. *Canadian Journal of Civil Engineering*, *40*(10), 988–998. https://doi.org/10.1139/cjce-2012-0544

Atkinson, G. M., Eaton, D. W., Ghofrani, H., Walker, D., Cheadle, B., Schultz, R., et al. (2016). Hydraulic fracturing and seismicity in the Western Canada Sedimentary Basin. *Seismological Research Letters*, *87*(3), 631–647. https://doi.org/10.1785/0220150263

Atkinson, G. M., Eaton, D. W., & Igonin, N. (2020). Developments in understanding seismicity triggered by hydraulic fracturing. *Nature Reviews Earth & Environment*, *1*(5), 264–277. https://doi.org/10.1038/s43017-020-0049-7

Atkinson, G. M., & Wald, D. J. (2007). "Did you feel it?" intensity data: A surprisingly good measure of earthquake ground motion. *Seismological Research Letters*, *78*(3), 362–368. https://doi.org/10.1785/gssrl.78.3.362

Atkinson, G. M., Worden, C. B., & Wald, D. J. (2014). Intensity prediction equations for North America. *Bulletin of the Seismological Society of America*, *104*(6), 3084–3093. https://doi.org/10.1785/0120140178

Baisch, S., Koch, C., Stang, H., Pittens, B., Drijver, B., & Buik, N. (2016). IF technology BV and Q-CON GmbH. In *"Defining the framework for seismic hazard assessment in geothermal projects V0.1." technical report, Kas Als Energiebron*. Retrieved from https://www.kasalsenergiebron.nl/content/user_upload/Kennisagenda_-_Defining_framework_for_Seismic_Hazard_Assessment_in_Geothermal_Projects_-_Technical_Report_-_161005.pdf

Baisch, S., Vörös, R., Rothert, E., Stang, H., Jung, R., & Schellschmidt, R. (2010). A numerical model for fluid injection induced seismicity at Soultz-sous-Forêts. *International Journal of Rock Mechanics and Mining Sciences*, *47*(3), 405–413. https://doi.org/10.1016/j.ijrmms.2009.10.001

Baker, J., Bradley, B., & Stafford, P. (2021). *Seismic hazard and risk analysis*. Cambridge University Press.

Baltay, A. S., Abercrombie, R., Chu, S., & Taira, T. A. (2024). The SCEC/USGS community stress drop validation study using the 2019 Ridgecrest earthquake sequence. *Seismica*, *3*(1), S15C. https://doi.org/10.26443/seismica.v3i1.1009

Baltay, A. S., Hanks, T. C., & Beroza, G. C. (2013). Stable stress-drop measurements and their variability: Implications for ground-motion prediction. *Bulletin of the Seismological Society of America*, *103*(1), 211–222. https://doi.org/10.1785/0120120161

Bassarak, C., Pfister, H. R., & Böhm, G. (2017). Dispute and morality in the perception of societal risks: Extending the psychometric model. *Journal of Risk Research*, *20*(3), 299–325. https://doi.org/10.1080/13669877.2015.1043571

Baumont, D., Manchuel, K., Traversa, P., Durouchoux, C., Nayman, E., & Ameri, G. (2018). Intensity predictive attenuation models calibrated in Mw for metropolitan France. *Bulletin of Earthquake Engineering*, *16*(6), 2285–2310. https://doi.org/10.1007/s10518-018-0344-6

Bazzurro, P., & Allin Cornell, C. (1999). Disaggregation of seismic hazard. *Bulletin of the Seismological Society of America*, *89*(2), 501–520. https://doi.org/10.1785/BSSA0890020501

Bell, A. F., Naylor, M., & Main, I. G. (2013). Convergence of the frequency-size distribution of global earthquakes. *Geophysical Research Letters*, *40*(11), 2585–2589. https://doi.org/10.1002/grl.50416

Benighaus, C., & Bleicher, A. (2019). Neither risky technology nor renewable electricity: Contested frames in the development of geothermal energy in Germany. *Energy Research & Social Science*, *47*, 46–55. https://doi.org/10.1016/j.erss.2018.08.022

Bentz, S., Kwiatek, G., Martínez-Garzón, P., Bohnhoff, M., & Dresen, G. (2020). Seismic moment evolution during hydraulic stimulations. *Geophysical Research Letters*, *47*(5), e2019GL086185. https://doi.org/10.1029/2019GL086185

Bohnhoff, M., Malin, P., ter Heege, J., Deflandre, J.-P., & Sicking, C. (2018). Suggested best practice for seismic monitoring and characterization of non-conventional reservoirs. *First Break*, *36*(2), 59–64. https://doi.org/10.3997/1365-2397.n0070

Bommer, J. J. (2002). Deterministic vs. probabilistic seismic hazard assessment: An exaggerated and obstructive dichotomy. *Journal of Earthquake Engineering*, *6*(sup001), 43–73. https://doi.org/10.1080/13632460209350432

Bommer, J. J. (2012). Challenges of building logic trees for probabilistic seismic hazard analysis. *Earthquake Spectra*, *28*(4), 1723–1735. https://doi.org/10.1193/1.4000079

Bommer, J. J. (2022). Earthquake hazard and risk analysis for natural and induced seismicity: Towards objective assessments in the face of uncertainty. *Bulletin of Earthquake Engineering*, *20*(6), 2825–3069. https://doi.org/10.1007/s10518-022-01357-4

Bommer, J. J., & Crowley, H. (2017). The purpose and definition of the minimum magnitude limit in PSHA calculations. *Seismological Research Letters*, *88*(4), 1097–1106. https://doi.org/10.1785/0220170015

Bommer, J. J., Crowley, H., & Pinho, R. (2015). A risk-mitigation approach to the management of induced seismicity. *Journal of Seismology*, *19*(2), 623–646. https://doi.org/10.1007/s10950-015-9478-z

Bommer, J. J., Dost, B., Edwards, B., Stafford, P. J., van Elk, J., Doornhof, D., & Ntinalexis, M. (2016). Developing an application-specific ground-motion model for induced seismicity. *Bulletin of the Seismological Society of America*, *106*(1), 158–173. https://doi.org/10.1785/0120150184

Bommer, J. J., Douglas, J., Scherbaum, F., Cotton, F., Bungum, H., & Fäh, D. (2010). On the selection of ground-motion prediction equations for seismic hazard analysis. *Seismological Research Letters*, *81*(5), 783–793. https://doi.org/10.1785/gssrl.81.5.783

Bommer, J. J., Edwards, B., Kruiver, P. P., Rodriguez-Marek, A., Stafford, P. J., Ntinalexis, M., et al. (2022). V7 ground-motion model for induced seismicity in the Groningen gas field, Revision 1, NAM Report (p. 282). Retrieved from https://nam-onderzoeksrapporten.data-app.nl/reports/download/groningen/en/06766b7a-1999-4f48-977c-33a5d94cdd82

Bommer, J. J., Oates, S., Cepeda, J. M., Lindholm, C., Bird, J., Torres, R., et al. (2006). Control of hazard due to seismicity induced by a hot fractured rock geothermal project. *Engineering Geology*, *83*(4), 287–306. https://doi.org/10.1016/j.enggeo.2005.11.002

Bommer, J. J., & Scherbaum, F. (2008). The use and misuse of logic-trees in probabilistic seismic hazard analysis. *Earthquake Spectra*, *24*(4), 997–1009. https://doi.org/10.1193/1.2977755

Bommer, J. J., & Stafford, P. J. (2020). Selecting ground-motion models for site-specific PSHA: Adaptability versus applicability. *Bulletin of the Seismological Society of America*, *110*(6), 2801–2815. https://doi.org/10.1785/0120200171

Bommer, J. J., Stafford, P. J., Edwards, B., Dost, B., van Dedem, E., Rodriguez-Marek, A., et al. (2017). Framework for a ground-motion model for induced seismic hazard and risk analysis in the Groningen Gas Field, The Netherlands. *Earthquake Spectra*, *33*(2), 481–498. https://doi.org/10.1193/082916EQS138M

Bommer, J. J., Stafford, P. J., Ruigrok, E., Rodriguez-Marek, A., Ntinalexis, M., Kruiver, P. P., et al. (2022). Ground-motion prediction models for induced earthquakes in the Groningen gas field, The Netherlands. *Journal of Seismology*, *26*(6), 1157–1184. https://doi.org/10.1007/s10950-022-10120-w

Bommer, J. J., & Verdon, J. P. (2024). The maximum magnitude of natural and induced earthquakes. *Geomechanics and Geophysics for Geo-Energy and Geo-Resources*. https://doi.org/10.22541/essoar.171826172.29972480/v1

Boore, D. M., Joyner, W. B., & Fumal, T. E. (1997). Equations for estimating horizontal response spectra and peak acceleration from Western north American earthquakes: A summary of recent work. *Seismological Research Letters*, *68*(1), 128–153. https://doi.org/10.1785/gssrl.68.1.128

Boore, D. M., Youngs, R. R., Kottke, A. R., Bommer, J. J., Darragh, R., Silva, W. J., et al. (2022). Construction of a ground-motion logic tree through host-to-target region adjustments applied to an adaptable ground-motion prediction model. *Bulletin of the Seismological Society of America*, *112*(6), 3063–3080. https://doi.org/10.1785/0120220056

Bourne, S. J., Oates, S. J., Bommer, J. J., Dost, B., van Elk, J., & Doornhof, D. (2015). A Monte Carlo method for probabilistic hazard assessment of induced seismicity due to conventional natural gas production. *Bulletin of the Seismological Society of America*, *105*(3), 1721–1738. https://doi.org/10.1785/0120140302

Boyd, O. S., Dreger, D. S., Gritto, R., & Garcia, J. (2018). Analysis of seismic moment tensors and in situ stress during Enhanced Geothermal System development at the Geysers geothermal field, California. *Geophysical Journal International*, *215*(2), 1483–1500. https://doi.org/10.1093/gji/ggy326

Braun, T., Danesi, S., & Morelli, A. (2020). Application of monitoring guidelines to induced seismicity in Italy. *Journal of Seismology*, *24*(5), 1015–1028. https://doi.org/10.1007/s10950-019-09901-7

Brzev, S., Scawthorn, C., Charleson, A. W., Allen, L., Greene, M., Jaiswal, K., & Silva, V. (2013). *GEM building taxonomy (version 2.0) (no. 2013-02)*. GEM Foundation.

Buijze, L., van Bijsterveldt, L., Cremer, H., Paap, B., Veldkamp, H., Wassing, B. B., et al. (2019). Review of induced seismicity in geothermal systems worldwide and implications for geothermal systems in The Netherlands. *Netherlands Journal of Geosciences*, *98*, e13. https://doi.org/10.1017/njg.2019.6

Cao, N. T., Eisner, L., & Jechumtálová, Z. (2020). Next record breaking magnitude for injection induced seismicity. *First Break*, *38*(2), 53–57. https://doi.org/10.3997/1365-2397.fb2020010

Cao, W., Durucan, S., Shi, J. Q., Cai, W., Korre, A., & Ratouis, T. (2022). Induced seismicity associated with geothermal fluids re-injection: Poroelastic stressing, thermoelastic stressing, or transient cooling-induced permeability enhancement? *Geothermics*, *102*, 102404. https://doi.org/10.1016/j.geothermics.2022.102404

CAPP, Canadian Association of Petroleum Producers. (2019). Anomalous induced seismicity due to hydraulic fracturing, industry shared practices report 2019-0026 (p. 18).

CEN. (2004). *Eurocode 8: Design of structures for earthquake resistance—Part 1: General rules, seismic actions and rules for buildings*. European Committee for Standardization. Retrieved from https://eurocodes.jrc.ec.europa.eu/EN-Eurocodes/eurocode-8-design-structures-earthquake-resistance

Cesca, S., Grigoli, F., Heimann, S., González, Á., Buforn, E., Maghsoudi, S., et al. (2014). The 2013 September–October seismic sequence offshore Spain: A case of seismicity triggered by gas injection? *Geophysical Journal International*, *198*(2), 941–953. https://doi.org/10.1093/gji/ggu172

Chavot, P., Ejderyan, O., Puts, H., Cees, W., Westaway, R., Vanegas, Y. S., et al. (2020). *Risk governance strategy report (Project H2020 DESTRESS)*. Université de Strasbourg Research Report. https://doi.org/10.13140/RG.2.2.17932.67209

Chavot, P., Heimlich, C., Masseran, A., Serrano, Y., Zoungrana, J., & Bodin, C. (2018). Social shaping of deep geothermal projects in Alsace: Politics, stakeholder attitudes and local democracy. *Geothermal Energy*, *6*(1), 26. https://doi.org/10.1186/s40517-018-0111-6

Chavot, P., Masseran, A., Bodin, C., Serrano, Y., & Zoungrana, J. (2019). Geothermal energy in France. A resource fairly accepted for heating but controversial for high-energy power plants. *Geothermal Energy and Society*, *105–122*, 105–122. https://doi.org/10.1007/978-3-319-78286-7_8

Chen, S., Zhang, Q., Andrews-Speed, P., & Mclellan, B. (2020). Quantitative assessment of the environmental risks of geothermal energy: A review. *Journal of Environmental Management*, *276*, 111287. https://doi.org/10.1016/j.jenvman.2020.111287

Chioccarelli, E., Cito, P., Iervolino, I., & Giorgio, M. (2019). REASSESS V2.0: Software for single-and multi-site probabilistic seismic hazard analysis. *Bulletin of Earthquake Engineering*, *17*(4), 1769–1793. https://doi.org/10.1007/s10518-018-00531-x

Cladouhos, T. T., Petty, S., Swyer, M. W., Uddenberg, M. E., Grasso, K., & Nordin, Y. (2016). Results from Newberry volcano EGS demonstration, 2010–2014. *Geothermics*, *63*, 44–61. https://doi.org/10.1016/j.geothermics.2015.08.009

Clerc, F., Harrington, R. M., Liu, Y., & Gu, Y. J. (2016). Stress drop estimates and hypocenter relocations of induced seismicity near Crooked Lake, Alberta. *Geophysical Research Letters*, *43*(13), 6942–6951. https://doi.org/10.1002/2016GL069800

Cochran, E. S., Wickham-Piotrowski, A., Kemna, K. B., Harrington, R. M., Dougherty, S. L., & Peña Castro, A. F. (2020). Minimal clustering of injection-induced earthquakes observed with a large-n seismic array. *Bulletin of the Seismological Society of America*, *110*(5), 2005–2017. https://doi.org/10.1785/0120200101

Coglianese, C. (2018). Listening, learning, leading: A framework for regulatory excellence. *Journal of Nursing Regulation*, *8*(4), 64. https://doi.org/10.1016/s2155-8256(17)30185-0

Convertito, V., Maercklin, N., Sharma, N., & Zollo, A. (2012). From induced seismicity to direct time-dependent seismic hazard. *Bulletin of the Seismological Society of America*, *102*(6), 2563–2573. https://doi.org/10.1785/0120120036

Cotton, F., Scherbaum, F., Bommer, J. J., & Bungum, H. (2006). Criteria for selecting and adjusting ground-motion models for specific target regions: Application to central Europe and rock sites. *Journal of Seismology*, *10*(2), 137–156. https://doi.org/10.1007/s10950-005-9006-7

Cousse, J., Trutnevyte, E., & Hahnel, U. J. J. (2021). Tell me how you feel about geothermal energy: Affect as a revealing factor of the role of seismic risk on public acceptance. *Energy Policy*, *158*, 112547. https://doi.org/10.1016/j.enpol.2021.112547

Cremen, G., Werner, M. J., & Baptie, B. (2020). A new procedure for evaluating ground-motion models, with application to hydraulic-fracture-induced seismicity in the United Kingdom. *Bulletin of the Seismological Society of America*, *110*(5), 2380–2397. https://doi.org/10.1785/0120190238

Criss, R. E. (2020). *Thermal models of the continental lithosphere* (pp. 151–174). Elsevier EBooks. https://doi.org/10.1016/b978-0-12-818430-1.00006-9

Crowley, H., & Bommer, J. J. (2006). Modelling seismic hazard in earthquake loss models with spatially distributed exposure. *Bulletin of Earthquake Engineering*, *4*(3), 249–273. https://doi.org/10.1007/s10518-006-9009-y

Crowley, H., Despotaki, V., Rodrigues, D., Silva, V., Toma-Danila, D., Riga, E., et al. (2020). Exposure model for European seismic risk assessment. *Earthquake Spectra*, *36*(1_suppl), 252–273. https://doi.org/10.1177/8755293020919429

Crowley, H., Pinho, R., van Elk, J., & Uilenreef, J. (2019). Probabilistic damage assessment of buildings due to induced seismicity. *Bulletin of Earthquake Engineering*, *17*(8), 4495–4516. https://doi.org/10.1007/s10518-018-0462-1

Cypser, D. A., & Davis, S. D. (1998). Induced seismicity and the potential for liability under US law. *Tectonophysics*, *289*(1–3), 239–255. https://doi.org/10.1016/S0040-1951(97)00318-1

Dabbeek, J., Crowley, H., Silva, V., Weatherill, G., Paul, N., & Nievas, C. I. (2021). Impact of exposure spatial resolution on seismic loss estimates in regional portfolios. *Bulletin of Earthquake Engineering*, *19*(14), 5819–5841. https://doi.org/10.1007/s10518-021-01194-x

D'Alessandro, A., Luzio, D., D'Anna, G., & Mangano, G. (2011). Seismic network evaluation through simulation: An application to the Italian National Seismic Network. *Bulletin of the Seismological Society of America*, *101*(3), 1213–1232. https://doi.org/10.1785/0120100066

Dallo, I., Corradini, M., Fallou, L., & Marti, M. (2022). How to fight misinformation about earthquakes? A communication guide. *Swiss Seismological Service at ETH Zurich*. https://doi.org/10.3929/ethz-b-000530319

Davis, S. D., & Frohlich, C. (1993). Did (or will) fluid injection cause earthquakes? Criteria for a rational assessment. *Seismological Research Letters*, *64*(3–4), 207–224. https://doi.org/10.1785/gssrl.64.3-4.207

Deichmann, N., & Giardini, D. (2009). Earthquakes induced by the stimulation of an enhanced geothermal system below Basel (Switzerland). *Seismological Research Letters*, *80*(5), 784–798. https://doi.org/10.1785/gssrl.80.5.784

De Landro, G., Picozzi, M., Russo, G., Adinolfi, G. M., & Zollo, A. (2020). Seismic networks layout optimization for a high-resolution monitoring of induced micro-seismicity. *Journal of Seismology*, *24*(5), 953–966. https://doi.org/10.1007/s10950-019-09880-9

Delavaud, E., Cotton, F., Akkar, S., Scherbaum, F., Danciu, L., Beauval, C., et al. (2012). Toward a ground-motion logic tree for probabilistic seismic hazard assessment in Europe. *Journal of Seismology*, *16*(3), 451–473. https://doi.org/10.1007/s10950-012-9281-z

Dialuce, G., Chiarabba, C., Di Bucci, D., Doglioni, C., Gasparini, P., Lanari, R., et al. (2014). *Indirizzi e linee guida per il monitoraggio della sismicità, delle deformazioni del suolo e delle pressioni di poro nell'ambito delle attività antropiche*. GdL MISE.

Diehl, T., Kraft, T., Kissling, E., & Wiemer, S. (2017). The induced earthquake sequence related to the St. Gallen deep geothermal project (Switzerland): Fault reactivation and fluid interactions imaged by microseismicity. *Journal of Geophysical Research: Solid Earth*, *122*(9), 7272–7290. https://doi.org/10.1002/2017jb014473

Dorbath, L., Cuenot, N., Genter, A., & Frogneux, M. (2009). Seismic response of the fractured and faulted granite of Soultz-sous-Forêts (France) to 5 km deep massive water injections. *Geophysical Journal International*, *177*(2), 653–675. https://doi.org/10.1111/j.1365-246X.2009.04030.x

Douglas, J. (2018). Capturing geographically-varying uncertainty in earthquake ground motion models or what we think we know may change. In *Recent advances in earthquake engineering in Europe: 16th European Conference on earthquake engineering-Thessaloniki 2018* (pp. 153–181). Springer International Publishing. https://doi.org/10.1007/978-3-319-75741-4_6

Douglas, J., & Aochi, H. (2014). Using estimated risk to develop stimulation strategies for enhanced geothermal systems. *Pure and Applied Geophysics*, *171*(8), 1847–1858. https://doi.org/10.1007/s00024-013-0765-8

Douglas, J., Edwards, B., Convertito, V., Sharma, N., Tramelli, A., Kraaijpoel, D., et al. (2013). Predicting ground motion from induced earthquakes in geothermal areas. *Bulletin of the Seismological Society of America*, *103*(3), 1875–1897. https://doi.org/10.1785/0120120197

Dowrick, D., & Rhoades, D. (2005). Revised models for attenuation of modified Mercalli intensity in New Zealand earthquakes. *Bulletin of the New Zealand Society for Earthquake Engineering*, *38*(4), 185–214. https://doi.org/10.5459/bnzsee.38.4.185-214

Dutch Mining Act. (2003). Dutch mining act effective 1st January 2003 (as amended up to 1st January 2019). Retrieved from https://www.nlog.nl/en/induced-seismicity

Edwards, B., Crowley, H., Pinho, R., & Bommer, J. J. (2021). Seismic hazard and risk due to induced earthquakes at a shale gas site. *Bulletin of the Seismological Society of America*, *111*(2), 875–897. https://doi.org/10.1785/0120200234

Edwards, B., & Fäh, D. (2013). A stochastic ground-motion model for Switzerland. *Bulletin of the Seismological Society of America*, *103*(1), 78–98. https://doi.org/10.1785/0120110331

Edwards, B., Staudenmaier, N., Cauzzi, C., & Wiemer, S. (2018). A hybrid empirical Green's function technique for predicting ground motion from induced seismicity: Application to the Basel enhanced geothermal system. *Geosciences*, *8*(5), 180. https://doi.org/10.3390/geosciences8050180

Ejderyan, O., Ruef, F., & Stauffacher, M. (2019). Geothermal energy in Switzerland: Highlighting the role of context. In A. Manzella, A. Allansdottir, & A. Pellizzone (Eds.), *Geothermal energy and society* (pp. 239–257). Springer International Publishing. https://doi.org/10.1007/978-3-319-78286-7_15

Ellsworth, W. L., Giardini, D., Townend, J., Ge, S., & Shimamoto, T. (2019). Triggering of the Pohang, Korea, earthquake (Mw 5.5) by enhanced geothermal system stimulation. *Seismological Research Letters*, *90*(5), 1844. https://doi.org/10.1785/0220190102

ERN-AI. (2020). Capra tool. Retrieved from http://ecapra.org/

Federal Emergency Management Agency (FEMA). (2013). Multi-hazard loss estimation methodology, earthquake model, Hazus-MH 2.1, technical manual.

Feng, Y., Mignan, A., Sornette, D., & Li, J. (2022). Hierarchical Bayesian modeling for improved high-resolution mapping of the completeness magnitude of earthquake catalogs. *Seismological Research Letters*, *93*(4), 2126–2137. https://doi.org/10.1785/0220210368

Field, E. H., Jordan, T. H., & Cornell, C. A. (2003). OpenSHA: A developing community-modeling environment for seismic hazard analysis. *Seismological Research Letters*, *74*(4), 406–419. https://doi.org/10.1785/gssrl.74.4.406

Fiori, R., Vergne, J., Schmittbuhl, J., & Zigone, D. (2023). Monitoring induced microseismicity in an urban context using very small seismic arrays: The case study of the Vendenheim EGS project. *Geophysics*, *88*(5), WB71–WB87. https://doi.org/10.1190/geo2022-0620.1

FKPE. (2013). Empfehlungen zur Ueberwachung induzierter Seismizitaet. Retrieved from https://www.gpi.kit.edu/downloads/fkpe_ueberw_ind_seis.pdf

Foulger, G. R., Wilkinson, M. W., Wilson, M. P., Mhana, N., Tezel, T., & Gluyas, J. G. (2023). Human-induced earthquakes: E-PIE—A generic tool for evaluating proposals of induced earthquakes. *Journal of Seismology*, *27*(1), 21–44. https://doi.org/10.1007/s10950-022-10122-8

Foulger, G. R., Wilson, M. P., Gluyas, J. G., Julian, B. R., & Davies, R. J. (2018). Global review of human-induced earthquakes. *Earth-Science Reviews*, *178*, 438–514. https://doi.org/10.1016/j.earscirev.2017.07.008

Franchin, P. (2014). A computational framework for systemic seismic risk analysis of civil infrastructural systems. In K. Pitilakis, P. Franchin, B. Khazai, & H. Wenzel (Eds.), *SYNER-G: Systemic seismic vulnerability and risk assessment of complex urban, utility, lifeline systems and critical facilities* (Vol. 31, pp. 23–56). Springer. https://doi.org/10.1007/978-94-017-8835-9

Galis, M., Ampuero, J. P., Mai, P. M., & Cappa, F. (2017). Induced seismicity provides insight into why earthquake ruptures stop. *Science Advances*, *3*(12), eaap7528. https://doi.org/10.1126/sciadv.aap7528

Gaucher, E., Schoenball, M., Heidbach, O., Zang, A., Fokker, P. A., van Wees, J. D., & Kohl, T. (2015). Induced seismicity in geothermal reservoirs: A review of forecasting approaches. *Renewable and Sustainable Energy Reviews*, *52*, 1473–1490. https://doi.org/10.1016/j.rser.2015.08.026

GEORISK. (2018). GEORISK project. Retrieved from https://www.georisk-project.eu

Gerstenberger, M. C., Marzocchi, W., Allen, T., Pagani, M., Adams, J., Danciu, L., et al. (2020). Probabilistic seismic hazard analysis at regional and national scales: State of the art and future challenges. *Reviews of Geophysics*, *58*(2). https://doi.org/10.1029/2019RG000653

Giardini, D. (2009). Geothermal quake risks must be faced. *Nature*, *462*(7275), 848–849. https://doi.org/10.1038/462848a

Gischig, V. S., Bethmann, F., Hertrich, M., Wiemer, S., Mignan, A., Broccardo, M., et al. (2019). Induced seismic hazard and risk analysis of hydraulic stimulation experiments at the Bedretto Underground Laboratory for Geoenergies (BULG). *ETH Report*. https://doi.org/10.3929/ethz-b-000384348

Gischig, V. S., Giardini, D., Amann, F., Hertrich, M., Krietsch, H., Loew, S., et al. (2020). Hydraulic stimulation and fluid circulation experiments in underground laboratories: Stepping up the scale towards engineered geothermal systems. *Geomechanics for Energy and the Environment*, *24*, 100175. https://doi.org/10.1016/j.gete.2019.100175

Goda, K., & Hong, H. P. (2009). Deaggregation of seismic loss of spatially distributed buildings. *Bulletin of Earthquake Engineering*, *7*(1), 255–272. https://doi.org/10.1007/s10518-008-9093-2

Goebel, T. H. W., Hauksson, E., Shearer, P. M., & Ampuero, J. P. (2015). Stress-drop heterogeneity within tectonically complex regions: A case study of San Gorgonio Pass, southern California. *Geophysical Journal International*, *202*(1), 514–528. https://doi.org/10.1093/gji/ggv160

Goertz-Allmann, B. P., Goertz, A., & Wiemer, S. (2011). Stress drop variations of induced earthquakes at the Basel geothermal site. *Geophysical Research Letters*, *38*(9), 1–5. https://doi.org/10.1029/2011GL047498

Grigoratos, I., Bazzurro, P., Rathje, E., & Savvaidis, A. (2021). Time-dependent seismic hazard and risk due to wastewater injection in Oklahoma. *Earthquake Spectra*, *37*(3), 2084–2106. https://doi.org/10.1177/8755293020988020

Grigoratos, I., Savvaidis, A., & Rathje, E. (2022). Distinguishing the causal factors of induced seismicity in the Delaware basin: Hydraulic fracturing or wastewater disposal? *Seismological Research Letters*, *93*(5), 2640–2658. https://doi.org/10.1785/0220210320

Grigoratos, I., Schultz, R., van Ginkel, J., Gunatilake, T., & Wiemer, S. (2023). Review of the Seismic Hazard and Risk Protocol for induced seismicity related to gas production from small gas fields in The Netherlands. In *SodM report*. Retrieved from https://www.sodm.nl/actueel/nieuws/2024/04/19/evaluatie-van-de-tijdelijke-leidraad-voor-seismische-risicoanalyse-van-kleine-gasvelden

Gupta, A., & Baker, J. W. (2019). A framework for time-varying induced seismicity risk assessment, with application in Oklahoma. *Bulletin of Earthquake Engineering*, *17*(8), 4475–4493. https://doi.org/10.1007/s10518-019-00620-5

Gutenberg, B., & Richter, C. F. (1944). Frequency of earthquakes in California. *Bulletin of the Seismological Society of America*, *34*(4), 185–188. https://doi.org/10.1785/BSSA0340040185

Hardt, M., & Scherbaum, F. (1994). The design of optimum networks for aftershock recordings. *Geophysical Journal International*, *117*(3), 716–726. https://doi.org/10.1111/j.1365-246X.1994.tb02464.x

Häring, M. O., Schanz, U., Ladner, F., & Dyer, B. C. (2008). Characterisation of the Basel 1 enhanced geothermal system. *Geothermics*, *37*(5), 469–495. https://doi.org/10.1016/j.geothermics.2008.06.002

Hauksson, E. (2015). Average stress drops of Southern California earthquakes in the context of crustal geophysics: Implications for fault zone healing. *Pure and Applied Geophysics*, *172*(5), 1359–1370. https://doi.org/10.1007/s00024-014-0934-4

Hirschberg, S., Wiemer, S., & Burgherr, P. (Eds.). (2014). *Energy from the Earth: Deep geothermal as a resource for the future?* (Vol. 62). vdf Hochschulverlag AG.

Hofmann, H., Zimmermann, G., Márton Pál, F., Ernst, H., Zang, A., Leonhardt, M., et al. (2019). First field application of cyclic soft stimulation at the Pohang Enhanced Geothermal System site in Korea. *Geophysical Journal International*, *217*(2), 926–949. https://doi.org/10.1093/gji/ggz058

Holenstein, M. (2016). *Comment mettre sur pied des mécanismes de gestion participative dans le cadre de projets énergétiques complexes? L'exemple de la géothermie profonde*. Fondation «Dialogue Risque».

Holl, H.-G. (2015). *What did we learn about EGS in the Cooper Basin?* Geodynamics Limited. https://doi.org/10.13140/RG.2.2.33547.49443

Hong, H. P., & Goda, K. (2006). A comparison of seismic-hazard and risk deaggregation. *Bulletin of the Seismological Society of America*, *96*(6), 2021–2039. https://doi.org/10.1785/0120050238

Hosseinpour, V., Saeidi, A., Nollet, M. J., & Nastev, M. (2021). Seismic loss estimation software: A comprehensive review of risk assessment steps, software development and limitations. *Engineering Structures*, *232*, 111866. https://doi.org/10.1016/j.engstruct.2021.111866

Huang, Y., Ellsworth, W. L., & Beroza, G. C. (2017). Stress drops of induced and tectonic earthquakes in the central United States are indistinguishable. *Science Advances*, *3*(8), e1700772. https://doi.org/10.1126/sciadv.1700772

Im, K., & Avouac, J. P. (2021). On the role of thermal stress and fluid pressure in triggering seismic and aseismic faulting at the Brawley Geothermal Field, California. *Geothermics*, *97*, 102238. https://doi.org/10.1016/j.geothermics.2021.102238

IMEPLS (Italian Ministry of the Environment and the Protection of Land and Sea). (2016). Linee Guida per l'utilizzazione della risorsa geotermica a media e alta entalpia. Retrieved from https://www.cngeologi.it/wp-content/uploads/2016/10/Linee_guida_geotermia.pdf

Ineris & BRGM. (2023). Guide de bonnes pratiques pour la maîtrise de la sismicité induite par les opérations de géothermie profonde. De Santis F., Maury J., Klein E., Peter-Borie M., Contrucci I., Dominique P. Retrieved from https://www.ecologie.gouv.fr/sites/default/files/Guide-geothermie.pdf

IRGC. (2020). Involving stakeholders in the risk governance process. Retrieved from https://irgc.org/risk-governance/irgc-risk-governance-framework/

Jayaram, N., & Baker, J. W. (2009). Correlation model for spatially distributed ground-motion intensities. *Earthquake Engineering & Structural Dynamics*, *38*(15), 1687–1708. https://doi.org/10.1002/eqe.922

Jeong, S. J., Stump, B. W., DeShon, H. R., & Quinones, L. (2021). Stress-drop estimates for induced seismic events in the Fort worth basin, Texas. *Bulletin of the Seismological Society of America*, *111*(3), 1405–1421. https://doi.org/10.1785/0120200268

Kallioras, S., Graziotti, F., & Penna, A. (2019). Numerical assessment of the dynamic response of a URM terraced house exposed to induced seismicity. *Bulletin of Earthquake Engineering*, *17*(3), 1521–1552. https://doi.org/10.1007/s10518-018-0495-5

Karytsas, S., & Polyzou, O. (2021). Social acceptance of geothermal power plants. In *Thermodynamic analysis and optimization of geothermal power plants* (pp. 65–79). Elsevier. https://doi.org/10.1016/B978-0-12-821037-6.00004-4

Kim, K.-H., Ree, J.-H., Kim, Y., Kim, S., Kang, S. Y., & Seo, W. (2018). Assessing whether the 2017Mw5.4 Pohang earthquake in South Korea was an induced event. *Science*, *360*(6392), 1007–1009. https://doi.org/10.1126/science.aat6081

Knoblauch, T. A. K., Trutnevyte, E., & Stauffacher, M. (2019). Siting deep geothermal energy: Acceptance of various risk and benefit scenarios in a Swiss-German cross-national study. *Energy Policy*, *128*, 807–816. https://doi.org/10.1016/j.enpol.2019.01.019

Kohrangi, M., Vamvatsikos, D., & Bazzurro, P. (2016). Implications of intensity measure selection for seismic loss assessment of 3-D buildings. *Earthquake Spectra*, *32*(4), 2167–2189. https://doi.org/10.1193/112215EQS177M

Koirala, R., Kwiatek, G., Shirzaei, M., Brodsky, E., Cladouhos, T., Swyer, M., & Goebel, T. (2024). Induced seismicity and surface deformation associated with long-term and abrupt geothermal operations in Blue Mountain, Nevada. *Earth and Planetary Science Letters*, *643*, 118883. https://doi.org/10.1016/j.epsl.2024.118883

Kraft, T., Mignan, A., & Giardini, D. (2013). Optimization of a large-scale microseismic monitoring network in northern Switzerland. *Geophysical Journal International*, *195*(1), 474–490. https://doi.org/10.1093/gji/ggt225

Kraft, T., Roth, P., & Wiemer, S. (2020). Good practice guide for managing induced seismicity in deep geothermal energy projects in Switzerland. Retrieved from www.research-collection.ethz.ch

Kwiatek, G., Bulut, F., Bohnhoff, M., & Dresen, G. (2014). High-resolution analysis of seismicity induced at Berlín geothermal field, El Salvador. *Geothermics*, *52*, 98–111. https://doi.org/10.1016/j.geothermics.2013.09.008

Kwiatek, G., Grigoratos, I., & Wiemer, S. (2024). Variability of seismicity rates and maximum magnitude for Adjacent hydraulic stimulations. *Seismological Research Letters*. https://doi.org/10.1785/0220240043

Kwiatek, G., Saarno, T., Ader, T., Bluemle, F., Bohnhoff, M., Chendorain, M., et al. (2019). Controlling fluid-induced seismicity during a 6.1-km-deep geothermal stimulation in Finland. *Science Advances*, *5*(5), eaav7224. https://doi.org/10.1126/sciadv.aav7224

Langenbruch, C., Ellsworth, W. L., Woo, J.-U., & Wald, D. J. (2020). Value at induced risk: Injection induced seismic risk from low-probability, high-impact events. *Geophysical Research Letters*, *47*(2), e2019GL085878. https://doi.org/10.1029/2019GL085878

Langenbruch, C., & Shapiro, S. A. (2010). Decay rate of fluid-induced seismicity after termination of reservoir stimulations. *Geophysics*, *75*(6), MA53–MA62. https://doi.org/10.1190/1.3506005

Law, R., Cotton, L., & Ledingham, P. (2019). The united downs deep geothermal power project. In *Conference proceedings, EGC 2019*. Retrieved from https://europeangeothermalcongress.eu/wp-content/uploads/2019/07/21.pdf

Le Goff, B., Borges, J. F., & Bezzeghoud, M. (2014). Intensity-distance attenuation laws for the Portugal mainland using intensity data points. *Geophysical Journal International*, *199*(2), 1278–1285. https://doi.org/10.1093/gji/ggu317

Lei, X., Huang, D., Su, J., Jiang, G., Wang, X., Wang, H., et al. (2017). Fault reactivation and earthquakes with magnitudes of up to Mw4. 7 induced by shale-gas hydraulic fracturing in Sichuan Basin, China. *Scientific Reports*, *7*(1), 7971. https://doi.org/10.1038/s41598-017-08557-y

Lei, X., Wang, Z., & Su, J. (2019a). The December 2018 M_L 5.7 and January 2019 M_L 5.3 earthquakes in South Sichuan basin induced by shale gas hydraulic fracturing. *Seismological Research Letters*, *90*(3), 1099–1110. https://doi.org/10.1785/0220190029

Lei, X., Wang, Z., & Su, J. (2019b). Possible link between long-term and short-term water injections and earthquakes in salt mine and shale gas site in Changning, south Sichuan Basin, China. *Earth and Planetary Physics*, *3*(6), 510–525. https://doi.org/10.26464/epp2019052

Leonard, M. (2014). Self-consistent earthquake fault-scaling relations: Update and extension to stable continental strike-slip faults. *Bulletin of the Seismological Society of America*, *104*(6), 2953–2965. https://doi.org/10.1785/0120140087

Lockman, A. B., & Allen, R. M. (2005). Single-station earthquake characterization for early warning. *Bulletin of the Seismological Society of America*, *95*(6), 2029–2039. https://doi.org/10.1785/0120040241

Luckett, R., Ottemöller, L., Butcher, A., & Baptie, B. (2019). Extending local magnitude M_L to short distances. *Geophysical Journal International*, *216*(2), 1145–1156. https://doi.org/10.1093/gji/ggy484

Mahani, A. B., Schultz, R., Kao, H., Walker, D., Johnson, J., & Salas, C. (2017). Fluid injection and seismic activity in the northern Montney play, British Columbia, Canada, with special reference to the 17 August 2015 Mw 4.6 induced earthquake. *Bulletin of the Seismological Society of America*, *107*(2), 542–552. https://doi.org/10.1785/0120160175

Majer, E., Nelson, J., Robertson-Tait, A., Savy, J., & Wong, I. (2012). *Protocol for addressing induced seismicity associated with enhanced geothermal systems*. US Department of Energy. https://doi.org/10.2172/1219482

Majer, E., Nelson, J., Robertson-Tait, A., Savy, J., & Wong, I. (2013). *Best practices for addressing induced seismicity associated with enhanced geothermal systems (EGS)*. Lawrence Berkeley National Laboratory & US Department of Energy. Retrieved from https://escholarship.org/uc/item/3446g9cf

Majer, E. L., & Peterson, J. E. (2007). The impact of injection on seismicity at the Geysers, California Geothermal Field. *International Journal of Rock Mechanics and Mining Sciences*, *44*(8), 1079–1090. https://doi.org/10.1016/j.ijrmms.2007.07.023

Mak, S., Cotton, F., & Schorlemmer, D. (2017). Measuring the performance of ground-motion models: The importance of being independent. *Seismological Research Letters*, *88*(5), 1212–1217. https://doi.org/10.1785/0220170097

Markhvida, M., & Baker, J. W. (2023). Modeling future economic costs and interdependent industry recovery after earthquakes. *Earthquake Spectra*, *39*(2), 914–937. https://doi.org/10.1177/87552930231162385

Martins, L., & Silva, V. (2020). Development of a fragility and vulnerability model for global seismic risk analyses. *Bulletin of Earthquake Engineering*, *19*(15), 6719–6745. https://doi.org/10.1007/s10518-020-00885-1

Martins, L., Silva, V., Crowley, H., & Cavalieri, F. (2021). Vulnerability modellers toolkit, an open-source platform for vulnerability analysis. *Bulletin of Earthquake Engineering*, *19*(13), 5691–5709. https://doi.org/10.1007/s10518-021-01187-w

Marzocchi, W., & Sandri, L. (2003). A review and new insights on the estimation of the b-value and its uncertainty. *Annals of Geophysics*. Retrieved from http://hdl.handle.net/2122/1017

Marzocchi, W., Spassiani, I., Stallone, A., & Taroni, M. (2020). How to be fooled searching for significant variations of the b-value. *Geophysical Journal International*, *220*(3), 1845–1856. https://doi.org/10.1093/gji/ggz541

Massa, M., Barani, S., & Lovati, S. (2014). Overview of topographic effects based on experimental observations: Meaning, causes and possible interpretations. *Geophysical Journal International*, *197*(3), 1537–1550. https://doi.org/10.1093/gji/ggt341

Master Plan Geothermal Energy in the Netherlands. (2018). A broad foundation for sustainable heat supply. Retrieved from https://geothermie.nl/images/bestanden/Masterplan_Aardwarmte_in_Nederland_ENG.pdf

Maxwell, S. C., Jones, M., Parker, R., Miong, S., Leaney, S., Dorval, D., & Hammermaster, K. (2009). Fault activation during hydraulic fracturing. In *SEG international exposition and annual meeting (SEG-2009)*. SEG.

Maxwell, S. C., Rutledge, J., Jones, R., & Fehler, M. (2010). Petroleum reservoir characterization using downhole microseismic monitoring. *Geophysics*, *75*(5), 75A129–75A137. https://doi.org/10.1190/1.3477966

McClure, M. W., & Horne, R. N. (2011). Investigation of injection-induced seismicity using a coupled fluid flow and rate/state friction model. *Geophysics*, *76*(6), WC181–WC198. https://doi.org/10.1190/geo2011-0064.1

McComas, K. A., Lu, H., Keranen, K. M., Furtney, M. A., & Song, H. (2016). Public perceptions and acceptance of induced earthquakes related to energy development. *Energy Policy*, *99*, 27–32. https://doi.org/10.1016/j.enpol.2016.09.026

McGarr, A. (2014). Maximum magnitude earthquakes induced by fluid injection. *Journal of Geophysical Research: Solid Earth*, *119*(2), 1008–1019. https://doi.org/10.1002/2013jb010597

McGarr, A., Simpson, D., & Seeber, L. (2002). 40 Case histories of induced and triggered seismicity. *International Geophysics*, *81*(PART A), 647–661. https://doi.org/10.1016/S0074-6142(02)80243-1

McGuire, R. K. (1995). Probabilistic seismic hazard analysis and design earthquakes: Closing the loop. *Bulletin of the Seismological Society of America*, *85*(5), 1275–1284. https://doi.org/10.1785/BSSA0850051275

McGuire, R. K. (2004). *Seismic hazard and risk analysis* (p. 221). Earthquake Engineering Research Institute, EERI Publication No. MNO-10.

Michael, A. J. (2014). How complete is the ISC-GEM global earthquake catalog? *Bulletin of the Seismological Society of America*, *104*(4), 1829–1837. https://doi.org/10.1785/0120130227

Mignan, A. (2012). Functional shape of the earthquake frequency-magnitude distribution and completeness magnitude. *Journal of Geophysical Research*, *117*(B8), 8302. https://doi.org/10.1029/2012JB009347

Mignan, A., Broccardo, M., Wiemer, S., & Giardini, D. (2017). Induced seismicity closed-form traffic light system for actuarial decision-making during deep fluid injections. *Scientific Reports*, *7*(1), 13607. https://doi.org/10.1038/s41598-017-13585-9

Mignan, A., Landtwing, D., Kaestli, P., Mena, B., & Wiemer, S. (2015). Induced seismicity risk analysis of the 2006 Basel, Switzerland, Enhanced Geothermal System project: Influence of uncertainties on risk mitigation. *Geothermics*, *53*, 133–146. https://doi.org/10.1016/j.geothermics.2014.05.007

Mignan, A., Werner, M. J., Wiemer, S., Chen, C.-C., & Wu, Y.-M. (2011). Bayesian estimation of the spatially varying completeness magnitude of earthquake catalogs. *Bulletin of the Seismological Society of America*, *101*(3), 1371–1385. https://doi.org/10.1785/0120100223

Mizrahi, L., Dallo, I., van der Elst, N. J., Christophersen, A., Spassiani, I., Werner, M. J., et al. (2024). Developing, testing, and communicating earthquake forecasts: Current practices and future directions. *Reviews of Geophysics*, *62*(3), e2023RG000823. https://doi.org/10.1029/2023RG000823

Moein, M. J., Langenbruch, C., Schultz, R., Grigoli, F., Ellsworth, W. L., Wang, R., et al. (2023). The physical mechanisms of induced earthquakes. *Nature Reviews Earth & Environment*, *4*(12), 847–863. https://doi.org/10.1038/s43017-023-00497-8

Molina, S., Lang, D. H., & Lindholm, C. D. (2010). SELENA—An open-source tool for seismic risk and loss assessment using a logic tree computation procedure. *Computers & Geosciences*, *36*(3), 257–269. https://doi.org/10.1016/j.cageo.2009.07.006

Moore, J., McLennan, J., Allis, R., Pankow, K., Simmons, S., Podgorney, R., et al. (2019). The Utah frontier observatory for research in geothermal energy (FORGE): An international laboratory for enhanced geothermal system technology development. In *44th workshop on geothermal reservoir engineering. Stanford*. Retrieved from https://pangea.stanford.edu/ERE/pdf/IGAstandard/SGW/2019/Moore.pdf

Muntendam-Bos, A. G., Hoedeman, G., Polychronopoulou, K., Draganov, D., Weemstra, C., van der Zee, W., et al. (2022). An overview of induced seismicity in The Netherlands. *Netherlands Journal of Geosciences*, *101*(e1), e1. https://doi.org/10.1017/njg.2021.14

Navas-Portella, V., González, Á., Serra, I., Vives, E., & Corral, Á. (2019). Universality of power-law exponents by means of maximum-likelihood estimation. *Physical Review E*, *100*(6), 062106. https://doi.org/10.1103/PhysRevE.100.062106

Nievas, C. I., Bommer, J. J., Crowley, H., & van Elk, J. (2019). Global occurrence and impact of small-to-medium magnitude earthquakes: A statistical analysis. *Bulletin of Earthquake Engineering*, *18*(1), 1–35. https://doi.org/10.1007/s10518-019-00718-w

Norbeck, J., & Latimer, T. (2023). Commercial-scale demonstration of a first-of-a-kind enhanced geothermal system. *EarthArXiv (California Digital Library)*. https://doi.org/10.31223/x52x0b

Novakovic, M., Atkinson, G. M., & Assatourians, K. (2018). Empirically calibrated ground-motion prediction equation for Oklahoma. *Bulletin of the Seismological Society of America*, *108*(5A), 2444–2461. https://doi.org/10.1785/0120170331
Ordaz, M., Salgado-Gálvez, M. A., & Giraldo, S. (2021). R-CRISIS: 35 years of continuous developments and improvements for probabilistic seismic hazard analysis. *Bulletin of Earthquake Engineering*, *19*(7), 2797–2816. https://doi.org/10.1007/s10518-021-01098-w
Oth, A. (2013). On the characteristics of earthquake stress release variations in Japan. *Earth and Planetary Science Letters*, *377*, 132–141. https://doi.org/10.1016/j.epsl.2013.06.037
Pagani, M., Monelli, D., Weatherill, G., Danciu, L., Crowley, H., Silva, V., et al. (2014). OpenQuake engine: An open hazard (and risk) software for the global earthquake model. *Seismological Research Letters*, *85*(3), 692–702. https://doi.org/10.1785/0220130087
Pankow, K., Rutledge, J., Wannamaker, P., & Whidden, K. (2023). *Utah FORGE induced seismicity mitigation plan* (p. 224). University of Utah Report. Retrieved from https://gdr.openei.org/submissions/1524
Paolucci, R., Mazzieri, I., Piunno, G., Smerzini, C., Vanini, M., & Özcebe, A. G. (2020). Earthquake ground motion modeling of induced seismicity in the Groningen gas field. *Earthquake Engineering & Structural Dynamics*, *50*(1), 135–154. https://doi.org/10.1002/eqe.3367
Papadopoulos, A. N., Bazzurro, P., & Marzocchi, W. (2020). Exploring probabilistic seismic risk assessment accounting for seismicity clustering and damage accumulation: Part I. Hazard analysis. *Earthquake Spectra*, *37*(2), 803–826. https://doi.org/10.1177/8755293020957338
Papadopoulos, A. N., Roth, P., & Danciu, L. (2024). Exposure manipulation strategies for balancing computational efficiency and precision in seismic risk analysis. *Bulletin of Earthquake Engineering*, *22*(9), 1–17. https://doi.org/10.1007/s10518-024-01929-6
Parisio, F., Vilarrasa, V., Wang, W., Kolditz, O., & Nagel, T. (2019). The risks of long-term re-injection in supercritical geothermal systems. *Nature Communications*, *10*(1), 4391. https://doi.org/10.1038/s41467-019-12146-0
Park, J., Bazzurro, P., & Baker, J. W. (2007). Modeling spatial correlation of ground motion intensity measures for regional seismic hazard and portfolio loss estimation. In T. Kanda & K. Faruta (Eds.), *Applications of statistics and probability in civil engineering*. Taylor & Francis Group.
Paulik, R., Horspool, N., Woods, R., Griffiths, N., Beale, T., Magill, C., et al. (2023). RiskScape: A flexible multi-hazard risk modelling engine. *Natural Hazards*, *119*(2), 1073–1090. https://doi.org/10.1007/s11069-022-05593-4
Pawley, S., Schultz, R., Playter, T., Corlett, H., Shipman, T., Lyster, S., & Hauck, T. (2018). The geological susceptibility of induced earthquakes in the Duvernay Play. *Geophysical Research Letters*, *45*(4), 1786–1793. https://doi.org/10.1002/2017gl076100
Petersen, M. D., Mueller, C. S., Moschetti, M. P., Hoover, S. M., Llenos, A. L., Ellsworth, W. L., et al. (2016). Seismic-hazard forecast for 2016 including induced and natural earthquakes in the central and eastern United States. *Seismological Research Letters*, *87*(6), 1327–1341. https://doi.org/10.1785/0220160072
Pitilakis, K., Crowley, H., & Kaynia, A. M. (2014). SYNER-G: Typology definition and fragility functions for physical elements at seismic risk. *Geotechnical, Geological and Earthquake Engineering*, *27*, 1–28. https://doi.org/10.1007/978-94-007-7872-6
Plenkers, K., Husen, S., & Kraft, T. (2015). A multi-step assessment scheme for seismic network site selection in densely populated areas. *Journal of Seismology*, *19*(4), 861–879. https://doi.org/10.1007/s10950-015-9500-5
Robertson-Tait, A., Villavert, M., Kennedy, M., Blankenship, D., Sullivan, P., Tang, J., et al. (2018). Communications and outreach for public acceptance of complex technical projects: Experience from the Fallon FORGE project. In *PROCEEDINGS, 43rd workshop on geothermal reservoir engineering Stanford University, Stanford, California, February 12–14, 2018 SGP-TR-213*.
Robinson, D., Fulford, G., & Dhu, T. (2005). *EQRM: Geoscience Australia's earthquake risk model: Technical manual: Version 3.0, GA record 2005/01*. Geoscience Australia.
Roy, C., Nowacki, A., Zhang, X., Curtis, A., & Baptie, B. (2021). Accounting for natural uncertainty within monitoring systems for induced seismicity based on earthquake magnitudes. *Frontiers in Earth Science*, *9*, 634688. https://doi.org/10.3389/feart.2021.634688
Ruef, F., Stauffacher, M., & Ejderyan, O. (2020). Blind spots of participation: How differently do geothermal energy managers and residents understand participation? *Energy Reports*, *6*, 1950–1962. https://doi.org/10.1016/j.egyr.2020.07.003
Ruigrok, E., Kruiver, P., & Dost, B. (2023). Construction of earthquake location uncertainty maps for The Netherlands. In *KNMI report number: TR-405* (p. 158).
Sandri, L., & Marzocchi, W. (2007). A technical note on the bias in the estimation of the b-value and its uncertainty through the Least Squares technique. *Annals of Geophysics*, *50*(3), 329–339. Retrieved from http://hdl.handle.net/2122/3671
Scherbaum, F., Delavaud, E., & Riggelsen, C. (2009). Model selection in seismic hazard analysis: An information-theoretic perspective. *Bulletin of the Seismological Society of America*, *99*(6), 3234–3247. https://doi.org/10.1785/0120080347
Scherbaum, F., & Kuehn, N. M. (2011). Logic tree branch weights and probabilities: Summing up to one is not enough. *Earthquake Spectra*, *27*(4), 1237–1251. https://doi.org/10.1193/1.3652744
Schmittbuhl, J., Lambotte, S., Lengliné, O., Grunberg, M., Jund, H., Vergne, J., et al. (2021). Induced and triggered seismicity below the city of Strasbourg, France from November 2019 to January 2021. *Comptes Rendus Geoscience*, *353*(S1), 561–584. https://doi.org/10.5802/crgeos.71
Schorlemmer, D., & Woessner, J. (2008). Probability of detecting an earthquake. *Bulletin of the Seismological Society of America*, *98*(5), 2103–2117. https://doi.org/10.1785/0120070105
Schultz, R. (2024). Inferring maximum magnitudes from the ordered sequence of large earthquakes. *Philosophical Transactions A*, *382*, 2276. https://doi.org/10.1098/rsta.2023.0185
Schultz, R., Atkinson, G., Eaton, D. W., Gu, Y. J., & Kao, H. (2018). Hydraulic fracturing volume is associated with induced earthquake productivity in the Duvernay play. *Science*, *359*(6373), 304–308. https://doi.org/10.1126/science.aao0159
Schultz, R., Baptie, B., Edwards, B., & Wiemer, S. (2023). Red-light thresholds for induced seismicity in the UK. *Seismica*, *2*(2). https://doi.org/10.26443/seismica.v2i2.1086
Schultz, R., Beroza, G., Ellsworth, W., & Baker, J. (2020). Risk-informed recommendations for managing hydraulic fracturing–induced seismicity via traffic light protocols. *Bulletin of the Seismological Society of America*, *110*(5), 2411–2422. https://doi.org/10.1785/0120200016
Schultz, R., Beroza, G. C., & Ellsworth, W. L. (2021a). A risk-based approach for managing hydraulic fracturing–induced seismicity. *Science*, *372*(6541), 504–507. https://doi.org/10.1126/science.abg5451
Schultz, R., Beroza, G. C., & Ellsworth, W. L. (2021b). A strategy for choosing red-light thresholds to manage hydraulic fracturing induced seismicity in North America. *Journal of Geophysical Research: Solid Earth*, *126*(12), e2021JB022340. https://doi.org/10.1029/2021jb022340
Schultz, R., Ellsworth, W. L., & Beroza, G. C. (2022). Statistical bounds on how induced seismicity stops. *Scientific Reports*, *12*(1), 1184. https://doi.org/10.1038/s41598-022-05216-9
Schultz, R., Ellsworth, W. L., & Beroza, G. C. (2023). An ensemble approach to characterizing trailing-induced seismicity. *Seismological Research Letters*, *94*(2A), 699–707. https://doi.org/10.1785/0220220352
Schultz, R., Muntendam-Bos, A., Zhou, W., Beroza, G. C., & Ellsworth, W. L. (2022). Induced seismicity red-light thresholds for enhanced geothermal prospects in The Netherlands. *Geothermics*, *106*, 102580. https://doi.org/10.1016/j.geothermics.2022.102580

Schultz, R., Quitoriano, V., Wald, D. J., & Beroza, G. C. (2021). Quantifying nuisance ground motion thresholds for induced earthquakes. *Earthquake Spectra*, *37*(2), 789–802. https://doi.org/10.1177/8755293020988025

Schultz, R., Skoumal, R. J., Brudzinski, M. R., Eaton, D., Baptie, B., & Ellsworth, W. (2020). Hydraulic fracturing-induced seismicity. *Reviews of Geophysics*, *58*(3), e2019RG000695. https://doi.org/10.1029/2019RG000695

Schultz, R., Wang, R., Gu, Y. J., Haug, K., & Atkinson, G. (2017). A seismological overview of the induced earthquakes in the Duvernay play near Fox Creek, Alberta. *Journal of Geophysical Research: Solid Earth*, *122*(1), 492–505. https://doi.org/10.1002/2016JB013570

Schultz, R., Yusifbayov, J., & Shipman, T. (2020). The scientific induced seismicity monitoring network (SCISMN). In *AER/AGS open file report 2019-09* (p. 16). Alberta Geological Survey/Alberta Energy Regulator.

Segall, P., & Lu, S. (2015). Injection-induced seismicity: Poroelastic and earthquake nucleation effects. *Journal of Geophysical Research: Solid Earth*, *120*(7), 5082–5103. https://doi.org/10.1002/2015JB012060

Shapiro, S. A. (2015). *Fluid-induced seismicity*. Cambridge University Press.

Shapiro, S. A., Dinske, C., Langenbruch, C., & Wenzel, F. (2010). Seismogenic index and magnitude probability of earthquakes induced during reservoir fluid stimulations. *The Leading Edge*, *29*(3), 304–309. https://doi.org/10.1190/1.3353727

Shapiro, S. A., Krüger, O. S., & Dinske, C. (2013). Probability of inducing given-magnitude earthquakes by perturbing finite volumes of rocks. *Journal of Geophysical Research: Solid Earth*, *118*(7), 3557–3575. https://doi.org/10.1002/jgrb.50264

Sharma, N., Convertito, V., De Matteis, R., & Capuano, P. (2022). Strong ground-motion prediction equations from induced earthquakes in St. Gallen geothermal field, Switzerland. *Journal of Geophysics and Engineering*, *19*(4), 820–832. https://doi.org/10.1093/jge/gxac044

Sharma, N., Convertito, V., Maercklin, N., & Zollo, A. (2013). Ground-motion prediction equations for the Geysers geothermal area based on induced seismicity records. *Bulletin of the Seismological Society of America*, *103*(1), 117–130. https://doi.org/10.1785/0120120138

Silva, V., Akkar, S., Baker, J., Bazzurro, P., Castro, J. M., Crowley, H., et al. (2019). Current challenges and future trends in analytical fragility and vulnerability modelling. *Earthquake Spectra*, *35*(4), 1927–1952. https://doi.org/10.1193/042418EQS101O

Silva, V., Amo-Oduro, D., Calderon, A., Costa, C., Dabbeek, J., Despotaki, V., et al. (2020). Development of a global seismic risk model. *Earthquake Spectra*, *36*(1_suppl), 372–394. https://doi.org/10.1177/8755293019899953

Silva, V., Brzev, S., Scawthorn, C., Yepes, C., Dabbeek, J., & Crowley, H. (2022). A building classification system for multi-hazard risk assessment. *International Journal of Disaster Risk Science*, *13*(2), 161–177. https://doi.org/10.1007/s13753-022-00400-x

Silva, V., Crowley, H., Pagani, M., Monelli, D., & Pinho, R. (2014). Development of the OpenQuake engine, the Global Earthquake Model's open-source software for seismic risk assessment. *Natural Hazards*, *72*(3), 1409–1427. https://doi.org/10.1007/s11069-013-0618-x

Silva, V., Yepes-Estrada, C., Dabbeek, J., Martins, L., & Brzev, S. (2018). *GED4ALL-Global exposure database for multi-hazard risk analysis–multi-hazard exposure taxonomy*. Global Earthquake Model Foundation.

Slovic, P. (1987). Perception of risk. *Science*, *236*(4799), 280–285. https://doi.org/10.1126/science.3563507

Sousa, R., Silva, V., & Rodrigues, H. (2022). The importance of indirect losses in the seismic risk assessment of industrial buildings—An application to precast RC buildings in Portugal. *International Journal of Disaster Risk Reduction*, *74*, 102949. https://doi.org/10.1016/j.ijdrr.2022.102949

Spampatti, T., Hahnel, U. J. J., Trutnevyte, E., & Brosch, T. (2022). Short and long-term dominance of negative information in shaping public energy perceptions: The case of shallow geothermal systems. *Energy Policy*, *167*, 113070. https://doi.org/10.1016/j.enpol.2022.113070

Stauffacher, M., Muggli, N., Scolobig, A., & Moser, C. (2015). Framing deep geothermal energy in mass media: The case of Switzerland. *Technological Forecasting and Social Change*, *98*, 60–70. https://doi.org/10.1016/j.techfore.2015.05.018

Strasser, F. O., Bommer, J. J., & Abrahamson, N. A. (2008). Truncation of the distribution of ground-motion residuals. *Journal of Seismology*, *12*(1), 79–105. https://doi.org/10.1007/s10950-007-9073-z

Sun, X., Yang, P., & Zhang, Z. (2017). A study of earthquakes induced by water injection in the Changning salt mine area, SW China. *Journal of Asian Earth Sciences*, *136*, 102–109. https://doi.org/10.1016/j.jseaes.2017.01.030

Taroni, M. (2022). The effect of magnitude uncertainty on the Gutenberg–Richter *b*-value estimation and the magnitude–frequency distribution: 'What hump? *Geophysical Journal International*, *231*(2), 907–911. https://doi.org/10.1093/gji/ggac219

Templeton, D. C., Schoenball, M., Layland-Bachmann, C., Foxall, W., Guglielmi, Y., Kroll, K., et al. (2021). *Recommended practices for managing induced seismicity risk associated with geologic Carbon storage; NRAP-TRS-I-001-2021; DOE.NETL-2021.2839; NRAP technical report series* (p. 80). U.S. Department of Energy, National Energy Technology Laboratory. https://doi.org/10.2172/1841840

Templeton, D. C., Schoenball, M., Layland-Bachmann, C. E., Foxall, W., Guglielmi, Y., Kroll, K. A., et al. (2023). A project lifetime approach to the management of induced seismicity risk at geologic carbon storage sites. *Seismological Research Letters*, *94*(1), 113–122. https://doi.org/10.1785/0220210284

Teng, G., Baker, J. W., & Wald, D. J. (2022). Evaluation of intensity prediction equations (IPEs) for small-magnitude earthquakes. *Bulletin of the Seismological Society of America*, *112*(1), 316–330. https://doi.org/10.1785/0120210150

Terrier, M., De Santis, F., Soliva, R., Valley, B., Bruel, D., Géraud, Y., & Schmittbuhl, J. (2022). Rapport Phase 1 du CE créé en appui à l'administration sur la boucle géothermique GEOVEN. Retrieved from https://www.bas-rhin.gouv.fr/Actions-de-l-Etat/Environnement/Geothermie

Trugman, D. T., Dougherty, S. L., Cochran, E. S., & Shearer, P. M. (2017). Source spectral properties of small to moderate earthquakes in southern Kansas. *Journal of Geophysical Research: Solid Earth*, *122*(10), 8021–8034. https://doi.org/10.1002/2017JB014649

Trugman, D. T., & Shearer, P. M. (2018). Strong correlation between stress drop and peak ground acceleration for recent M 1–4 earthquakes in the San Francisco Bay area. *Bulletin of the Seismological Society of America*, *108*(2), 929–945. https://doi.org/10.1785/0120170245

Trutnevyte, E., & Ejderyan, O. (2018). Managing geoenergy-induced seismicity with society. *Journal of Risk Research*, *21*(10), 1287–1294. https://doi.org/10.1080/13669877.2017.1304979

Trutnevyte, E., & Wiemer, S. (2017). Tailor-made risk governance for induced seismicity of geothermal energy projects: An application to Switzerland. *Geothermics*, *65*, 295–312. https://doi.org/10.1016/j.geothermics.2016.10.006

van der Elst, N. J. (2021). B-Positive: A robust estimator of aftershock magnitude distribution in transiently incomplete catalogs. *Journal of Geophysical Research: Solid Earth*, *126*(2), e2020JB021027. https://doi.org/10.1029/2020JB021027

van der Elst, N. J., Page, M. T., Weiser, D. A., Goebel, T. H. W., & Hosseini, S. M. (2016). Induced earthquake magnitudes are as large as (statistically) expected. *Journal of Geophysical Research: Solid Earth*, *121*(6), 4575–4590. https://doi.org/10.1002/2016jb012818

van Eijs, R., Mulders, F. M. M., Nepveu, M., Kenter, C. J., & Scheffers, B. C. (2006). Correlation between hydrocarbon reservoir properties and induced seismicity in The Netherlands. *Engineering Geology*, *84*(3–4), 99–111. https://doi.org/10.1016/j.enggeo.2006.01.002

van Elk, J., Bourne, S. J., Oates, S. J., Bommer, J. J., Pinho, R., & Crowley, H. (2019). A probabilistic model to evaluate options for mitigating induced seismic risk. *Earthquake Spectra*, *35*(2), 537–564. https://doi.org/10.1193/050918EQS118M

van Ginkel, J., Ruigrok, E., Stafleu, J., & Herber, R. (2022). Development of a seismic site-response zonation map for The Netherlands. *Natural Hazards and Earth System Sciences*, *22*(1), 41–63. https://doi.org/10.5194/nhess-22-41-2022

Vargas-Payera, S., Martínez-Reyes, A., & Ejderyan, O. (2020). Factors and dynamics of the social perception of geothermal energy: Case study of the Tolhuaca exploration project in Chile. *Geothermics*, *88*, 101907. https://doi.org/10.1016/j.geothermics.2020.101907

Verdon, J. P., Baptie, B. J., & Bommer, J. J. (2019). An improved framework for discriminating seismicity induced by industrial activities from natural earthquakes. *Seismological Research Letters*, *90*(4), 1592–1611. https://doi.org/10.1785/0220190030

Verdon, J. P., & Bommer, J. J. (2020). Green, yellow, red, or out of the blue? An assessment of traffic light schemes to mitigate the impact of hydraulic fracturing-induced seismicity. *Journal of Seismology*, *25*(1), 301–326. https://doi.org/10.1007/s10950-020-09966-9

Vörös, R., & Baisch, S. (2022). Induced seismicity and seismic risk management—A showcase from the Californië geothermal field (The Netherlands). *Netherlands Journal of Geosciences*, *101*, e15. https://doi.org/10.1017/njg.2022.12

Walsh, F. R., & Zoback, M. D. (2016). Probabilistic assessment of potential fault slip related to injection-induced earthquakes: Application to north-central Oklahoma, USA. *Geology*, *44*(12), 991–994. https://doi.org/10.1130/g38275.1

Walter, W. R., Yoo, S.-H., Mayeda, K., & Gök, R. (2017). Earthquake stress via event ratio levels: Application to the 2011 and 2016 Oklahoma seismic sequences. *Geophysical Research Letters*, *44*(7), 3147–3155. https://doi.org/10.1002/2016GL072348

Walters, R. J., Zoback, M. D., Baker, J. W., & Beroza, G. C. (2015). *Version 1—Spring 2015 scientific principles affecting protocols for site-characterization and risk assessment related to the potential for seismicity triggered by Saltwater disposal and hydraulic fracturing*. Stanford University. Retrieved from https://scits.stanford.edu/sites/g/files/sbiybj22081/files/media/file/scitsguidelines_final_spring2015_0_0.pdf

Wannamaker, P. E., Simmons, S. F., Miller, J. J., Hardwick, C. L., Erickson, B. A., Bowman, S. D., et al. (2020). Geophysical activities over the Utah FORGE site at the Outset of project phase 3. In *45th Workshop on geothermal reservoir engineering*. Retrieved from https://pangea.stanford.edu/ERE/pdf/IGAstandard/SGW/2020/Wannamaker.pdf

Watkins, T. J., Verdon, J. P., & Rodríguez-Pradilla, G. (2023). The temporal evolution of induced seismicity sequences generated by low-pressure, long-term fluid injection. *Journal of Seismology*, *27*(2), 243–259. https://doi.org/10.1007/s10950-023-10141-z

Weber, D., & Brian, M. (2014). *Öffentlichkeitsarbeit für Geothermieprojekte*. Omniprint. Retrieved from https://www.enerchange.de/sites/default/files/pr-leitfaden-geothermie-enerchange.pdf

Weichert, D. H. (1980). Estimation of the earthquake recurrence parameters for unequal observation periods for different magnitudes. *Bulletin of the Seismological Society of America*, *70*(4), 1337–1346. https://doi.org/10.1785/BSSA0700041337

Wentinck, H. M., & Kortekaas, M. (2023). Induced seismicity in the Groningen gas field—Arrest of ruptures by fault plane irregularities. *Netherlands Journal of Geosciences*, *102*, e11. https://doi.org/10.1017/njg.2023.9

Wiemer, S., Kraft, T., & Landtwing, D. (2014). Seismic risk. In S. Hirschberg, S. Wiemer, & P. Burgherr (Eds.), *Energy from the Earth: Deep geothermal as a resource for the future? TA Swiss geothermal project final report* (pp. 263–295). Paul Scherrer Institute.

Wiemer, S., Kraft, T., Trutnevyte, E., & Roth, P. (2017). "Good practice" guide for managing induced seismicity in deep geothermal energy projects in Switzerland. In *ETH report*. https://doi.org/10.3929/ethz-b-000254161

Wiemer, S., & Wyss, M. (2000). Minimum magnitude of complete reporting in earthquake catalogs: Examples from Alaska, the Western United States, and Japan. *Bulletin of the Seismological Society of America*, *90*, 859–869. https://doi.org/10.1785/0119990114

Woessner, J., & Wiemer, S. (2005). Assessing the quality of earthquake Catalogues: Estimating the magnitude of completeness and its uncertainty. *Bulletin of the Seismological Society of America*, *95*(2), 684–698. https://doi.org/10.1785/0120040007

Wong, I., Bubeck, A., Gray, B., Lewandowski, N., McGregor, I., Smith, S., et al. (2023). Quantifying the potential for induced seismicity and the associated hazard and risk for EGS projects in Nevada and Oregon. In *ARMA, ARMA-2023*.

Woo, J. U., Kim, M., Sheen, D. H., Kang, T. S., Rhie, J., Grigoli, F., et al. (2019). An in-depth seismological analysis revealing a causal link between the 2017 M_W 5.5 Pohang earthquake and EGS project. *Journal of Geophysical Research: Solid Earth*, *124*(12), 13060–13078. https://doi.org/10.1029/2019JB018368

Wood, H. O., & Neumann, F. (1931). Modified Mercalli intensity scale of 1931. *Bulletin of the Seismological Society of America*, *21*(4), 277–283. https://doi.org/10.1785/BSSA0210040277

Wu, Q., Chapman, M., & Chen, X. (2018). Stress-drop variations of induced earthquakes in Oklahoma. *Bulletin of the Seismological Society of America*, *108*(3A), 1107–1123. https://doi.org/10.1785/0120170335

Wu, Y. M., Yen, H. Y., Zhao, L., Huang, B. S., & Liang, W. T. (2006). Magnitude determination using initial P waves: A single-station approach. *Geophysical Research Letters*, *33*(5), L05306. https://doi.org/10.1029/2005GL025395

Yaghoubi, A., Schultz, R., Hickson, C., Wigston, A., & Dusseault, M. B. (2024). Induced seismicity traffic light protocol at the Alberta No. 1 geothermal project site. *Geothermics*, *117*, 102860. https://doi.org/10.1016/j.geothermics.2023.102860

Yepes-Estrada, C., Calderon, A., Costa, C., Crowley, H., Dabbeek, J., Hoyos, M. C., et al. (2023). Global building exposure model for earthquake risk assessment. *Earthquake Spectra*, *39*(4), 2212–2235. https://doi.org/10.1177/87552930231194048

Yepes-Estrada, C., Silva, V., Valcárcel, J., Acevedo, A. B., Tarque, N., Hube, M. A., et al. (2017). Modeling the residential building inventory in South America for seismic risk assessment. *Earthquake Spectra*, *33*(1), 299–322. https://doi.org/10.1193/101915eqs155dp

Yu, H., Harrington, R. M., Kao, H., Liu, Y., Abercrombie, R. E., & Wang, B. (2020). Well proximity governing stress drop variation and seismic attenuation associated with hydraulic fracturing induced earthquakes. *Journal of Geophysical Research: Solid Earth*, *125*(9), e2020JB020103. https://doi.org/10.1029/2020JB020103

Zalachoris, G., & Rathje, E. M. (2019). Ground motion model for small-to-moderate earthquakes in Texas, Oklahoma, and Kansas. *Earthquake Spectra*, *35*(1), 1–20. https://doi.org/10.1193/022618eqs047m

Zang, A., Oye, V., Jousset, P., Deichmann, N., Gritto, R., McGarr, A., et al. (2014). Analysis of induced seismicity in geothermal reservoirs—An overview. *Geothermics*, *52*, 6–21. https://doi.org/10.1016/j.geothermics.2014.06.005

Zeiler, C., & Velasco, A. A. (2009). Developing local to near-regional Explosion and earthquake discriminants. *Bulletin of the Seismological Society of America*, *99*(1), 24–35. https://doi.org/10.1785/0120080045

Zhang, F., Wang, R., Chen, Y., & Chen, Y. (2022). Spatiotemporal variations in earthquake triggering mechanisms during multistage hydraulic fracturing in Western Canada. *Journal of Geophysical Research: Solid Earth*, *127*(8), e2022JB024744. https://doi.org/10.1029/2022JB024744

Zhao, Y., Jiang, G., Lei, X., Xu, C., Zhao, B., & Qiao, X. (2023). The 2021 Ms 6.0 Luxian (China) earthquake: Blind reverse-fault rupture in deep sedimentary formations likely induced by pressure perturbation from hydraulic fracturing. *Geophysical Research Letters*, *50*(7), e2023GL103209. https://doi.org/10.1029/2023GL103209

Zhou, Y., Zhou, S., & Zhuang, J. (2018). A test on methods for Mc estimation based on earthquake catalog. *Earth and Planetary Physics*, *2*(2), 150–162. https://doi.org/10.26464/epp2018015

Zoback, M. D., & Gorelick, S. M. (2012). Earthquake triggering and large-scale geologic storage of carbon dioxide. *Proceedings of the National Academy of Sciences*, *109*(26), 10164–10168. https://doi.org/10.1073/pnas.1202473109